Fixed-Rate Transmission of Correlated Analog Sources over Fading Multiple-Access Channels: Performance Bounds and Code Design

by

Chathura Illangakoon

A Thesis submitted to the Faculty of Graduate Studies of The University of Manitoba,
in Partial Fulfilment of the Requirements for the degree of

Doctor of Philosophy

Department of Electrical and Computer Engineering
University of Manitoba
Winnipeg

Abstract

Reliable and efficient communication of analog observations over a fading multiple access channel (MAC) is important in wireless sensor networks. A sensor network can be well modelled by a set of correlated Gaussian sources communicating to a common receiver over a fading Gaussian MAC (GMAC). It is known that traditional separate source-channel (SSC) coding is sub-optimal when channel state information (CSI) is not available to the transmitters. For this case, neither the optimum performance theoretical achievable (OPTA) nor any practical coding schemes that can outperform traditional coding, are known.

This thesis investigates the minimum mean square error (MMSE) of communicating a pair of Gaussian sources over a bandwidth-matched GMAC with block Rayleigh fading (BF-GMAC) in the absence of transmitter CSI. We derive several upper-bounds to the MMSE as a function of transmitter powers, channel signal-to-noise ratio (CSNR), and the correlation coefficient of the two sources. To derive nontrivial upper bounds which improve on those of SSC coding and uncoded transmission, we incorporate ideas from joint source-channel coding and hybrid digital–analog (HDA) coding to construct coding schemes for which the achievable MMSE can be determined.

One main contribution is two new MMSE upper bounds, which appear to be the best known characterizations of the OPTA to date. These bounds (JSC-VQ and HDA-JSC-VQ bounds) are derived by considering a transmission scheme where optimally vector quantized Gaussian sources are directly transmitted in analog form over the BF-GMAC. A comparison of these bounds with the MMSE bound for traditional SSC coding shows a gap that grows with source correlation and CSNR. Although there exists a gap even

when the sources are uncorrelated, this gap is relatively small. It is shown that, for highly correlated sources and low average CSNR, uncoded transmission can achieve performance approaching the HDA-JSC-VQ bound.

The difficulty of designing a practical coding scheme based on JSC-VQ scheme is the requirement of infinite-dimensional vector quantizers (VQ) for each Gaussian source and the joint detection of long codewords at the receiver. We present a practical coding method constructed by replacing the VQs by trellis coded quantizers (TCQ), which can perform close to the JSC-VQ bound.

Acknowledgements

I would like to express my deepest gratitude to my advisor Prof. Pradeepa Yahampath for his guidance and insight throughout my Ph.D. thesis. His encouraging words, constructive criticism, fair judgment and patience helped me to grow as a researcher as well as a person. In addition, his well-taught Topics in Signal Compression and Coding, and Information Theory courses boosted my enthusiasm towards information and communication theoretic research work. I owe him much gratitude to his prompt and constructive feedback, and for his numerous proofreads. This thesis would not have been possible without his guidance. I wish to acknowledge the financial support from National Science and Research Council (NSERC) and the University of Manitoba.

I would like to thank all the professors in our department for their help and guidance. Also I wish to thank the administrative staff of the Faculty of Graduate Studies and the Department of Electrical and Computer Engineering.

My sincere gratitude goes to all my colleagues in the communication lab whose support and friendship was invaluable. Also I must thank all my friends in Winnipeg for making the years so enjoyable.

I would like to thank my parents for inspiring a love of learning and giving me the freedom to follow my passion. I can't imagine coming so far without their love and dedication. My deepest thanks to my wife Godawari for her kindness and support during these tough academic years.

Contents

List of Figures

List of Tables

List of Abbreviations

AWGN	additive white Gaussian noise
BFMAC	block-fading multiple-access channel
CSI	channel state information
CSNR	channel signal-to-noise ratio
HDA	hybrid digital-analog
iid	independent and identically distributed
JSC	joint source-channel
LDPC	low-density parity check
MAC	multiple-access channel
MAP	maximum a posterior
ML	maximum-likelihood
MMSE	minimum mean-squared error
MSE	mean-squared error
pdf	probability density function
pmf	probability mass function
SCS	source-channel separation
SNR	signal-to-noise ratio
SSC	separate source-channel
SW	Slepian-Wolf
TCQ	trellis-coded quantization
TCVQ	trellis-coded vector quantization
VQ	vector quantizer/ vector quantization

Notation

General Mathematical Notation

$a \in \mathcal{A}$	a is an element of $\mathcal{A}$
$a \notin \mathcal{A}$	a is not an element of $\mathcal{A}$
$\mathcal{A} \subseteq \mathcal{B}$	$\mathcal{A}$ is a subset of $\mathcal{B}$
$\mathcal{A} \subset \mathcal{B}$	$\mathcal{A}$ is a proper subset of $\mathcal{B}$
$\mathcal{A} \cap \mathcal{B}$	intersection of $\mathcal{A}$ and $\mathcal{B}$
$\mathcal{A} \cup \mathcal{B}$	union of $\mathcal{A}$ and $\mathcal{B}$
$\mathcal{A}^c$	complement of $\mathcal{A}$
$\mathcal{A} \times \mathcal{B}$	Cartesian product of $\mathcal{A}$ and $\mathcal{B}$
$\mathbf{x}^*$	complex conjugate of x
$\mathbf{X}^T$	transpose of x
$\mathbf{X}^H$	conjugate transpose of x
$\|x\|$	absolute value of x
$\|\mathbf{x}\|$	L_2-norm of $\mathbf{x}$
$\langle \mathbf{x}, \mathbf{y} \rangle$	inner product between $\mathbf{x}$ and $\mathbf{y}$
$\sphericalangle(\mathbf{x}, \mathbf{y})$	angle between $\mathbf{x}$ and $\mathbf{y}$
$\mathrm{E}[X]$	expectation of X
$I(X;Y)$	mutual information between X and Y
$I(X;Y\|Z)$	cond. mutual information between X and Y cond. on Z
K_{XX}	covariance matrix of random vector X
$\tilde{K}_{XX}$	pseudo covariance matrix of random vector X
$\log_2(x)$	logarithm, to the base 2, of x
lim	limit
max	maximum

min	minimum
$\mathbb{C}$	set of complex numbers
$\mathbb{N}$	set of natural numbers
$\mathcal{CN}(\mu, \nu)$	complex Gaussian distribution of mean μ and covariance ν
Pr$[\mathcal{A}]$	probability of event $\mathcal{A}$
Pr$[\mathcal{A}\|\mathcal{B}]$	conditional probability of event $\mathcal{A}$ conditioned on $\mathcal{B}$
$\mathbb{R}$	set of real numbers
$\mathbb{Z}$	set of integer numbers

Problem Specific Notation

α_i, β_i	scaling coefficients
$\mathcal{C}_i$	codebooks
D, D_i	mean squared-error distortion
$D^{\text{JCS-VQ}}$	distortion resulting from JSC-VQ coding scheme
$D^{\text{JCS-VQ-HDA}}$	distortion resulting from JSC-VQ-HDA coding scheme
D^{HDA}	distortion resulting from HDA coding scheme
D^{SSC}	distortion resulting from SSC coding scheme
D^{U}	distortion resulting from uncoded scheme
$f_i^{(n)}$	encoding functions of transmitter
γ_i	fading power
h_i	fading gain
i	user index
k	time index
μ, μ_i	power-to-noise ratios
n	block-length
N	additive noise variance
P, P_i	average power constraints
$\phi_i^{(n)}$	reconstruction functions of receivers
R, R_i	rates of vector-quantizer
ρ	correlation coefficient between sources
$\tilde{\rho}$	asymptotic correlation between VQ source codewords

$S_{i,k}$	time-k sample of source i
t, t_i	power sharing ratio between digital part and analog part in HDA coding
$\tilde{\mathbf{S}}_i$	vector-quantized version of $\mathbf{S}_i$
$\hat{S}_{i,k}$	estimate of $S_{i,k}$
σ^2	source variance
$\mathbf{U}_i^o$	vector-quantized version of $\mathbf{S}_i$
$\hat{\mathbf{U}}_i^o$	estimate of vector-quantized sequence $\mathbf{U}_i^o$
W_k	time-k additive noise
$X_{i,k}$	time-k channel input of transmitter i
Y_k	time-k MAC output
$\mathbf{Z}_i$	quantization error sequence of vector-quantized $\mathbf{S}_i$

Chapter 1

Introduction and Background

A well designed communication system sends information from sources to the destinations for *reliable* reconstruction of the source. Figure 1.1 illustrates a communication system which sends information to the destination over a communication channel. The source encoder converts a sequence of source symbols into another sequence of symbols, drawn from a finite alphabet. Source encoding is often referred to as data compression. The data compression can be *lossy* or *lossless*. Lossless data compression is when the source can be reproduced exactly through a decompression process. The main goal of lossless compression is to represent the source by minimum number of symbols (say bits). The average number of bits representing one source symbol at the output of the source encoder is called the *rate of the code*. The *entropy rate* of the source provides a lower bound to the rate for lossless data compression [1, 2].

Lossless data compression is only possible when the source produces discrete-valued symbols from a finite alphabet. However, when the source produces continuous amplitude symbols, lossless data compression is not possible as the source entropy rate is infinite, and hence lossy compression has to be employed. The loss due to compression measured, according to an error criterion, is called distortion. Rate-distortion theory describes the minimum achievable average distortion for a given rate and vice versa [2–4].

This thesis is concerned with communicating continuous-amplitude sources and hence

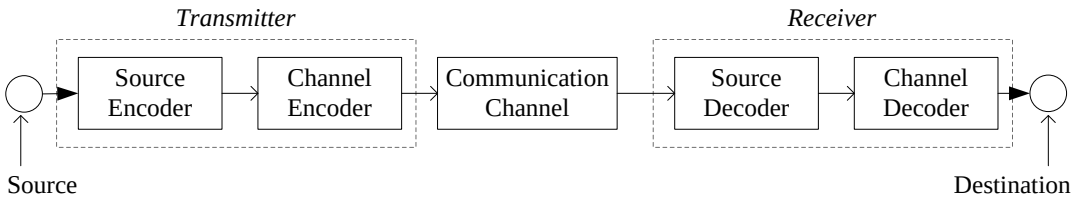

Figure 1.1: A communication system.

lossy compression. The problem of interest is communicating multiple continuous sources to a single receiver over a common wireless channel. Such systems are referred to as multiple access communication systems. We start by introducing the reader to the basic problem of communicating information from a single source to a single receiver in Section 1.1. In Section 1.2 multiple-access systems are introduced. In Section 1.3, the main problem studied in this thesis is introduced, and the specific contributions are summarized.

1.1 Single Continuous Source over a Point-to-point Channel

In the system shown in Fig. 1.1, the channel encoder maps the source encoder outputs into a sequence of channel input symbols such that the source encoder output can be "reliably" decoded at the channel decoder. Here, by relaible decoding, we mean the ability of making a decoding error is arbitrarily small by choosing the coding scheme appropriately. In Shannon's landmark paper [1], it is shown that reliable communication can be achieved even if the channel is noisy. According to the *channel capacity theorem* [2], reliable communication is possible when the transmission rate is less than the channel capacity, i.e., the channel capacity provides an upper bound to the transmission rate.

Consider transmission of a source over a point-to-point noisy channel using the communication model depicted in Figure 1.1. According to the *source-channel transmission theorem* [1, 2], lossless transmission of a source is possible when the entropy rate of the source is less than the channel capacity, and not possible when the rate is greater than the

channel capacity. The entropy rate of an analog source is infinite and the capacity of a noisy channel is finite. Therefore, lossless transmission of an analog source is not possible over a noisy channel. The goal in this case is to transmit the source to achieve the minimum possible distortion at a given bit rate. An unbeatable lower bound on the minimum achievable distortion is given by [1–3]

$$D_{opt} = D(bC),$$

where $D(.)$ is the distortion-rate function of the source [2–4], C is the capacity of the channel, and b is the number of channel uses per source sample. D_{opt} is often referred to as the *theoretically optimal performance* or the *Shannon limit*.

There are two broad approaches to communicating an information source: (I) *Digital communication* and (II) *Analog communication*. The communication model that is depicted by Fig. 1.1 is based on a digital communication method which uses so called separate source-channel coding. According to Shannon's source-channel separation theorem, such systems can be designed to achieve the theoretically optimal performance for a broad class of source and channels [1–3]. But, in most cases, this may require very complex encoding and decoding algorithms involving long processing delays. In such optimal systems, the source encoder compresses the source to achieve $D(bC)$, and the channel coder (encoding-decoding) achieves error free communication at a transmission rate equal to the channel capacity.

An inherent problem of digital communication based on source-channel separation is the "threshold effect" as shown in Figure 1.2. The threshold effect can be described as follows. The channel code is designed for a particular channel signal-to-noise ratio (CSNR), and therefore a system can be designed to achieve a certain performance when the true CSNR is not less than the design CSNR. However, when the true CSNR falls below the design CSNR, as for example in wireless systems with fading, the performance of the system degrades drastically. Also, the performance of systems based on the source-channel separation principle will not improve as the true CSNR increases, as the loss due to the source

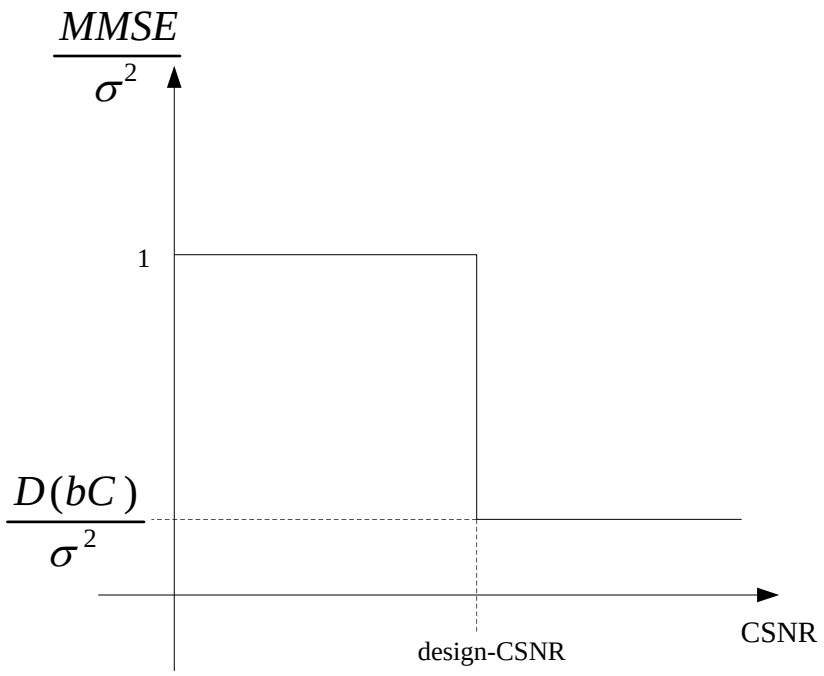

Figure 1.2: An example of threshold effect in digital communication based on source-channel separation (σ^2 is the source variance).

compression cannot be recovered. Furthermore, the threshold effect is more pronounced when a system operates close to the theoretically optimum performance.

In order to reduce the threshold effect, digital systems are designed by combining source and channel coding in to a single code. This approach is called *joint source-channel coding*. Joint source-channel coding schemes attempt to mitigate the threshold effect by exploiting the channel and source characteristics jointly. Some examples for such techniques are (a) channel optimized vector quantization (COVQ) where the quantizer for the source is optimized to both the source and the channel [5–8]; (b) unequal error protection where source data is protected from channel errors according to their relative importance [9]; (c) optimal index assignments [9, 10]; (d) by using the redundancies at the source encoder output to correct channel errors [11–14].

Both separate source-channel coding and joint source-channel coding schemes have finite transmission rates, and hence these are called digital coding schemes. In digital

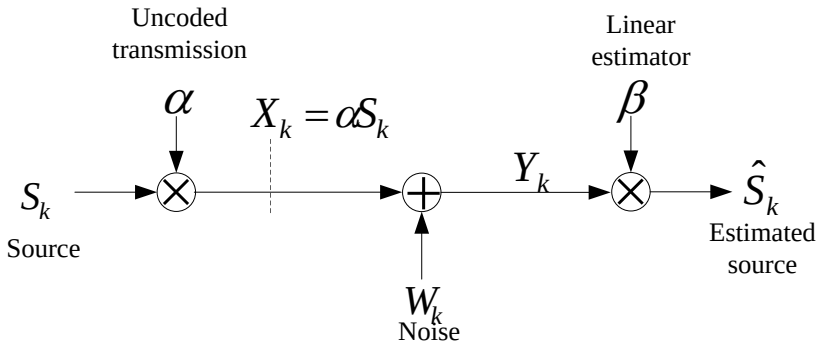

Figure 1.3: Uncoded transmission of continuous source over additive noise channel.

systems used to transmit continuous information sources, we cannot recover the loss due to quantization used for source encoding. Therefore, the performance of digital systems do not improve as the CSNR increases beyond a certain value.

Another approach to transmitting an analog information source is through analog modulation (see Figure 1.3). Since analog systems do not quantize the source, the transmitter output has a continuous valued alphabet. Therefore, analog systems have an infinite rate at the transmitter output. As a result the quality of the received signal gradually changes with the CSNR [15]. But all practical analog transmission systems such as those based on amplitude modulation (AM) or frequency modulation (FM), perform substantially below most digital systems, as it is difficult to exploit the source and channel characteristics well using analog signal processing.

The problem of sending an analog source over a noisy channel is well studied and a large body of literature exists. Shannon [16] discussed the issue of sending an analog source over a noisy channel. Shannon represented the source output and the transmitter input as "points in geometrical spaces", and viewed encoder-decoder operations are mappings between two spaces of different dimentionality. It was shown that when the source and channel bandwidths are mismatched the optimal encoder and decoder mappings will be highly nonlinear and complex.

Goblick [15] compared the mean-squared error distortion performance of various analog schemes when analog data is transmitted over an additive white Gaussian noise (AWGN)

channel. Wyner and Ziv [17] considered a problem of transmitting a discrete-time analog data belonging to a bounded set with variety of fidelity criteria. Bounds on the minimum achievable distortion are obtained for finite and infinite delay coding. Ziv [18] studied performance and derived lower bounds of general modulation schemes for a class of distortion functions.

So far, we discussed the problem of transmitting an analog source over channels that do not vary with time. In many practical situations such as in wireless communication, the channel characteristics vary with time. In this type of situations, the communication system performance depends on the degree of knowledge that the transmitter and/or receiver has about the channel state at a given time instant. The knowledge about the instantaneous channel characteristics is called *channel state information* (CSI). In most cases, it is easier for a receiver to acquire CSI using the signal it observes at the channel output. It is however, more difficult for the transmitter to acquire CSI. Depending on the availability of CSI, communication systems can be divided into two main categories:

1. Fully informed: CSI available at both receiver and transmitter.

2. Partially informed: CSI available only at the receiver or the transmitter,

The most common instance of partially informed systems is those in which CSI only available to the receiver. Such systems are also called systems with to no transmitter CSI.

An assumption that is made commonly regarding time varying channels is that the channel transitions over all possible fading states during the transmission of a codeword. This type of a channel is referred to as an ergodic channel. Shannon [3] proved that separate source-channel coding can achieve the optimum performance for transmitting a source over an ergodic channel. When CSI is not available at the transmitter, the encoding rate cannot be varied to match the channel, which forces the transmitter to use constant rate encoding and to distribute the instantaneous power randomly over a codeword to maintain its average power constraint. In such scenarios, the achievable upper-bound on the transmission rate can be severely restricted if the probability of channel undergoing low CSNR values is

larger than that for the high CSNR values. The Shannon capacity for an ergodic channel is given by

$$C_{erg} = \int_0^\infty C(\tau) f(\tau) d\tau,$$

where τ is the instantaneous CSNR which is available to the decoder, $C(\tau)$ is the instantaneous capacity of the channel, and $f(\tau)$ is the pdf of τ. The minimum achievable distortion can be written as

$$D_{opt} = D(bC_{erg}).$$

In order to achieve the Shannon limit, the length of the transmitted codeword must be long enough to capture the ergodic nature of the channel. As a result, the slower the channel varies the longer codeword length required. Therefore, a channel must exhibit sufficiently fast variation in order for us to be able to use the Shannon capacity as a basis for communication system design (see [19] for details).

When the channel varies slowly in such a manner such that the instantaneous CSNR τ remains constant over a large number of channel symbols, the Shannon capacity may not be suitable for designing communication systems. For example, should the randomly varying channel realizes a CSNR equal to zero, the Shannon capacity is equal to zero. Unlike in the case of fast varying channels, it is more meaningful to design digital systems for slow varying channels based on the notion of outage capacity. An outage occurs when the realized CSNR falls below a certain value say τ_{des}, i.e, the instantaneous channel capacity is less than the transmission rate. Consequently, a higher rate than the Shannon capacity is possible at the expense of reliability during deep fading states that occur in fast-fading channels [20].

The design parameter τ_{des} determines the outage probability P_{out} and the transmission rate to be used. When there is no transmitter CSI, data is transmitted at a constant rate which is equal to the channel capacity evaluated at the design CSNR τ_{des}. The outage

probability of the system is given by

$$P_{out} = \Pr(\tau < \tau_{des}).$$

Consequently, the probability of successful decoding is $1 - P_{out}$. In this case, the expected distortion can be evaluated over the fading distribution as

$$D_{av} = D\left(bC(\tau_{des})\right)\left(1 - P_{out}\right) + d_0 P_{out},$$

where d_0 is the average source reconstruction distortion during channel outages. This result can be interpreted as follows: either the source data is received successfully with distortion $D\left(C(\tau_{des})\right)$, or the system is in outage in which case the distortion is equal to d_0. The communication system can be designed to minimize the average distortion with respect to the design CSNR.

It is well known that direct, or *uncoded*, transmission of a memoryless Gaussian source over a memoryless Gaussian channel is optimum when the distortion is measured by mean square error and the source bandwidth is equal to the channel bandwidth (bandwidth matched) [15, 21]. The performance degradation of uncoded transmission in bandwidth mismatched cases can be attributed to the inefficiency due to lack of data compression. In bandwidth mismatched case, joint source-channel (JSC) coding schemes have been developed based on hybrid digital-analog (HDA) coding techniques to improve the performance over separate source-channel coding systems. In HDA schemes, the efficient data compression in digital schemes are combined with graceful channel adaptation property of analog coding schemes. In a number of previous work, it has been demonstrated that, in situations where transmitter-side CSI is not available (such as broadcast or multicast), HDA coding schemes can be used to design systems that perform well over a large range of CSNRs [22–25].

In [22], it is conjectured that no code is optimal simultaneously at different CSNRs when the source and channel bandwidth are not equal. For unequal source and channel bandwidths, [22] proposes a number of "nearly robust" JSC coding schemes based on HDA coding techniques to improve the performance over separate source-channel cod-

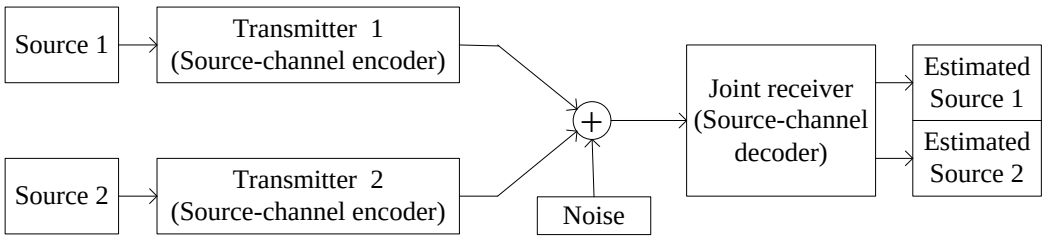

Figure 1.4: Transmission of two sources over a two-to-one MAC.

ing systems. The HDA systems proposed in [22] are designed to be optimum at a target CSNR but improve or degrade gracefully should the true CSNR deviate from the target.

A digital code aimed at sending information from a single transmitter to many receivers experiencing different CSNRs is called a broadcast strategy [26]. Two extreme approaches are to send data at a rate equal to the capacity of the worst channel or to send data at a rate equal to the capacity of the best channel. Obviously such approaches result in poor overall performance. However, [26] shows that by distributing high-rate information across low-rate messages, a broadcast system can improve its overall performance. An uncertain channel with finite states may be visualized as a transmitter broadcasting data to a set of virtual receivers with different CSNRs. Therefore, fading channels without CSI at the transmitter can be modeled as a broadcast channel. A layered broadcast strategy for Gaussian fading channel is studied in [27]. In [27], it is shown that layered broadcast strategies enable to implement a continuum of capacity versus outage values rather than a single pair as is in the standard digital coding approach. In [28], a layered broadcast strategy is considered for sending a Gaussian source over a fading Gaussian channel with a finite number of states. In particular, [28] obtains the operating point inside the capacity region of the equivalent broadcast channel that minimizes the expected distortion.

1.2 Multiple Sources over a Multiple Access Channel

So far we have considered point-to-point communication. Now we turn our attention to multiple-access communication which is the main focus of this thesis. The problem of

sending multiple sources over a multiple-access channel (MAC) to a single receiver captures many practical communication systems. Common examples include ground stations sending voice data to a satellite, cellular devices sending data to a cell-tower, or a network of sensors sending observed data to a central monitoring station. A simple example in which two information sources are transmitted to a single receiver over a MAC is illustrated in Figure 1.4. Slepian and Wolf [29] considered the problem of lossless compression of two or more correlated sources separately while decompression of the sources are performed jointly. The well known Slepian-Wolf theorem [29] gives necessary and sufficient conditions for achievable rate tuples. Wyner and Ziv [30] considered lossy compression of a source with a fidelity criterion when the decoder has side information about the source and derived a lower bound for achievable rates for a given distortion. Berger [31] and Tung [32] introduced multi-terminal source coding problem by considering separate compression and joint decompression subject to distortion constraints. Finding the achievable rate region in the general multi-terminal source coding problem is known to be very hard, hence many work in the literature has mostly focused on the quadratic Gaussian case in which the sources are jointly Gaussian and the mean-squared error is used as the distortion measure. The work by Oohoma [33] and Wagner [34] present the complete solution to the quadratic Gaussian two-terminal source coding problem under an individual distortion criterion.

In the MAC case, the capacity of the channel is the closure of all rate tuples for which the all encoded messages can be decoded with an arbitrary small probability of error. The capacity region of the discrete Gaussian MAC with transmitter powers P_1 and P_2, and noise variance N is illustrated in Figure 1.5 [2]. It is known that when there is no constraint on the transmission delay, any rate pair (R_1, R_2) inside the capacity region can be achieved by using independent Gaussian random codes at the transmitters.

One way to transmit multiple sources over a MAC is to employ a system based on the principle of source-channel separation. However, it is well known that the separate source-channel coding is not optimal for sending multiple sources over a MAC. Except

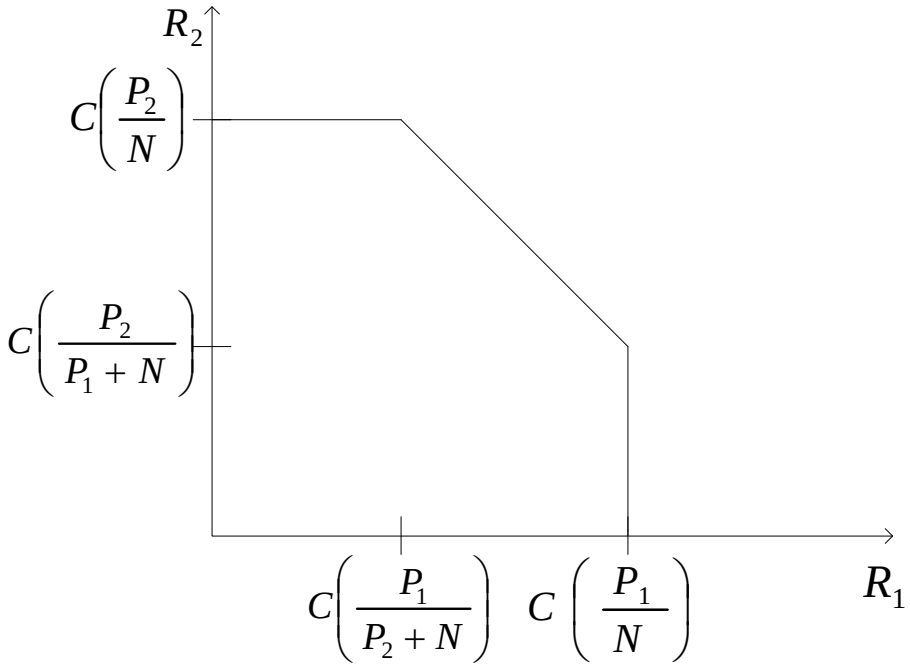

Figure 1.5: Gaussian multiple-access channel capacity ($C(x) = \frac{1}{2}\log(1+x)$).

for a few special network models in which sources and channels are suitably "matched" [21, 35–39], optimally sending multiple sources over a MAC requires joint optimization of data compression and channel coding. The problem of lossless transmission of two finite-alphabet correlated sources over a two-to-one MAC is addressed by Cover, El Gamal and Salehi [40]. In [40], sufficient conditions for the existence of a code which achieves an arbitrarily small decoding error probability are presented. It has been shown that such a code rely on direct mapping of the source symbols to channel inputs, rather than data compression followed by channel coding. Other related work on lossless transmission of correlated sources are [41] and [42].

In work, more directly related to the work in this thesis, Salehi [43] studied a lossy version of the problem with two finite-alphabet sources and arbitrary distortion measures on each source. Lapidoth and Tinguely [44] considered the problem of sending Gaussian sources over the two-to-one Gaussian MAC with an average power constraint on each transmitter. In [44], the authors focus on the bandwidth matched case and present necessary and

sufficient conditions for the achievability of a distortion pair. Moreover, [44] introduces a "source-channel vector-quantizer" scheme, relies on the optimal source compression by VQ and the constructive interference created by correlated channel inputs. This scheme plays a central role in new developments presented in Chapters 3 and 4 of this thesis.

When the channel state of a MAC is a random variable there is an instantaneous capacity region corresponding to the realized channel state. When the CSI is not available to the transmitters, fixed transmission rates have to be used in all transmitters. The ergodic capacity region based on the standard interpretation of the Shannon capacity is well defined for a fast fading MAC with no transmitter CSI [19, chapter, p. 215]. When the MAC is slowly varying, parallel to the point-to-point case, a common outage probability is defined as the probability that the tuple of transmission rates lies outside the capacity region. For heterogeneous networks, it is necessary to evaluate the individual outage probabilities corresponding to each transmitter. Individual outage probabilities without transmitter CSI are discussed in [45] for a MAC with transmitters and the receiver equipped with multiple antennas. Narasimhan [46] computes the explicit individual outage rate regions for a quasi-static fading MAC by assuming Gaussian multiple-access interference.

In [47], the digital transmission of a pair of uncorrelated Gaussian sources using separate source-channel coding over a slow-fading two-to-one MAC without the transmitter CSI is considered. The average distortion is obtained using the individual outage regions computed in [46], and the transmission rates that minimize the average sum MSE for the independent Rayleigh fading are obtained numerically. A different approach for transmitting sources over a the static Gaussian MAC using a CDMA like access scheme, based on analog JSC coding techniques [21, 48, 49] is proposed in [50]. In the analog JSC coding approach a block of source samples is directly mapped to a block of channel input symbols using a non-linear transformation. In [50], simulation results were obtained using practical analog JSC codes optimized for point-to-point communications, and simulation results show that the performance of these practical systems are close to the theoretical limit.

1.3 Contribution of the Thesis

1.3.1 Objectives of this thesis

The MMSE achievable in communicating correlated Gaussian sources over a block-fading GMAC, when CSI is not available at the transmitters, is not known. To this end, one objective of this thesis is to establish upper-abounds to the unknown MMSE by considering JSC coding methods that accounts for channel uncertainty at the transmitters. In practical communication systems with finite delays and limited encoder-decoder processing powers, an important problem is designing practical coding schemes that mimic an effective theoretical coding principle to approach the best achievable performance. The problem of practical code design for communicating correlated sources over MAC with no CSI at transmitters is not addressed in the literature. To this end, another objective of this thesis is to propose a practical code, with finite coding delay and tractable computational complexity, for correlated sources and fading MAC.

1.3.2 Contributions

- In Chapter 2, we establish several upper bounds to the unknown MMSE by considering a superposition-based HDA coding to exploits the benefits of both digital and analog coding to counteract the channel uncertainty and to exploit source correlation. The achievable MMSE of source-channel separation-based coding and uncoded transmission are also derived and used as benchmarks.

- In Chapter 3, we derive upper bounds to the achievable MMSE by considering JSC coding schemes that use source dependent channel codewords allowing constructive and destructive interference between digital channel inputs. The MMSE derived for a source-channel vector quantization scheme and an HDA extension of it provide the best known upper bound to the achievable MMSE for communicating correlated Gaussian source over block Rayleigh fading Gaussian MAC. The MMSE of the two

schemes are derived by considering the three possible outage cases. Through numerical performance evaluations, it is shown that, unlike in the case of fixed GMAC, uncoded transmission is no longer optimal at low CSNRs, when there is channel fading and CSI is not available to the transmitters.

- In Chapter 4, we propose a practical JSC coding scheme that mimics the coding principle used in the source-channel vector quantizer scheme presented in Chapter 3. The encoder achieves source-channel coding by employing trellis coded quantization with an expanded codebook. We propose a four state joint decoder based on the Viterbi algorithm. Simulation results show that the proposed JSC coding scheme perform closer to the source-channel vector quantizer bound than the other alternatives such as separate source-channel (SSC) coding, uncoded transmission, and HDA coding considered in Chapter 2.

Chapter 2

HDA Coding for Sending Information from Gaussian Sources over BF-MAC

2.1 Introduction

One important design consideration arises that in wireless communication is the channel uncertainty at the transmitters. In many practical systems the CSI is estimated periodically at the transmitters by sending a burst of training data from the transmitters to the receiver. The receiver typically communicate the estimated CSI to the transmitters via feedback channels. Therefore, the CSI available to the transmitters can be limited by the capacity of the feedback channels. Moreover, when such feedback channels are unavailable due to spectrum scarcity, the transmitters have to deal with a large degree of channel uncertainty. Due to this channel uncertainty at the transmitters, the conventional digital coding scheme based on source-channel separation suffers from the cliff effect. On the other hand, JSC coding schemes based on HDA techniques have the potential to have better average performance under channel uncertainty as the performance of HDA coding changes gracefully with the channel quality. In order to examine the aforementioned claim, we consider the following problem of sending Gaussian sources over a slow-fading two-to-one MAC, as shown in Fig. 2.1.

We consider sending a pair of Gaussian sources over a block-fading Gaussian MAC. The sources can be mutually correlated. We consider a communication model with no CSI at the transmitters while the perfect CSI is available to the receiver. As discussed in Chapter 1, the property of graceful improvement-degradation in HDA schemes is well understood for the point-to-point case [22]. However, the performance of HDA coding with random channel variations is not straightforward as the reliable transmission from the digital encoders depends on the achievable rate region for the BF-MAC. Therefore, the individual outage regions must be computed according to the decodability of the digital codewords. In [46], the individual outage regions are computed for the channel coding over block-fading Gaussian MAC when the CSI is not available to the transmitters.

The HDA technique uses optimal VQ for digital compression of the source, which will be transmitted using a channel code. The analog information to be transmitted is the quantization error obtained by subtracting the VQ source codeword from the source sequence. The block of continuous-valued uncoded quantization error samples are transmitted over the same channel bandwidth used by the digital transmission of the source, by power splitting between the uncoded (analog) and the digital transmissions. The analog channel inputs act as additive noise to the digital codewords. The outage events of the digital codewords are defined based on the decodability of the channel codewords for given encoder parameters and the current channel gains which are constant for the channel codewords in the case of block fading. The necessary and sufficient conditions for joint decodability of the channel codewords are used to compute individual outage regions for the channel fading gains. We assume that the number of channel symbols transmitted per source symbol is one (i.e., bandwidth matched).

For comparison, the performance of an alternative HDA coding scheme where the analog and digital components are sent by orthogonal channel access is considered. The comparison of the performance of the HDA coding over the two-to-one MAC and a comparable orthogonal MAC can be justified by the following reasons:

1. The outage events creates different levels of interference

2. Effect of different channel uses per source symbol in digital coding

3. Sub-optimality of the uncoded transmission when the source-channel bandwidths are mismatched

The optimum outage rates and the power splitting ratio of the above systems, that minimize the average distortion, assuming the independent Rayleigh fading, are obtained using numerical optimization techniques. The problem we consider is related to multi-user communication systems with real-time traffic where it is difficult for the transmitters to obtain the current CSI. For example, in an upstream voice communication between ground stations and a satellite, a desirable design criteria is to minimize the average distortion over uncertain channels.

Contribution

The MMSE achievable in communicating correlated Gaussian sources over a fading GMAC is not known. To this end, this chapter establishes several upper bounds to the unknown MMSE by considering a coding schemes which uses superposition-based HDA transmission to combine the benefits of both digital coding and uncoded transmission. The achievable MMSE of source-channel separation-based coding and uncoded transmission are also derived an used as bench marks.

2.2 Problem Statement

The basic problem considered in Chapters 2-4 can be stated as follows. Two information sources S_1 and S_2 are observed at different locations and there is no communication link between the two locations. We wish to communicate and reproduce these two sources at a central location, where the communication is to takes place over a wireless channel modeled by a Gaussian MAC with Rayleigh fading. Each source is a circularly symmetric complex-valued Gaussian variable $S_i \in \mathbb{C}$ with mean zero and variance $\mathrm{E}\{|S_i|\} = \sigma_i^2$. Let

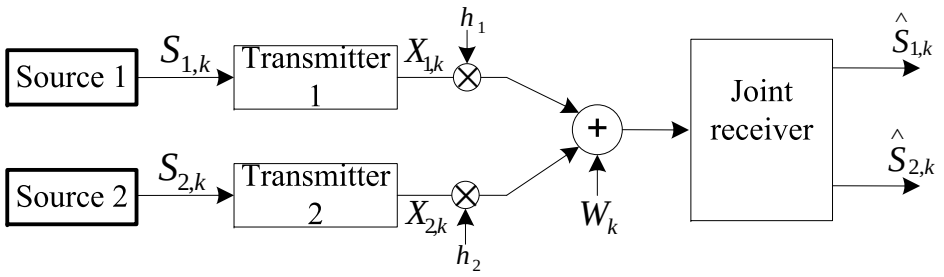

Figure 2.1: Communicating a pair of Gaussian sources over a two-to-one block fading Gaussian multiple-access channel.

the covariance matrix and the pseudo-covariance matrix of (S_1, S_2) be [51]

$$K_{SS} = \begin{pmatrix} \sigma_1^2 & \rho\sigma_1\sigma_2 \\ \rho\sigma_1\sigma_2 & \sigma_2^2 \end{pmatrix},$$

and $\tilde{K}_{SS} = \mathbf{0}_{2\times 2}$, respectively, where $|\rho| < 1$. A sequence of n outputs from the source S_i, denoted by $\mathbf{S}_i = (S_{i,1}, \ldots, S_{i,n})$, is assumed to be independent and identically distributed (iid). It is assumed that source and channel bandwidths are identical, so that a sequence of n source symbols are transmitted by n uses of the MAC. The encoder for each source S_i is therefore a mapping $f_i^{(n)} : \mathbb{C}^n \to \mathbb{C}^n$, and

$$\mathbf{X}_i = f_i^{(n)}(\mathbf{S}_i)$$

is the channel codeword $\mathbf{X}_i = (X_{i,1}, \ldots, X_{i,n})$ and $X_{i,n} \in \mathbb{C}$ is channel input for S_i at time $k = 1, \ldots, n$ (the superscript in $f_i^{(n)}$ emphasizes the fact each encoder is a block-encoder for n consecutive source symbols.) The transmitter for S_i has an average power constraint $P_i > 0$ so that

$$\frac{1}{n}\sum_{k=1}^{n} \mathrm{E}\left\{|X_{i,k}|^2\right\} \le P_i, \quad i = 1, 2.$$

Let the MAC output for channel input $(\mathbf{X}_1, \mathbf{X}_2)$ be the sequence $\mathbf{Y} = (Y_1, \ldots, Y_n)$, where $Y_k \in \mathbb{C}$ is the MAC output at time k given by

$$Y_k = h_1 X_{1,k} + h_2 X_{2,k} + W_k,$$

$h_{i,k} \in \mathbb{C}$ is the gain of the channel between S_i and the receiver at time k and $W_k \in \mathbb{C}$ is complex-valued channel noise. As usual it is assumed that $(h_{1,k}, h_{2,k})$ is iid complex Gaussian random variables with mean zero and independent real and complex parts. In this thesis we are concerned with a MAC with block fading, i.e., $h_{1,k}$ and $h_{2,k}$ remain constant during the transmission of a length n codeword. Therefore, henceforth we will denote the channel gains by h_1 and h_2. The channel noise W_k is assumed to be circularly symmetric Gaussian random variable with mean zero and variance N. The noise sequence $\mathbf{W} = (W_1, \ldots, W_n)$ is assumed to be an iid sequence.

Finally, we use a decoder which can be described by a pair of mappings $\phi_i^{(n)} : \mathbb{C}^n \to \mathbb{C}^n$, $i = 1; 2$, such that the decoded source sequences are given by

$$\hat{\mathbf{S}}_i = \phi_i^{(n)}(\mathbf{Y}).$$

The mean square reconstruction error of the source S_i is given by

$$D_i(h_1, h_2) = \frac{1}{n} \sum_{i=1}^{n} \mathrm{E}\{|S_{i,k} - \hat{S}_{i,k}|^2\}, \tag{2.1}$$

where the expected values is over the joint distribution of S_1, S_2 and the distributions of the two independent variables h_1 and h_2. We assume the codeword length n can be made large enough so that source codes achieving the rate-distortion bound and channel codes with vanishingly small error probabilities can be found. In this case, the optimal $(f_i^{(n)}, \phi_i^{(n)})$, $i = 1, 2$ are those which minimize the average MMSE,

$$D^* = \frac{1}{2} \int \left(D_1(h_1, h_2) + D_2(h_1, h_2)\right) f(h_1) f(h_2) dh_1 dh_2, \tag{2.2}$$

where $f(h_i), i = 1, 2$, is the pdf of the fading gains h_1 and h_2. This would be an optimal JSC coding scheme for our set-up. However, finding the optimal JSC coding scheme for this set-up appears to be very difficult. Therefore, our end goal is to find the MMSE achievable with good JSC coding schemes based on HDA coding which can acheive a D lower than that of: (1) the best separate source-channel coding scheme, and (2) the simplest JSC coding scheme of uncoded transmission.

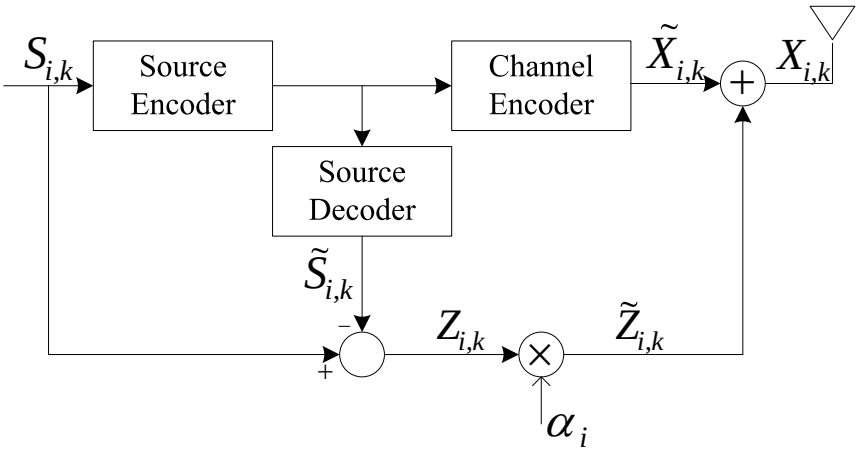

Figure 2.2: HDA encoder.

2.3 Superposition-based HDA Coding for Correlated Gaussian Sources and BF-GMAC

In this section we consider a conventional HDA coding scheme to establish an upper bound to the minimum achievable MSE in communicating a pair of correlated Gaussian sources over a two-to-one BF-GMAC. In [22], HDA coding techniques based on superposition is considered for broadcasting a Gaussian source over a AWGN channel when the source channel bandwidths are mismatched. In the broadcast setup a single source is communicated to multiple receivers experiencing different channel SNR values.It is shown in [22] that certain JSC coding based on HDA techniques are 'nearly robust' when source-channel bandwidths are mismatched, where a coding scheme is considered robust when it is optimal over a wide range of CSNRs. In our problem, the channel uncertainty at the transmitters may be mitigated by considering such robust HDA coding techniques. However, since the CSI is not available at the transmitters and the channel varies, a good coding scheme must be matched to the distribution of the channel fading gains. Below we describe a JSC coding system which is based on a conventional HDA technique where analog source information is superimposed on digital codewords to describe the source to the common receiver.

The coding scheme uses a power splitting between the digital and analog parts, and the channel inputs generated by the digital and the analog parts are superimposed and

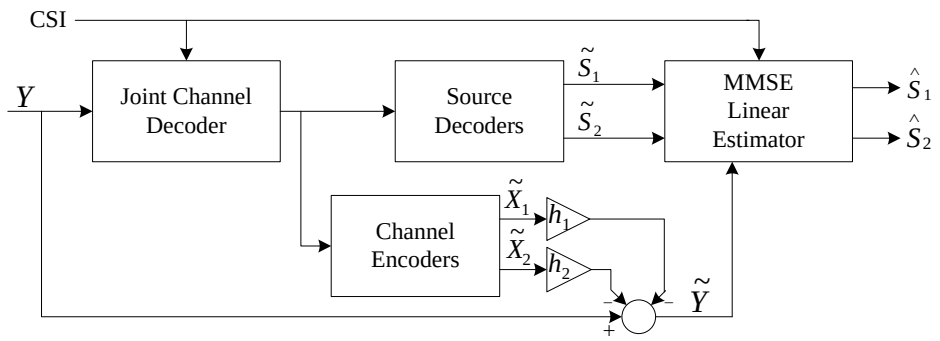

Figure 2.3: HDA decoder.

transmitted over the block fading two-to-one MAC. The block diagrams of the encoder and the joint decoder are shown in Fig. 2.2 and Fig. 2.3, respectively. First, the source sequence $\mathbf{S}_i$ is vector-quantized using an optimal VQ, and the VQ index $m = \Pi_i(\mathbf{S}_i)$ is input to a digital channel encoder which outputs the digital channel codeword $\tilde{\mathbf{X}}_i = \Lambda_i(m)$, where functions $\Pi_i : \mathbb{C}^n \to \{0, 1, \ldots, 2^{nR_i} - 1\}$ and $\Lambda_i : \{0, 1, \ldots, 2^{nR_i} - 1\} \to \mathbb{C}^n$ represent the VQ encoder and the channel encoder functions, respectively, and R_i is the encoding rate. Analog data is generated by obtaining the sequence of VQ errors $\mathbf{Z}_i = \mathbf{S}_i - \tilde{\mathbf{S}}_i$, where $\tilde{\mathbf{S}}_i = \Pi_i^{-1}(m)$ is the output of the VQ decoder $\Pi_i^{-1} : \{0, 1, \ldots, 2^{nR_i} - 1\} \to \mathbb{C}^n$. The channel input sequence $\mathbf{X}_i$ is the addition of the channel codeword and the scaled VQ error sequence, given by

$$\mathbf{X}_i = \tilde{\mathbf{X}}_i + \alpha_i \mathbf{Z}_i,$$

where $\alpha_i = \sqrt{nt_iP_i/\mathrm{E}\{\|Z_i\|^2\}}$, and $0 \leq t_i \leq 1$ is the ratio between the average power of the analog channel input and the expected average power constraint. Consequently, the average power of the digital channel codewords is subject to the constraint $\frac{1}{n}\mathrm{E}\{\|\tilde{\mathbf{X}}_i\|^2\} \leq (1 - t_i)P_i$. The joint reconstruction of the two sources is performed in two stages: 1. joint decoding of the digital channel codewords $\{\tilde{\mathbf{X}}_i\}$, 2. MMSE estimation of the source sequences based on decoded source codewords and the MAC output. A function $\Lambda^{-1} : \mathbb{C}^n \to \mathbb{C}^n \times \mathbb{C}^n$ is used in the receiver to jointly decode the digital codewords for both

sources based on the channel output sequence $\mathbf{Y}$, i.e.,

$$(\hat{\tilde{\mathbf{X}}}_1, \hat{\tilde{\mathbf{X}}}_2) = \Lambda^{-1}(\mathbf{Y}),$$

where $(\hat{\tilde{\mathbf{X}}}_1, \hat{\tilde{\mathbf{X}}}_2)$ is the pair of decoded digital codewords. The decoding function Λ^{-1} depends on the current fading gains, the transmission rates, and the power allocation ratio. Now we describe the three scenarios according to the decodability of the digital codewords, which we call outage events. The three outage events are:

1. Both digital codewords are successfully decoded (no outage)
2. Only one digital codeword successfully decoded (partial outage)
3. Either of the digital codewords cannot be decoded successfully (total outage)

The digital codebooks are constructed using a random code, whos symbols $\{\tilde{\mathbf{X}}_{i,k}\}$, $i \in \{1,2\}$ and $k = 1, \ldots, n$, are iid circularly symmetric complex Gaussian random variables $\tilde{X}_{i,k} \in \mathbb{C} \sim \mathcal{CN}(0, (1-t_i)P_i)$, so that the probability of successful decoding of both digital codewords are maximized [2, 20]. Also note that as $n \to \infty$, the optimal VQ splits the Gaussian source into two iid circularly symmetric complex Gaussian sequences, $\{\tilde{\mathbf{S}}_{i,k}\}$ and $\mathbf{Z}_{i,k}$, where $i \in \{1,2\}$ and $k = 1, \ldots, n$. Therefore, the analog channel input sequences $\alpha_i \mathbf{Z}_i$, $i = 1, 2$ act as AWGN to the digital channel inputs.

Case I: Both digital codewords can be decoded successfully

For given fading gains (h_1, h_2), the MAC between the digital channel inputs and the channel output can be seen as an AWGN MAC, i.e.,

$$Y_k = h_1 \tilde{X}_{1,k} + h_2 \tilde{X}_{2,k} + (h_1 \alpha_1 Z_{1,k} + h_2 \alpha_2 Z_{2,k} + W_k), \quad k = 1, \ldots, n. \tag{2.3}$$

The two channel input sequences $\{h_1 \tilde{X}_{1,k}\}$ and $\{h_2 \tilde{X}_{2,k}\}$ of the AWGN MAC given by (2.3) are subject to the average power constraints $\gamma_1(1-t_1)P_1$ and $\gamma_2(1-t_2)P_2$, respectively, where $\gamma_i = |h_i|^2$, $i = 1, 2$. The two input sequences are corrupted by AWGN with

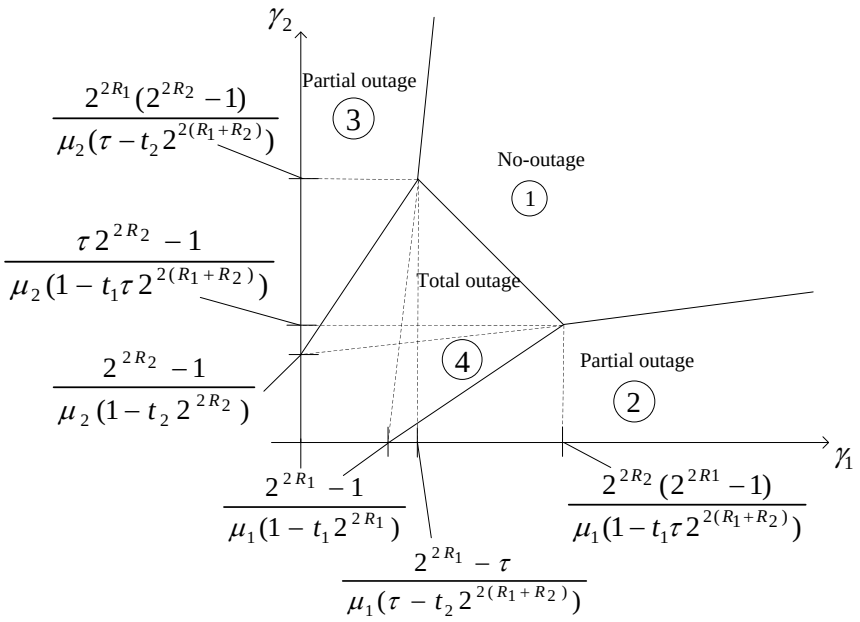

Figure 2.4: (γ_1, γ_2) pair regions corresponding to outage events in HDA coding of uncorrelated sources. $\tau = \frac{1-t_2}{1-t_1}$

average power $\gamma_1 t_1 P_1 + \gamma_2 t_2 P_2 + 2\text{Re}\{h_1 h_2^*\}\rho_Z \sqrt{t_1 t_2 P_1 P_2} + N$, where ρ_Z is the correlation coefficient between the VQ error symbols $Z_{1,k}$ and $Z_{2,k}$. Therefore the successful decoding of both codewords are determined by the achievable rate region of the AWGN MAC [2], and the necessary and sufficient conditions for this case given by the conditions

$$\begin{aligned}
(I):\ R_1 &< I(\tilde{X}_1; Y|\tilde{X}_2) \\
&= \frac{1}{2}\log\left(1 + \frac{\gamma_1(1-t_1)\mu_1}{\gamma_1 t_1\mu_1 + \gamma_2 t_2\mu_2 + 2\text{Re}\{h_1 h_2^*\}\rho_z\sqrt{t_1 t_2\mu_1\mu_2} + 1}\right) \quad (2.4) \\
(II):\ R_2 &< I(\tilde{X}_2; Y|\tilde{X}_1) \\
&= \frac{1}{2}\log\left(1 + \frac{\gamma_2(1-t_2)\mu_2}{\gamma_1 t_1\mu_1 + \gamma_2 t_2\mu_2 + 2\text{Re}\{h_1 h_2^*\}\rho_z\sqrt{t_1 t_2\mu_1\mu_2} + 1}\right) \quad (2.5) \\
(III):\ R_1 + R_2 &< \frac{1}{2} I(\tilde{X}_1, \tilde{X}_2; Y) \\
&= \frac{1}{2}\log\left(1 + \frac{\gamma_1(1-t_1)\mu_1 + \gamma_2(1-t_2)\mu_2}{\gamma_1 t_1\mu_1 + \gamma_2 t_2\mu_2 + 2\text{Re}\{h_1 h_2^*\}\rho_z\sqrt{t_1 t_2\mu_1\mu_2} + 1}\right) \quad (2.6)
\end{aligned}$$

where $\mu_i = P_i/N$ and $I(.;.)$ denotes the mutual information (for clarity we have dropped the time-index k), and ρ_Z is given by

$$\rho_z = \frac{\frac{1}{n}\langle \mathbf{Z}_1, \mathbf{Z}_2 \rangle}{\sigma_{z_1}\sigma_{z_2}},$$

where

$$\sigma_{z_i}^2 = 2^{-2R_i}\sigma^2, \quad i \in \{1, 2\}.$$

At the For given encoder parameters (R_1, t_1) and (R_2, t_2), the individual outage regions for digital coding over γ_1 and γ_2, for uncorrelated sources, are illustrated in Fig. 2.4. In Fig. 2.4, the "no-outage" region, denoted by $\mathcal{H}_{no}^h$, is the region indicated by ①. For correlated sources, the outage regions cannot be described explicitly in terms of the fading powers γ_1 and γ_1 due the interference term $2\text{Re}\{h_1 h_2^*\}\rho_z\sqrt{t_1 t_2 \mu_1 \mu_2}$.

In this case the sources are estimated based on the recovered source codewords $\tilde{\mathbf{S}}_1$ and $\tilde{\mathbf{S}}_2$, and the residual MAC output sequence

$$\begin{aligned}\tilde{Y}_k &= Y_k - (h_1\tilde{X}_{1,k} + h_2\tilde{X}_{2,k}) \\ &= h_1\alpha_1 Z_{1,k} + h_2\alpha_2 Z_{2,k} + W_k, \quad k = 1, \ldots, n.\end{aligned}$$

Since $\{\tilde{S}_{1,1}, \ldots, \tilde{S}_{1,n}\}$, $\{\tilde{S}_{2,1}, \ldots, \tilde{S}_{2,n}\}$, and $\{\tilde{Y}_1, \ldots, \tilde{Y}_n\}$ are iid sequences which are jointly Gaussian, the optimal MMSE estimator is linear, and the estimate of the source sequence $\mathbf{S}_i$ is given by

$$\hat{S}_{i,k} = q_{i,1}\tilde{S}_{1,k} + q_{i,2}\tilde{S}_{1,k} + q_{i,3}\tilde{Y}_k, \quad k = 1, \ldots, n,$$

where $q_{i,1}, q_{i,2}$ and $q_{i,3}$ are the coefficients of the linear estimator, which can be found by solving

$$\underbrace{\begin{bmatrix} k_{11} & k_{12} & k_{13} \\ k_{21} & k_{22} & k_{23} \\ k_{31} & k_{32} & k_{33} \end{bmatrix}}_{\mathbf{K}} \underbrace{\begin{bmatrix} q_{i,1} \\ q_{i,2} \\ q_{i,3} \end{bmatrix}}_{\mathbf{q}_i} = \underbrace{\begin{bmatrix} c_{i1} \\ c_{i2} \\ c_{i3} \end{bmatrix}}_{\mathbf{c}_i},$$

where

$$\mathbf{K} = \begin{bmatrix} \frac{1}{n}E\|\tilde{\mathbf{S}}_1\|^2 & \frac{1}{n}E\langle\tilde{\mathbf{S}}_2, \tilde{\mathbf{S}}_1\rangle & \frac{1}{n}E\langle\tilde{\mathbf{Y}}, \tilde{\mathbf{S}}_1\rangle \\ \frac{1}{n}E\langle\tilde{\mathbf{S}}_1, \tilde{\mathbf{S}}_2\rangle & \frac{1}{n}E\|\tilde{\mathbf{S}}_1\|^2 & \frac{1}{n}E\langle\tilde{\mathbf{Y}}, \tilde{\mathbf{S}}_2\rangle \\ \frac{1}{n}E\langle\tilde{\mathbf{S}}_1, \tilde{\mathbf{Y}}\rangle & \frac{1}{n}E\langle\tilde{\mathbf{S}}_2, \tilde{\mathbf{Y}}\rangle & \frac{1}{n}E\|\tilde{\mathbf{Y}}\|^2 \end{bmatrix}$$

and

$$\mathbf{c}_i = \begin{bmatrix} \frac{1}{n}E\langle\mathbf{S}_i, \tilde{\mathbf{S}}_1\rangle \\ \frac{1}{n}E\langle\mathbf{S}_i, \tilde{\mathbf{S}}_2\rangle \\ \frac{1}{n}E\langle\mathbf{S}_i, \mathbf{Y}\rangle \end{bmatrix}.$$

For optimal VQ of Gaussian sources, $\mathbf{K}$, $\mathbf{c}_1$ and $\mathbf{c}_2$ can be verified to have the following values [44]:

$$\begin{aligned}
k_{11} &= \sigma^2(1 - 2^{-2R_1}) \\
k_{12} &= k_{21}^* = \sigma^2(1 - 2^{-2R_1})(1 - 2^{-2R_2}) \\
k_{13} &= k_{31}^* = \alpha_2 h_2 \rho 2^{-2R_2} k_{11} \\
k_{22} &= \sigma^2(1 - 2^{-2R_2}) \\
k_{23} &= k_{32}^* = \alpha_1 h_1 \rho 2^{-2R_1} k_{11} \\
k_{33} &= \gamma_1 t_1 P_1 + \gamma_2 t_2 P_2 + 2\mathrm{Re}\{h_1 h_2^*\}\rho_z\sqrt{t_1 t_2 P_1 P_2} + N \\
c_{11} &= k_{11} \\
c_{12} &= \rho k_{22} \\
c_{13} &= (\alpha_1 h_1^* 2^{-2R_1} + \alpha_2 h_2^* \rho 2^{-2R_2})\sigma^2 \\
c_{21} &= \rho k_{22} \\
c_{22} &= k_{22} \\
c_{23} &= (\alpha_1 h_1^* \rho 2^{-2R_1} + \alpha_2 h_2^* 2^{-2R_2})\sigma^2
\end{aligned}$$

Then the optimal MMSE estimator $\mathbf{q}_i$ is given by

$$\mathbf{q}_i = \mathbf{K}^{-1}\mathbf{c}_i, \quad i = 1, 2.$$

The MSE of the optimal estimator reconstructing the source $\mathbf{S}_i$ is

$$D^h_{no_1}(h_1, h_2) = \sigma^2 - q^*_{i,1}c_{i1} - q^*_{i,2}c_{i2} - q^*_{i,3}c_{i3}.$$

The average MMSE for given (R_1, R_2, t_1, t_2) can be found by evaluating

$$D^h_{no}(R_1, R_2, t_1, t_2) = \int_{\mathcal{H}^h_{no}} \frac{D^h_{no_1}(h_1, h_2) + D^h_{no_2}(h_1, h_2)}{2} f(h_1)f(h_2)d\mathbf{h}.$$

Case II: Only one codeword can be decoded successfully

Lets consider the case in which only the codeword $\tilde{\mathbf{X}}_1$ can be decoded correctly. A sufficient condition for decoding $\tilde{\mathbf{X}}_1$ can be obtained by simply considering codeword $\tilde{\mathbf{X}}_2$ as Gaussian interference. When a necessary condition for correct decoding of codeword $\tilde{\mathbf{X}}_2$ given codeword $\tilde{\mathbf{X}}_1$ correctly decoded is false, it provides a sufficient condition to say codeword $\tilde{\mathbf{X}}_2$ cannot be decoded correctly. Following those argument we can write necessary and sufficient conditions to this case as

$$\begin{aligned}(I):\ R_1 &< (X_1; Y) \\ &= \frac{1}{2}\log\left(1 + \frac{\gamma_1(1-t_1)\mu_1}{\gamma_1 t_1\mu_1 + \gamma_2\mu_2 + 2\text{Re}\{h_1h_2^*\}\rho_z\sqrt{t_1t_2\mu_1\mu_2} + 1}\right) \qquad (2.7)\\ (II):\ R_2 &> I(X_2; Y|X_1) \\ &= \frac{1}{2}\log\left(1 + \frac{\gamma_2(1-t_2)\mu_2}{\gamma_1 t_1\mu_1 + \gamma_2 t_2\mu_2 + 2\text{Re}\{h_1h_2^*\}\rho_z\sqrt{t_1t_2\mu_1\mu_2} + 1}\right). \qquad (2.8)\end{aligned}$$

This "partial outage" region $\mathcal{H}^{(2)h}_{po}$, for uncorrelated source, is indicated by ② in Fig. 2.4. The region indicated by ③ is the partial outage region $\mathcal{H}^{(1)h}_{po}$ where only Codeword 2 can be decoded successfully.

Upon decoding $\tilde{\mathbf{X}}_1$, the residual sequence $\tilde{\mathbf{Y}}$ is obtained by computing $\mathbf{Y} - h_1\tilde{\mathbf{X}}_1$, which is given by

$$\tilde{Y}_k = h_1\alpha_1 Z_{1,k} + h_2(\tilde{X}_{2,k} + \alpha_2 Z_{2,k}) + W_k, \quad k = 1, \ldots, n.$$

The optimal estimate of the source sequence is

$$\hat{S}_{i,k} = q_{i,1}\tilde{S}_{1,k} + q_{i,2}\tilde{Y}_k, \quad k = 1, \ldots, n.$$

The linear estimator $q_{i,1}$ and $q_{i,2}$ can be found by solving

$$\underbrace{\begin{bmatrix} k_{11} & k_{12} \\ k_{21} & k_{22} \end{bmatrix}}_{\mathbf{K}} \underbrace{\begin{bmatrix} q_{i,1} \\ q_{i,2} \end{bmatrix}}_{\mathbf{q}_i} = \underbrace{\begin{bmatrix} c_{i1} \\ c_{i2} \end{bmatrix}}_{\mathbf{c}_i},$$

where

$$\mathbf{K} = \begin{bmatrix} \frac{1}{n}E\|\tilde{\mathbf{S}}_1\|^2 & \frac{1}{n}E\langle\tilde{\mathbf{Y}}, \tilde{\mathbf{S}}_1\rangle \\ \frac{1}{n}E\langle\tilde{\mathbf{S}}_1, \tilde{\mathbf{Y}}\rangle & \frac{1}{n}E\|\tilde{\mathbf{Y}}\|^2 \end{bmatrix},$$

and

$$\mathbf{c}_i = \begin{bmatrix} \frac{1}{n}E\langle\mathbf{S}_i, \tilde{\mathbf{S}}_1\rangle \\ \frac{1}{n}E\langle\mathbf{S}_i, \mathbf{Y}\rangle \end{bmatrix}.$$

$\mathbf{K}$, $\mathbf{c}_1$ and $\mathbf{c}_2$ can be verified to have the following values:

$$\begin{aligned}
k_{11} &= \sigma^2(1 - 2^{-2R_1}) \\
k_{12} &= k_{21}^* = \alpha_2 h_2 \rho 2^{-2R_2}(1 - 2^{-2R_1})\sigma^2 \\
k_{22} &= \gamma_1 t_1 P_1 + \gamma_2 P_2 + 2\text{Re}\{h_1 h_2^*\}\rho_z\sqrt{t_1 t_2 P_1 P_2} + N \\
c_{11} &= k_{11} \\
c_{12} &= (\alpha_1 h_1^* 2^{-2R_1} + \alpha_2 h_2^* \rho 2^{-2R_2})\sigma^2 \\
c_{21} &= \rho\sigma^2(1 - 2^{-2R_1}) \\
c_{22} &= (\alpha_1 h_1^* \rho 2^{-2R_1} + \alpha_2 h_2^* 2^{-2R_2})\sigma^2
\end{aligned}$$

The optimal MMSE estimator $\mathbf{q}_i$ is given by $\mathbf{q}_i = \mathbf{K}^{-1}\mathbf{c}_i, \quad i = 1, 2$. The MSE of the optimal estimator reconstructing the source $\mathbf{S}_i$ is

$$D_{po_i}^{(2)h}(h_1, h_2) = \sigma^2 - q_{i,1}^* c_{i1} - q_{i,2}^* c_{i2}.$$

The average MMSE for given (R_1, R_2, t_1, t_2) can be found by evaluating

$$D^{(2)h}(R_1, R_2, t_1, t_2) = \int_{\mathcal{H}_{po}^{(1)h}} \frac{D_{no_1}^h(h_1, h_2) + D_{no_2}^h(h_1, h_2)}{2} f(h_1) f(h_2) d\mathbf{h}.$$

Similarly, the average MSE $D^{(1)h}(R_1, R_2, t_1, t_2)$ corresponding to the case where only codeword 2 can be decoded can be calculated.

Case III: Either of the codewords can not be decoded successfully

A "total-outage" of the digital transmission occurs when neither of the digital codewords can be decoded correctly in the given channel state. The rate region for this scenario can be obtained by excluding the union of the three rate regions in the no-outage and the partial-outage cases. Then it follows that the necessary and sufficient conditions for the total-outage are

$$\begin{aligned}
(I):\ R_1 &> I(\tilde{X}_1; Y) \\
&= \frac{1}{2}\log\left(1 + \frac{\gamma_1(1-t_1)\mu_1}{\gamma_1 t_1\mu_1 + \gamma_2\mu_2 + 2\mathrm{Re}\{h_1 h_2^*\}\rho_z\sqrt{t_1 t_2\mu_1\mu_2} + 1}\right) \qquad (2.9) \\
(II):\ R_2 &> I(\tilde{X}_2; Y) \\
&= \frac{1}{2}\log\left(1 + \frac{\gamma_2(1-t_2)\mu_2}{\gamma_1\mu_1 + \gamma_2 t_2\mu_2 + 2\mathrm{Re}\{h_1 h_2^*\}\rho_z\sqrt{t_1 t_2\mu_1\mu_2} + 1}\right) \qquad (2.10) \\
(III):\ R_1 + R_2 &> I(\tilde{X}_1, \tilde{X}_2; Y) \\
&= \frac{1}{2}\log\left(1 + \frac{\gamma_1(1-t_1)\mu_1 + \gamma_2(1-t_2)\mu_2}{\gamma_1 t_1\mu_1 + \gamma_2 t_2\mu_2 + 2\mathrm{Re}\{h_1 h_2^*\}\rho_z\sqrt{t_1 t_2\mu_1\mu_2} + 1}\right). \qquad (2.11)
\end{aligned}$$

The total-outage region $\mathcal{H}_{to}^h$, for uncorrelated sources, is indicated by ④ in Fig. 2.4. The optimal estimate of the source sequence is computed based on the MAC output $\mathbf{Y}$

$$\hat{S}_{i,k} = q_i Y_k, \quad k = 1, \ldots, n.$$

The optimal MSE estimate of source $\mathbf{S}_i$ is given by

$$\hat{S}_{i,k} = q_i Y_k, \quad k = 1, \ldots, n,$$

where q_i is the optimal estimator, given by

$$\begin{aligned} q_1 &= \frac{\frac{1}{n}E\langle \mathbf{S}_1, \mathbf{Y}\rangle}{\frac{1}{n}\|\mathbf{Y}^2\|} \\ &= \frac{(\alpha_1 h_1^* 2^{-2R_1} + \alpha_2 h_2^* \rho 2^{-2R_2})\sigma^2}{\gamma_1 P_1 + \gamma_2 P_2 + 2\mathrm{Re}\{h_1 h_2^*\}\rho_z\sqrt{t_1 t_2 P_1 P_2} + N} \\ q_2 &= \frac{\frac{1}{n}E\langle \mathbf{S}_2, \mathbf{Y}\rangle}{\frac{1}{n}\|\mathbf{Y}^2\|} \\ &= \frac{(\alpha_1 h_1^* \rho 2^{-2R_1} + \alpha_2 h_2^* 2^{-2R_2})\sigma^2}{\gamma_1 P_1 + \gamma_2 P_2 + 2\mathrm{Re}\{h_1 h_2^*\}\rho_z\sqrt{t_1 t_2 P_1 P_2} + N}. \end{aligned}$$

The corresponding MSE values of the optimal estimators are

$$\begin{aligned} D^h_{to_1}(h_1, h_2) &= \sigma^2 - \frac{|(\alpha_1 h_1^* 2^{-2R_1} + \alpha_2 h_2^* \rho 2^{-2R_2})\sigma^2|^2}{\gamma_1 P_1 + \gamma_2 P_2 + 2\mathrm{Re}\{h_1 h_2^*\}\rho_z\sqrt{t_1 t_2 P_1 P_2} + N} \\ D^h_{to_2}(h_1, h_2) &= \sigma^2 - \frac{|(\alpha_1 h_1^* \rho 2^{-2R_1} + \alpha_2 h_2^* 2^{-2R_2})\sigma^2|^2}{\gamma_1 P_1 + \gamma_2 P_2 + 2\mathrm{Re}\{h_1 h_2^*\}\rho_z\sqrt{t_1 t_2 P_1 P_2} + N}. \end{aligned}$$

The average MMSE for given (R_1, R_2, t_1, t_2) can be found by evaluating

$$D^h_{to}(R_1, R_2, t_1, t_2) = \int_{\mathcal{H}^h_{to}} \frac{D^h_{o_1}(h_1, h_2) + D^h_{o_2}(h_1, h_2)}{2} f(h_1) f(h_2) d\mathbf{h}.$$

The optimal encoder parameters (R_1, R_2, t_1, t_2) and the achievable average MMSE is found by solving

$$\begin{aligned} D^{HDA} = \min_{R_1, R_2, t_1, t_2} & D^h_{no}(R_1, R_2, t_1, t_2) + D^{(1)h}(R_1, R_2, t_1, t_2) \\ & + D^{(2)h}(R_1, R_2, t_1, t_2) + D^h_o(R_1, R_2, t_1, t_2). \end{aligned} \tag{2.12}$$

The solution to the above optimization problem can be numerically evaluated using a global optimization tool. This gives us a computable upper bound to the MMSE achievable in communicating correlated Gaussian sources over a BF-GMAC.

In Sections 2.4-2.7 to follow, we derive the MMSE of several other coding schemes which can be used as benchmarks for the upper bound we established above.

2.4 HDA Coding over Orthogonal MAC

In the HDA coding in section 2.3 channel inputs to the two-to-one MAC, analog data from both transmitters interfere the digital coding, and therefore the additional interference due to the analog data reduces the effective channel capacity. Furthermore, when a codeword is in outage, the non decodable codeword acts as interference to the analog data. Another useful benchmark can be derived by considering a simple HDA scheme where analog and digital components in a non-interfering manner by orthogonalizing the BF-GMAC. However the disadvantage of this scheme is the number of channel uses available for sending a source sample decreases.

The two-to-one MAC is used as two point-to-point channels by splitting the number of channel uses between the two transmitters. Assume that the transmitter i ($i \in \{1, 2\}$) transmits n_i channel symbols over n channel access time-shared between the two transmitters, i.e., $n = n_1 + n_2$. In the digital part of the encoder optimal VQ at rate $r_i R_i$ is applied to the source block $\mathbf{S}_i \in \mathbb{C}^n$, where $r_i = n_i/n$. The VQ output $I_i \in \{1, 2, \ldots, 2^{n_i R_i}\}$ is mapped to digital channel codeword $\tilde{\mathbf{X}}_i \in \mathbb{C}^{n_i}$. In the analog part, VQ error vector $\mathbf{Z}_i$ is obtained and split into two blocks, i.e., $\mathbf{Z}_i = (\mathbf{Z}_i^{(1)}, \mathbf{Z}_i^{(2)})$, where $\mathbf{S}_i^{(1)} \in \mathbb{C}^{n_1}$ and $\mathbf{Z}_i^{(2)} \in \mathbb{C}^{n_2}$ are blocks with length n_1 and n_2, respectively. Transmitter i transmits the $\mathbf{Z}_i^{(i)}$ superimposed with the digital codeword. At the joint decoder, the digital codeword is recovered if it can be decoded error-free (no-outage). Then the VQ error sequence is estimated from the channel output, after canceling the interference due to the digital codeword. The corresponding part of the source sequence is reconstructed by adding the VQ error sequence to the decoded digital codeword. Now we explain the computation of the average MSE by considering outage events for the digital codewords.

The necessary and sufficient condition for the successful decodability of each digital codeword is given by the channel capacity of the AWGN channel, i.e.,

$$R_i < \frac{1}{2}\log\left(1 + \frac{\frac{\mu_i}{r_i}(1 - t_i)\gamma_i}{\frac{\mu_i}{r_i}t_i\gamma_i + 1}\right).$$

Given rate R_i, power allocation ratio t_i and bandwidth ratio r_i, decoding can be done successfully, if and only if $\gamma_i > \bar{\gamma}_i$, where $\bar{\gamma}_i$ is given by

$$\bar{\gamma}_i = \frac{r_i}{\mu_i}\left(\frac{2^{2R_i}}{1 - t_i 2^{2R_i}}\right).$$

We can now obtain the average distortion as shown below.

Case I: The codeword can be decoded successfully

Consider when $\gamma_i > \bar{\gamma}_i$, i.e., when the codeword can be successfully decoded. Source block $\mathbf{S}_i^{(i)}$ of source $\mathbf{S}_i$ is reconstructed as follows.

$$\hat{S}_{i,k} = \tilde{S}_{i,k} + \hat{Z}_{i,k}, \forall S_{i,k} \in \mathbf{S}_i^{(i)}.$$

The end-end-end MSE in reconstructing $\mathbf{S}_i^{(i)}$ is given by

$$D_{no_i,i}^{(ortho)}(\gamma) = \frac{1}{t_i \frac{\mu_i}{r_i}\gamma_i + 1}\sigma_{Z_o,i}^2,$$

where $\sigma_{Z_o,i}^2 = 2^{-2r_1R_1}\sigma^2$. The end-to-end MSE in reconstructing $\mathbf{S}_i^{(j)}$, $j \neq i$ is simply $D_{no_2}^{(ortho)}(\gamma) = \sigma_{Z_o,i}^2$. The average MSE for this case can be evaluated as

$$D_{no,i}^{(ortho)}(R_i, t_i, r_i) = \int_{\bar{\gamma}}^{\infty} \frac{1}{2}\left(D_{no_i,i}^{(ortho)}(\gamma) + D_{no_j,i}^{(ortho)}(\gamma)\right) f(\gamma_i) d\gamma, \quad i \in \{1,2\}, j \neq i,$$

where $f(\gamma_i)$ is the pdf of the fading gain power.

Case II: The codeword can not be decoded successfully

Consider when $\gamma_i < \bar{\gamma}_i$, i.e., when the codeword cannot be successfully decoded. Source block $\mathbf{S}_i^{(i)}$ of source $\mathbf{S}_i$ is reconstructed as

$$\hat{S}_{i,k} = \hat{Z}_{i,k}, \forall S_{i,k} \notin \mathbf{S}_i^{(i)},$$

and the resulting MSE in reconstructing $\mathbf{S}_i^{(i)}$ is given by

$$D_{o_i,i}^{(ortho)}(\gamma) = \left(1 - 2^{-2r_iR_i}\right)\sigma^2 + \frac{(1-t_i)\frac{\mu_i}{r_i}\gamma_i + 1}{\frac{\mu_i}{r_i}\gamma_i + 1}\sigma_{Z_o,i}^2.$$

The end-to-end MSE in reconstructing $\mathbf{S}_i^{(j)}$, $j \neq i$ is simply the source variance, i.e., $D_{o_j,i}^{(ortho)}(\gamma) = \sigma^2$. Therefore the average MSE, when the digital transmission is in outage, is

$$D_{o,i}^{(ortho)}(R_i, t_i, r_i) = \int_0^{\bar{\gamma}} \frac{1}{2}\left(D_{o_i,i}^{(ortho)}(\gamma) + D_{o_j,i}^{(ortho)}(\gamma)\right) f(\gamma) d\gamma_i \quad i \in \{1,2\}, j \neq i.$$

The minimum achievable MSE cab be obtained by minimizing the overall MSE with respect to the transmission rate R_i, power allocation ratio t_i and the channel splitting ration r_i, i.e.,

$$D^{(ortho)} = \min_{R_1,R_2,t_1,t_2,r_1,r_2} \sum_{i=1}^{2} D_{no,i}^{(ortho)}(R_i, t_i, r_i) + D_{o,i}^{(ortho)}(R_i, t_i, r_i).$$

2.5 Separate Source-Channel Coding

As a benchmark we now consider the source-channel separation (SCS) approach which ignores any correlation between GMAC inputs. In [47], the rate pairs corresponding to different outage events for digital channel codes over BF-MAC are computed. The corresponding outage regions can be obtained by letting $t_i = 0$, $i = 1, 2$ in the HDA coding described in Section 2.3. The (γ_1, γ_2) regions corresponding to the outage events in separate source-channel (SSC) coding is depicted in Fig. 2.5. The average distortion of reconstructing S_1 and S_2 in each outage scenario is calculated as follows.

Case I: Both codewords can be decoded correctly

The corresponding necessary and sufficient conditions can be obtained by simply letting $t_i = 0$, $i = 1, 2$ in (2.4)-(2.6). The probability of no-outage (P_{no}) can be calculated by

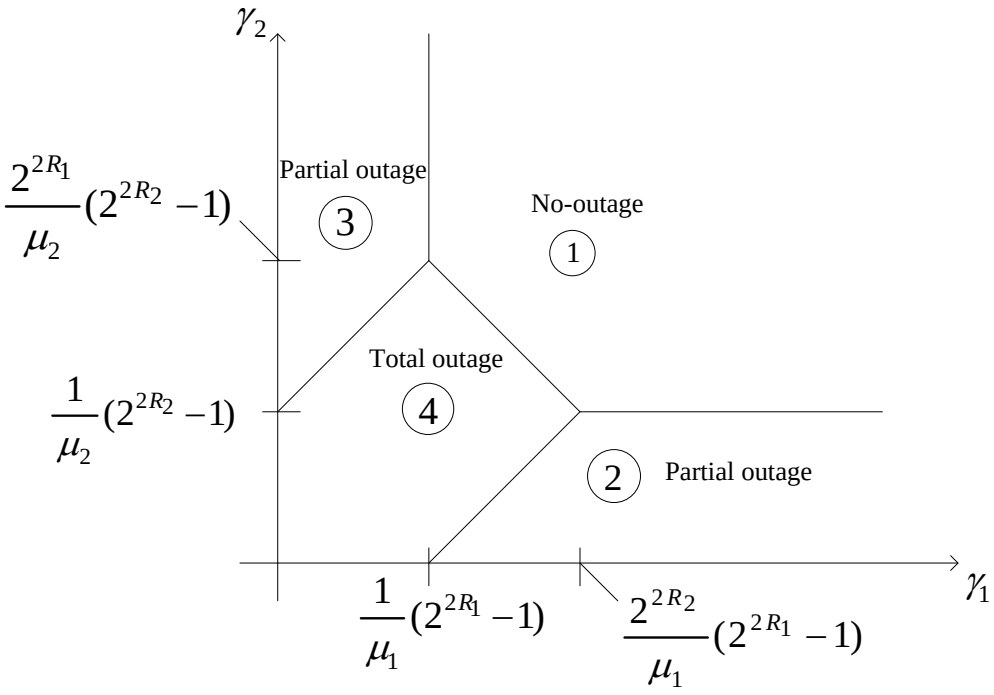

Figure 2.5: Individual outage regions for conventional source-channel separation coding.

evaluating the following integral

$$P_{no} \stackrel{\Delta}{=} \int_{\mathcal{H}_{no}} f(\gamma_1, \gamma_2) d\gamma_1 d\gamma_2,$$

where $\mathcal{H}_{no}^{\lceil}$ denote the no-outage region which is indicated by ① in Figure 2.5. An explicit expression for the probability of no-outage for the case of Rayleigh fading can be computed as follows:

$$\begin{aligned}
P_{no} = & \int_{\frac{1}{\mu_2}(2^{2R_2}-1)}^{\infty} \int_{\frac{2^{2R_2}}{\mu_1}(2^{2R_1}-1)}^{\infty} e^{-(\gamma_1+\gamma_2)} d\gamma_1\gamma_2 + \\
& \int_{\frac{1}{\mu_1}(2^{2R_2}-1)}^{\frac{2^{2R_2}}{\mu_1}(2^{2R_1}-1)} \int_{\frac{1}{\mu_2}(2^{2(R_1+R_2)}-1-\mu_1\gamma_1)}^{\infty} e^{-(\gamma_1+\gamma_2)} d\gamma_1\gamma_2 \\
= & \, e^{-\frac{2^{2R_2}}{\mu_1}(2^{2R_1}-1)} + \int_{\frac{1}{\mu_1}(2^{2R_2}-1)}^{\frac{2^{2R_2}}{\mu_1}(2^{2R_1}-1)} e^{-(1-\frac{\mu_1}{\mu_2})\gamma_1} e^{-\frac{1}{\mu_2}(2^{2(R_1+R_2)}-1)} d\gamma_1 \\
= & \, e^{-\frac{1}{\mu_2}(2^{2(R_1+R_2)}-1)} \left\{ e^{-\frac{(\mu_2-\mu_1)2^{2R_1}(2^{2R2}-1)}{\mu_2^2}} - e^{-\frac{(\mu_2-\mu_1)(2^{2R_1}-1)}{\mu_1\mu_2}} \right\} +
\end{aligned}$$

$$e^{-(2^{2R_2}-1)(\frac{1}{\mu_2}+\frac{2^{2R_1}}{\mu_1})}. \tag{2.13}$$

The average reconstruction distortion given that both channel codewords are decoded correctly is

$$D_{no} = \frac{(2^{-2R_1} + 2^{-2R_2})\sigma^2}{2}.$$

Case II: Only one codeword can be decoded correctly

Consider channel codeword $\mathbf{X}_1$ can be decoded correctly while channel codeword $\mathbf{X}_2$ cannot be decoded correctly. Necessary and sufficient conditions for this case can be obtained by letting $t_i = 0$, $i = 1, 2$, in (2.7) and (2.8). Then the probability of no-outage ($P_{po}^{(1)}$) can be calculated by evaluating the following integral

$$P_{po}^{(1)} \triangleq \int_{\mathcal{H}_{po}^{(1)}} f(\gamma_1, \gamma_2) d\gamma_1 d\gamma_2,$$

where $\mathcal{H}_{po}^{(1)}$ denote the partial-outage region which is indicated by ② in Figure 2.5. The probability of this outage scenario ($P_{no}^{(1)}$) can be computed as follows:

$$\begin{aligned} P_{no}^{(1)} &= \int_0^{\frac{1}{\mu_2}(2^{2R_2}-1)} \int_{\frac{1}{\mu_1}(2^{2R_1}-1)(\mu_2\gamma_2+1)}^{\infty} e^{-(\gamma_1+\gamma_2)} d\gamma_1 d\gamma_2 \\ &= e^{\frac{1}{\mu_1}(2^{2R_1}-1)} \int_0^{\frac{1}{\mu_2}(2^{2R_2}-1)} e^{(\frac{\mu_2}{\mu_1}(2^{2R_1}-1)-1)\gamma_2} d\gamma_2 \\ &= e^{-\frac{2R_1(2^{2R_2}-1)}{\mu_1}} \left\{ 1 - e^{-\frac{(2^{2R_1}-1)}{\mu_2}} \right\}. \end{aligned}$$

Since $\mathbf{X}_1$ can be decoded correctly while $\mathbf{X}_2$ cannot be decoded correctly, the average distortion of reconstructing S_1 and S_2 are equal to $2^{-2R_1}\sigma^2$ and σ^2, respectively. Therefore, the average distortion in this case ($D_{no}^{(1)}$) is given by

$$D_{no}^{(1)} = \frac{(1 + 2^{-2R_1})\sigma^2}{2}.$$

Similarly, the probability of partial-outage, when only the channel codeword $\mathbf{X}_2$ can be decoded correctly ($P_{po}^{(1)}$), can be found by calculating the integral

$$P_{po}^{(1)} \triangleq \int_{\mathcal{H}_{po}^{(1)}} f(\gamma_1, \gamma_2) d\gamma_1 d\gamma_2,$$

where $\mathcal{H}_{po}^{(2)}$ denote the partial-outage region which is indicated by ③ in Figure 2.5. The probability of this outage scenario ($P_{no}^{(2)}$) can be computed as follows:

$$\begin{aligned} P_{no}^{(2)} &= \int_0^{\frac{1}{\mu_1}(2^{2R_1}-1)} \int_{\frac{1}{\mu_2}(2^{2R_2}-1)(\mu_1\gamma_1+1)}^{\infty} e^{-(\gamma_1+\gamma_2)} d\gamma_2 d\gamma_1 \\ &= e^{\frac{1}{\mu_2}(2^{2R_2}-1)} \int_0^{\frac{1}{\mu_1}(2^{2R_1}-1)} e^{(\frac{\mu_1}{\mu_2}(2^{2R_2}-1)-1)\gamma_1} d\gamma_1 \\ P_{no}^{(2)} &= e^{-\frac{2R_2(2^{2R_1}-1)}{\mu_2}} \left\{ 1 - e^{-\frac{(2^{2R_2}-1)}{\mu_1}} \right\}. \end{aligned}$$

The average distortion in this case ($D_{no}^{(2)}$) is given by

$$D_{no}^{(2)} = \frac{(1+2^{-2R_2})\sigma^2}{2}.$$

Case III: Neither of the codewords can be decoded successfully

The corresponding necessary and sufficient conditions for this case can be obtained by letting $t_i = 0, i = 1, 2$ in (2.9)-(2.11). Since the three outage scenarios are mutually exclusive, the probability of total-outage (P_{no}) can be computed from

$$P_{to} = 1 - (P_{no} + P_{po}^{(1)} + P_{po}^{(2)}).$$

The average reconstruction distortion in this case (D_{to}) is equal to the source variance, i.e.,

$$D_{to} = \sigma^2.$$

Therefore, the average reconstruction distortion over the fading distribution is

$$D^{SSC}(R_1, R_2) = P_{no} D_{no} + P_{po}^{(1)} D_{po}^{(1)} + P_{po}^{(2)} D_{po}^{(2)} + P_{to} D_{to}.$$

The optimal transmitter rates (R_1^0, R_2^0) and the corresponding minimum achievable MSE is

found by solving the minimization problem:

$$D^{SSC}(R_1^0, R_2^0) = \min_{R_1, R_2} D^{SSC}(R_1, R_2). \tag{2.14}$$

The problem stated in (2.14) can be solved numerically using a global optimization tool.

2.6 Distributed VQ Combined with Channel Coding

In Section 2.5, we described a SSC coding scheme as a benchmark for our problem. In this section, we describe source-channel separation approach which can achieve a lower MMSE. The distortion pairs that are achievable for sending correlated sources over the fixed GMAC by combining the optimal distributed VQ coding with the optimal channel coding is discussed in [44]. In our problem setup, we can approach source-channel separation through two coding strategies. First, by combining the distributed VQ of the sources with the channel coding over the block-fading MAC. The other strategy is to simply to ignore source correlation and encode the sources independently using an optimal VQ followed by channel coding. This was the approach used in Section 2.5. Note that, for given source-channel coding rates, while the achievable distortion region due to optimal distributed VQ is a lower bound to the achievable distortion region due to non-distributed VQ, the optimal distributed VQ requires both VQ indexes to be recovered at the receiver. However, the source reconstruction in non-distributed VQ is performed independently. Therefore, the average performance of the source-channel separation coding with distributed source VQ which takes advantage of source correlation is not necessarily superior to the average performance of the source-channel separation coding with non-distributed VQ which ignores source correlation. Below, we determine the minimum achievable MMSE of distributed VQ-based SSC scheme. Assuming that channel codewords are decoded error free, the achievable distortion regions for given coding rates R_1 and R_2 can be deduced from the rate-distortion region of the distributed source coding problem for a bivariate Gaussian source [33]. Below, we use this result to determine the average MSE of the SSC coding

scheme over the BF-GMAC.

For given coding rates $R_1 > 0$ and $R_2 > 0$, a distortion-pair (D_1, D_2) is achievable, if and only if

$$(D_1, D_2) \in \mathcal{D}_1(R_1, R_2) \cap \mathcal{D}_2(R_1, R_2) \cap \mathcal{D}_{\text{prod}}(R_1, R_2)$$

where

$$\begin{aligned}
\mathcal{D}_1(R_1, R_2) &= \left\{ D_1 : D_1 \geq \Delta_1 \text{ and } D_1 \leq \sigma^2 \right\} \\
\mathcal{D}_2(R_1, R_2) &= \left\{ D_2 : D_2 \geq \Delta_1 \text{ and } D_2 \leq \sigma^2 \right\} \\
\mathcal{D}_{\text{prod}}(R_1, R_2) &= \left\{ (D_1, D_2) : D_1 D_2 \geq \Delta_{12} \right\},
\end{aligned}$$

with

$$\begin{aligned}
\Delta_1 &= \sigma^2 2^{-2R_1}(1 - \rho^2(1 - 2^{-2R_2})) \\
\Delta_2 &= \sigma^2 2^{-2R_2}(1 - \rho^2(1 - 2^{-2R_1})) \\
\Delta_{12} &= \sigma^4 \left[(1 - \rho^2) 2^{-2(R_1 + R_2)} + \rho^2 2^{-4(R_1 + R_2)} \right].
\end{aligned}$$

The problem is to find the minimum $(D_1 + D_2)$ subject to the above constraints for the achievable distortion region for given (R_1, R_2) and ρ. Let $D_1 + D_2 = \delta_s$, where $\delta_s > 0$, is a line connecting $(\delta_s, 0)$ and $(0, \delta_s)$ on the (D_1, D_2) plane. Note that for given $D_i, i = 1, 2$, the corresponding achievable minimum $D_j, j \neq i$ lies on the boundary of the achievable distortion region. Therefore the achievable MMSE is found when at least one of the above constraint is satisfied with equality. This will result in three different scenarios to be considered to determine the MMSE for given rate-pair, as illustrated in Figure 2.6.

Case I:

Assume line $D_1 + D_2 = d_s$ just touches the curve defined by $D_1 D_2 = \Delta_{12}$ while the point at which they satisfies the other two constraints (see Figure 2.6 (b)). Since $D_1 D_2 = \Delta_{12}$, $\Delta_{12} > 0$, is symmetrical about the line $D_1 = D_2$, line $D_1 + D_2 = d_s$ just touches

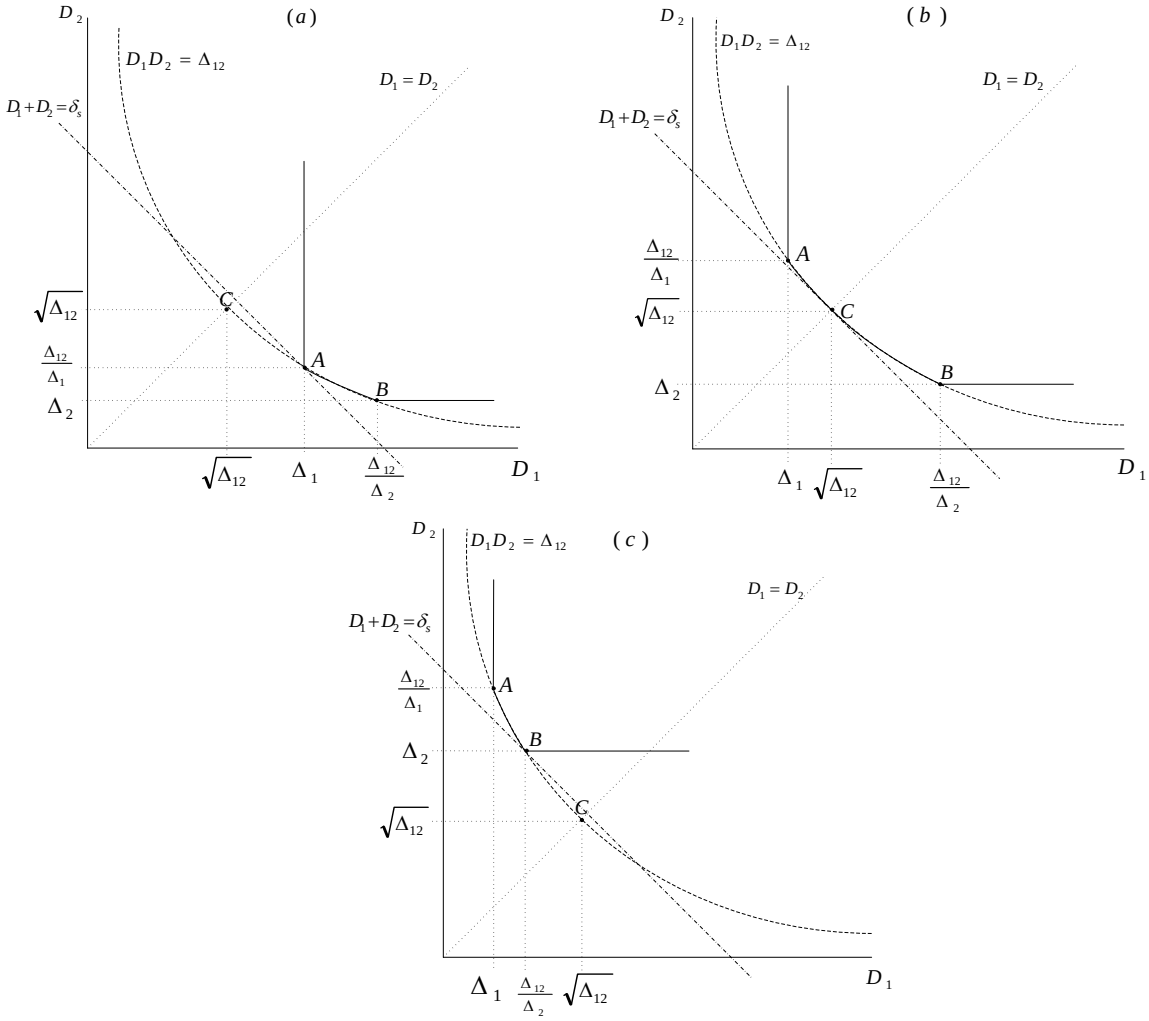

Figure 2.6: Distortion pairs achievable in distributed VQ of two correlated Gaussian sources at a fixed rate pair (R_1, R_2).

$D_1D_2 = \Delta_{12}$ when $D_1 = D_2$. Therefore, the minimum distortion is given by

$$D^* = \sqrt{\Delta_{12}}.$$

Case II:

Assume, when line $D_1 + D_2 = \delta_s$ just touches the curve defined by $D_1D_2 = \Delta_{12}$ while the point at which the distortion pair satisfies the constraint defined by $\mathcal{D}_2(R_1, R_2)$ (i.e., $D_2 \geq \Delta_2$), it does not satisfy the constraint defined by $\mathcal{D}_1(R_1, R_2)$ (i.e., $D_1 < \Delta_1$). In this

case, in order to find the achievable MMSE $(D_1 + D_2)/2$, δ_s must be increased until line $D_1 + D_2 = \delta_s$ touches the intersection of curve $D_1 D_2 = \Delta_{12}$ and line $D_1 = \Delta_1$ (see Figure 2.6 (a)). The achievable D_1 and D_2, so that $D_1 + D_2$ is minimized, is given by

$$D_1^* = \Delta_1$$
$$D_2^* = \frac{\Delta_{12}}{\Delta_1}.$$

The resulting MMSE is $D^* = (D_1^* + D_2^*)/2$.

Case III:

The remaining case is when line $D_1 + D_2 = \delta_s$ just touches the curve defined by $D_1 D_2 = \Delta_{12}$ while the point at which they touch satisfies the constraint defined by $\mathcal{D}_1(R_1, R_2)$ (i.e., $D_1 \geq \Delta_1$), it does not satisfy the constraint defined by $\mathcal{D}_2(R_1, R_2)$ (i.e., $D_2 \leq \Delta_2$). In order to find the achievable MMSE $(D_1 + D_2)/2$, δ_s should be further increased until line $D_1 + D_2 = \delta_s$ touches the intersection of curve $D_1 D_2 = \Delta_{12}$ and line $D_2 = \Delta_2$ (see Figure 2.6 (c)). The achievable D_1 and D_2, so that $D_1 + D_2$ is minimized, is given by

$$D_2^* = \Delta_2$$
$$D_1^* = \frac{\Delta_{12}}{\Delta_2}.$$

The resulting MMSE is $D^* = (D_1^* + D_2^*)/2$.

Finding the optimum encoding rates

Recall that the above MSE is computed assuming both channel codewords are correctly decoded at the receiver. Therefore with transmitters transmit at rates R_1 and R_2 with correct decoding, the achievable MMSE (D^*) is determined by one the above three cases. Let $D_{no.dVQ}$ is the distortion corresponding to the no-outage case. Then, the average distortion is given by

$$D_{min}(R_1, R_2) = D_{no.dVQ} P_{no} + \sigma^2 (1 - P_{no}),$$

where P_{no} is the probability of decoding both codewords correctly (for given R_1 and R_2), which is given by (2.13). The minimum average distortion and the optimum encoding rates

are computed by minimizing $D_{min}(R_1, R_2)$ with respect to R_1 and R_2. It is difficult to establish the convexity of this minimization problem. Therefore, we use numerical optimization to find the optimum transmission rates and the corresponding MMSE.

2.7 Uncoded Transmission

In the relation to sending correlated Gaussian sources over fixed GMAC, [44] proves that the uncoded transmission is optimal when the transmitter powers, noise variance, and the correlation coefficient satisfy a certain condition. In particular, in the symmetrical case, for given source correlation the uncoded transmission is optimal below a certain power-to-noise ratio value. However, when the channel varies, such optimality is unlikely. Below, we determine the minimum achievable MMSE of this scheme for the BF-GMAC.

At each transmitter, the channel input symbols are generated by scaling the source symbols so that the average power constraint of the channel input sequence is satisfied with equality. That is

$$X_{i,k} = \sqrt{\frac{P_i}{\sigma^2}} S_{i,k}, \quad k \in \{1, 2, \ldots, n\}.$$

Based on the resulting channel output Y_k, the decoder then compute the MMSE estimate $\hat{S}_{i,k}$ of the source symbol $S_{i,k}$. That is

$$\hat{S}_{i,k} = \mathrm{E}[S_{i,k}|Y_k], \quad k \in \{1, 2, \ldots, n\}.$$

Note that, since the channel output Y_k and the source symbol $S_{i,k}$ are jointly Gaussian, the MMSE estimator is linear. Then the MMSE estimate of $S_{i,k}$ can be written as

$$\hat{S}_{i,k} = A_i Y_k, \quad k \in \{1, 2, \ldots, n\},$$

where $A_i \in \mathbb{C}$ denotes the linear MMSE estimator of $S_{i,k}$, and can be found evaluating

$$A_i = \frac{\mathrm{E}[S_{i,k} Y_k^*]}{\mathrm{E}[|Y_k|^2]}, \quad k \in \{1, 2, \ldots, n\},$$

where Y_k^* is the complex conjugate of the Y_k. Note that A_i is constant over one block of transmission since the fading gains remain unchanged during the transmission, and $S_{i,k}$ and Y_k are iid. sequence of random symbols. The corresponding MMSE error is given by

$$D_i(\gamma_1, \gamma_2) = \mathrm{E}[|S_{i,k}|^2] - \frac{|\mathrm{E}[S_{i,k}Y_k^*]|^2}{\mathrm{E}[|Y_k|^2]}, \quad k \in \{1, 2, \ldots, n\}.$$

The MMSE in estimating $S_{1,k}$ is evaluated as

$$\begin{aligned} D_1(\gamma_1, \gamma_2) &= \sigma^2 - \sigma^2 \frac{\gamma_1 P_1 + \rho^2 \gamma_2 P_2 + 2\rho \mathrm{Re}\{h_1 h_2^*\}\sqrt{P_1 P_2}}{\gamma_1 P_1 + \gamma_2 P_2 + 2\rho \mathrm{Re}\{h_1 h_2^*\}\sqrt{P_1 P_2} + N} \\ &= \sigma^2 \frac{(1-\rho^2)\gamma_2 P_2 + N}{\gamma_1 P_1 + \gamma_2 P_2 + 2\rho \mathrm{Re}\{h_1 h_2^*\}\sqrt{P_1 P_2} + N}. \end{aligned}$$

Similarly, the MMSE in estimating $S_{2,k}$ can be computed, and is given by

$$D_2(\gamma_1, \gamma_2) = \sigma^2 \frac{(1-\rho^2)\gamma_1 P_1 + N}{\gamma_1 P_1 + \gamma_2 P_2 + 2\rho \mathrm{Re}\{h_1 h_2^*\}\sqrt{P_1 P_2} + N}$$

The average expected distortion (D) can be computed by evaluating

$$D = \int_{(\gamma_1, \gamma_2) \in \mathbb{R}^+ \times \mathbb{R}^+} \frac{D_1(\gamma_1, \gamma_2) + D_2(\gamma_1, \gamma_2)}{2} f(\gamma_1, \gamma_2) d\gamma_1 d\gamma_2.$$

We can further simplify this expression for the special case $P_1 = P_2$, and $\rho = 0$. For this case, given that fading follows the Rayleigh distribution, we can obtain

$$D^U = \sigma^2 e^{\frac{1}{\mu}} \left[\left(1 + \frac{1}{\mu}\right) e^{-\frac{1}{\mu}} - \frac{1}{\mu^2} E_1\left(\frac{1}{\mu}\right) \right],$$

where $\mu = P_1/N (= P_2/N)$, where $E_1(x)$ is the exponential integral defined by

$$E_1(x) = \int_x^\infty \frac{e^{-t}}{t} dt, \quad x > 0.$$

2.8 Numerical Results and Discussion

In this section, we compare the MMSE upper bound derived in Section 2.3 using superposition-based HDA coding with other bench mark bounds. The MMSE is evaluated over the independent Rayleigh fading MAC with $E\{\gamma_i\} = 1$, $i \in \{1, 2\}$. We use a global optimization

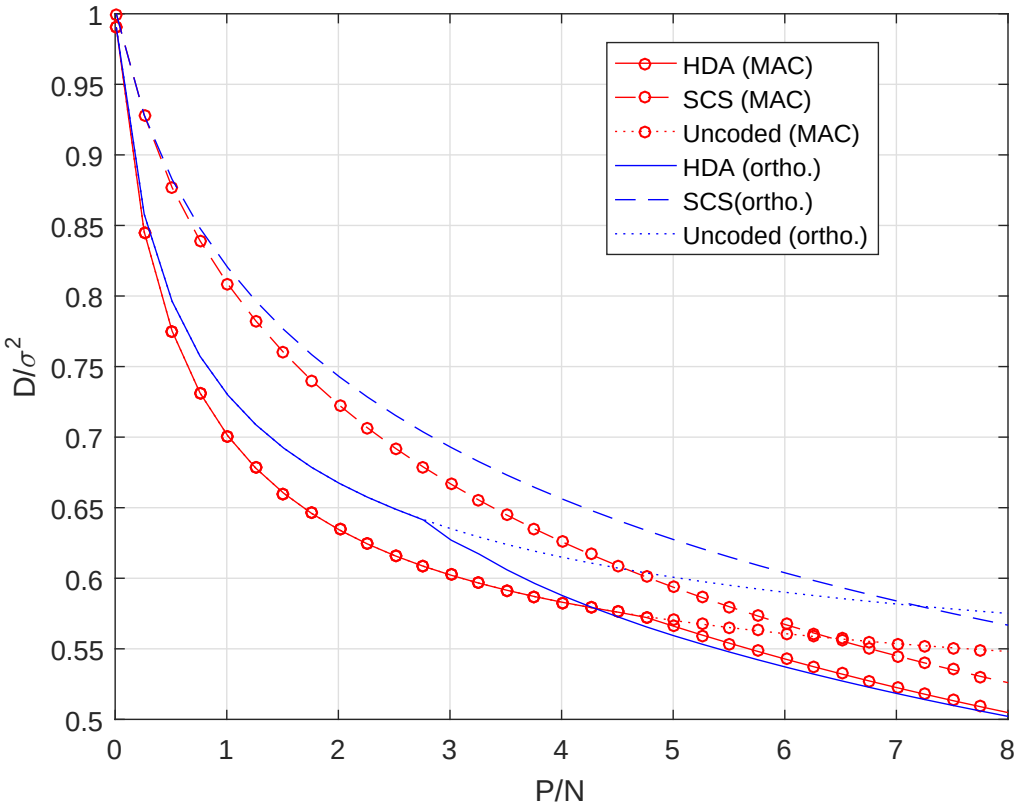

Figure 2.7: Performance comparison for sending uncorrelated sources over Rayleigh BF-MAC.

tool in Matlab to to evaluate all MMSE bounds. Fig. 2.7 shows the performance of the HDA coding, the SSC coding, and the uncoded schemes, for sending uncorrelated ($\rho = 0$) Gaussian sources over both the two-to-one MAC (MAC) and the orthogonal MAC (ortho.).

The performance of the uncoded transmission is significantly better compared to separation-based approach for a range of low P/N values (1-3). However, as the P/N increases the performance of the uncoded scheme levels off as $P/N \to \infty$. In uncoded transmission, the channel inputs by one transmitter act as independent noise to the other transmitter. In the symmetric ($P_1 = P_2$) case the average distortion of the uncoded scheme approaches $\sigma^2/2$. The HDA scheme outperforms both the uncoded scheme and the separation-based approach after some P/N value. Below this P/N value, the HDA scheme operates as an uncoded scheme, i.e., $t = 1$. As P/N increases, the performance of the HDA scheme and the performance of the separation-based approach converge as the uncoded approach

is significantly outperformed by the separation-based approach. A similar observation can be made regarding the orthogonal MAC case as well.

The performance of the HDA scheme based on orthogonal channel access HDA (ortho.) is slightly better than the HDA (MAC) in the P/N range of $5 - 10$. This is due to the fact that in the two-to-one MAC case, when P/N is low, the probability of either of the transmitters being in outage is higher than the probability of one transmitter being in outage in the orthogonal MAC case. Therefore, there is a higher level of noise for the analog transmission in the two-to-one MAC. However, the HDA (MAC) scheme outperforms the HDA (ortho.) scheme as P/N increases. For instance, at $P/N = 20$, D/σ^2 values of the HDA (MAC) and the HDA (ortho.) schemes are 0.3859 and 0.3948, respectively. The no-outage region of the HDA (MAC) scheme becomes relatively dominant for larger P/N values. The performance of HDA coding as a function CSNR for correlated sources will be discussed in Chapter 3.

Fig. 2.8 compares the performance of various coding schemes for different values of the source correlation coefficient ρ. As can be observed, at $P/N = 10$ dB, the SCS based coding schemes are inferior to HDA coding and the uncoded transmission. This is due to the fact that digital channel code experiences outages more frequently, in which case decoder cannot estimate the source sequences. At lower ρ values SSC coding which ignores the source correlation shows a slightly lower MSE compared to SSC coding with distributed VQ. This may be attributed to the fact that distributed VQ requires both channel codewords to reconstruct each source. In Fig.2.9, a similar performance comparison is presented for $P/N = 30$ dB. At high CSNR values SSC coding with distributed VQ achieves a lower MSE compared to the uncoded transmission for up to $\rho = 0.9$. This is due to the obvious fact that the digital code is in no-outage with high probability. However, as $\rho \to 1$ the uncoded transmission causes negligible interference between the channel inputs, and therefore becomes optimal. In both CSNR values 10 dB and 30 dB, the HDA coding shows superior performance over the other coding schemes for different ρ values. This is due to the fact that HDA coding can be matched to the fading distribution and the source

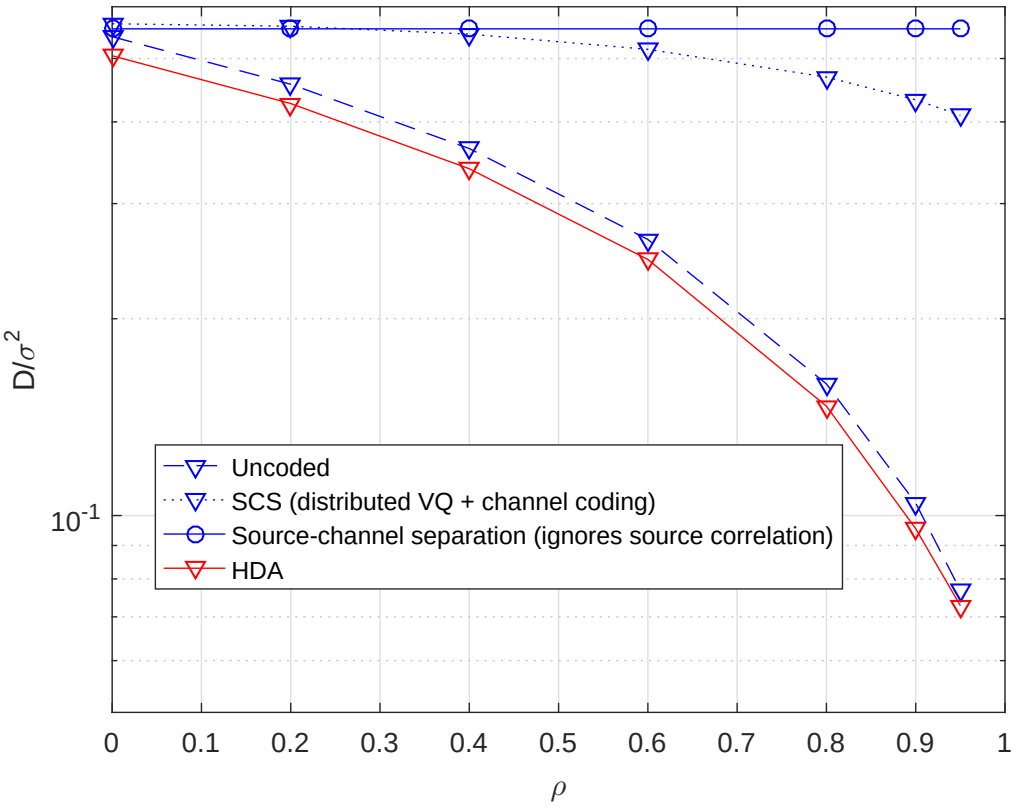

Figure 2.8: MSE vs ρ at P/N = 10 dB.

correlation by optimizing the encoder parameters.

2.9 Conclusion

The best performance achievable in communicating correlated Gaussian sources over a BF-GMAC is an open problem. In this chapter several upper bounds to the minimum achievable MMSE have been obtained and compared. The lowest MMSE bound is found by considering an HDA coding scheme, which we refer to as HDA (MAC). In this case, by computing the individual outage regions of digital coding, we were able to compute the average MSE and optimize the encoder to find an achievable bound for communicating Gaussian sources over BF-MAC. Through numerical result we have shown that the HDA (MAC) scheme can outperform the source-channel separation approach and the uncoded

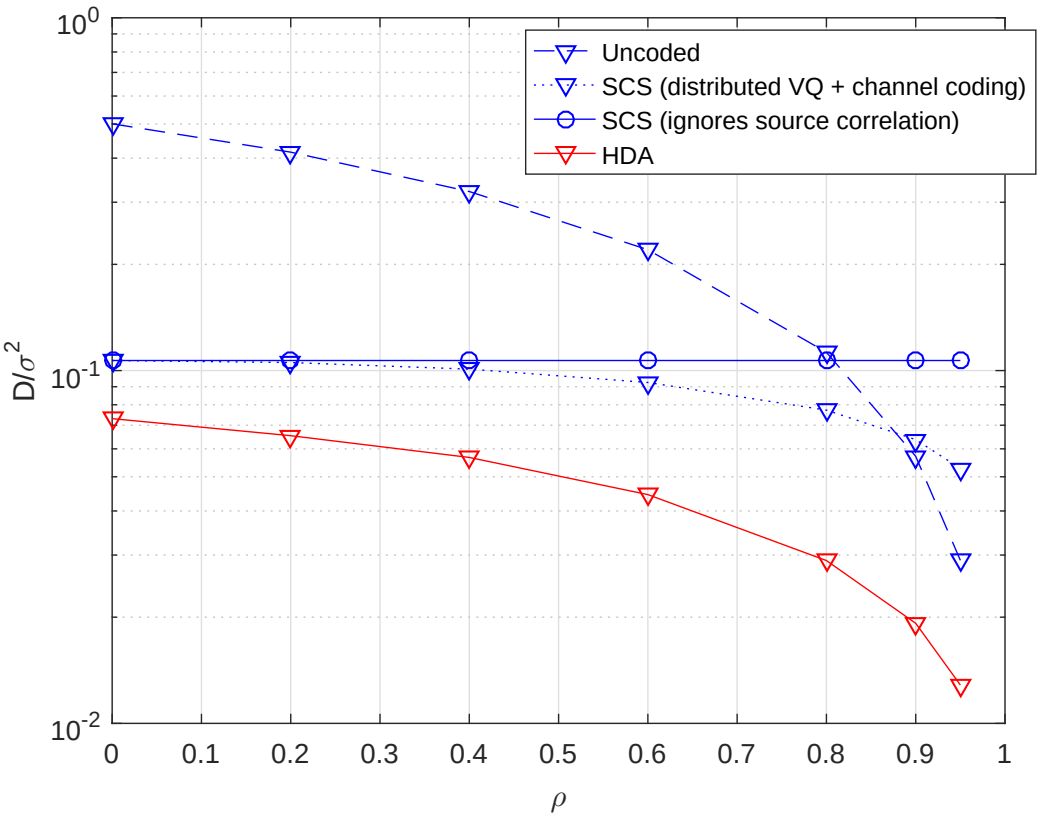

Figure 2.9: MSE vs ρ at 30 dB.

scheme as P/N increases. The SSC coding (SCS) shows inferior performance at low to moderate CSNR. Furthermore, We have compared the performance of the HDA coding with orthogonal channel access. The numerical results show that the HDA (MAC) scheme outperforms HDA (ortho.) scheme at moderate to high P/N values, which indicates the advantage of sharing the bandwidth of the MAC between the transmitters when the probability of the outage events are low.

Chapter 3

Source Dependent Channel Coding for Correlated Sources and BF-GMAC

3.1 Introduction

In this chapter, we study distortion versus average CSNR performance of communication of two correlated Gaussian sources over two-to-one block-fading MAC, using JSC coding schemes with source dependent channel codewords. In [44], a lower bound for achievable MMSE is derived for communicating correlated Gaussian sources over a fixed GMAC with source-channel bandwidth matched. In [44], authors present a JSC coding scheme that performs close to the MSE lower bound in the symmetric case. One of the key contributing factors to the performance enhancement of the JSC scheme in [44] is the enhanced capacity region due to the correlated channel codewords, generated by mapping VQ source codewords directly to channel inputs. The fundamental difference between the problem studied in this chapter and that in [44] is the outages in the channel code due to fading in the channel. A decoder outage occurs when a channel codeword cannot be decoded error-free. Since the channel codes can be seen as noisy source sequences, even during an outage the channel codewords carries some information about the source, and therefore can be used to reconstruct the sources to some accuracy. As the fading gains are unknown at the trans-

mitters, a pair of fixed rates have to be used through out the transmission. However, when random channel fading gains drops below a certain value fixed-rate channel codes can become undecodable. Therefore, the decodabitiy of the channel codewords depends on the particular realization of the fading gain observed during the transmission of the codewords. There can be different decoder outage scenarios in a two-input GMAC: both codewords decodable, only one of the codewords decodable, or both codewords undecodable. The key challenge in our problem setup is computing the average MMSE under different outage scenarios at the receiver.

Contribution

- The source-channel vector quantization scheme and an HDA extension of it provide the best known lower bounds for the MMSE of transmitting correlated Gaussian sources of a GMAC with no fading [44]. In this chapter we derive the MMSE lower bounds of these schemes for BF-GMAC with no CSI at the transmitters, by considering three possible cases of decoder outage.

- Through numerical performance evaluations, it is shown that, unlike in the case of non-fading GMAC as considered in [44], uncoded transmission is no longer optimal at low CSNRs, when there is channel fading and CSI is not available to the transmitters. In particular, it is shown that JSC coding which combines both coded and uncoded source components can outperform uncoded transmission at low CSNRs.

3.2 JSC Coding Based on Vector Quantization

A simple yet effective coding scheme which can be used to communicate a pair of Gaussian sources to a common receiver over a non-fading MAC is presented in [44]. In this scheme, each source is quantized by a rate-distortion optimal vector quantizer [2] and the real-valued quantized vectors are directly transmitted over the GMAC, without any further

channel coding. Since the correlated sources will produce correlated vector quantizer outputs, this JSC scheme produces correlated channel codewords at the GMAC inputs, and is able to exploit the correlation between the sources to improve the effective channel "capacity" . Also, when one of the codewords is decoded correctly, the effective CSNR of the other codeword increases due to the correlation between the codewords. In case where only one codeword can be decoded, the correlation between the channel output and the transmitted codewords may be used to increase the effective CSNR.

This chapter investigates the best achievable performance of a *source-channel vector quantization* (JSC-VQ) scheme [44] for a GMAC with Rayleigh fading and no transmitter-side CSI. This scheme is illustrated in Fig. 3.1. As in HDA coding, the achievable MMSE is determined by three possible outage conditions at the decoder. However, the advantage here is that, even when none of the codewords can be decoded correctly some estimates of the two sources can still be obtained from the observed channel output.

The JSC-VQ encoder i vector-quantizes the source sequences $\mathbf{S}_i$ using a rate R_i codebook, scales the resulting codeword $\mathbf{U}_i^o$ to satisfy its average power constraint P_i, and transmits the scales codeword $\mathbf{X}_i = \beta_i \mathbf{U}_i^o$ over the BF-MAC, where

$$\beta_i = \sqrt{\frac{P_i}{\sigma^2(1-2^{-2R_i})}}, \quad i = 1, 2. \tag{3.1}$$

Note that, since VQ source codewords are mapped to the channel codewords, correlated source sequence generates maximally correlated channel inputs $X_{1,k}$ and $X_{2,k}$, and hence the advantage of this scheme. The estimation of the source sequence is done in two steps. First, upon observing the resulting channel output $\mathbf{Y}$, the decoder uses the same VQ codebooks used by the encoders to jointly detect the transmitted codewords $(\mathbf{U}_1^o, \mathbf{U}_2^o)$, by considering their correlation or the asymptotic angle (detection-step). Note that $(\mathbf{S}_1, \mathbf{S}_2, \mathbf{U}_1^o, \mathbf{U}_2^o, \mathbf{Y})$ are asymptotically jointly Gaussian and hence the optimal (MMSE) estimator is linear. Let the codeword pair found in the detection-step be $(\hat{\mathbf{U}}_1, \hat{\mathbf{U}}_2)$. In general, the estimated source

sequences are given by

$$\hat{\mathbf{S}}_i = \gamma_{i,1}\hat{\mathbf{U}}_1 + \gamma_{i,2}\hat{\mathbf{U}}_2 + \gamma_{i,3}\mathbf{Y}, \quad i = 1, 2,$$

where coefficients $\gamma_{i,1}, \gamma_{i,2}$ and $\gamma_{i,3}$ of the optimal linear estimator are to be determined. For given encoder parameters $(R_1, R_2, \beta_1, \beta_2)$, it is not guaranteed that $(\hat{\mathbf{U}}_1, \hat{\mathbf{U}}_2) = (\mathbf{U}_1^o, \mathbf{U}_2^o)$ at the current channel state (h_1, h_2), hence $\gamma_{i,1}, \gamma_{i,2}$ and $\gamma_{i,3}$ will depend on the state (outage-event) of the decoder. We next consider the all possible outage events to determine the MMSE.

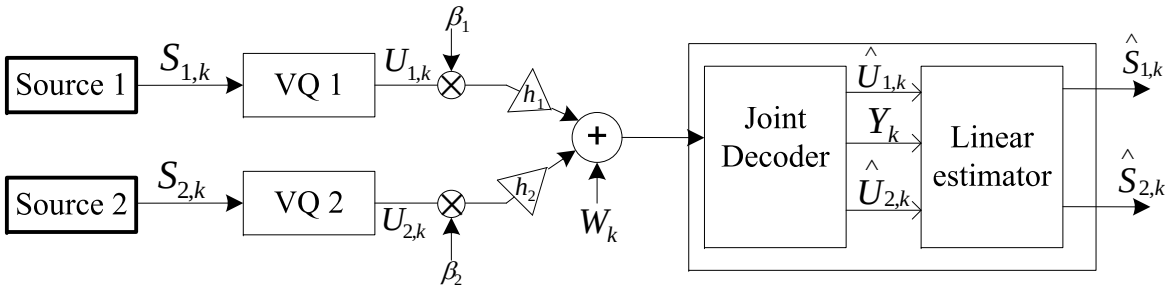

Figure 3.1: Vector-quantized source sequences are transmitted over slow fading MAC.

3.2.1 Both codewords can be decoded correctly

The set of all rate-pairs for which both codewords can be decoded correctly are given by the following Lemma.

Lemma 3.1. *For given $(P_1, P_2), (h_1, h_2), (\beta_1, \beta_2)$ and ρ, both source-channel VQ codewords can be detected with an arbitrarily small error probability, if (R_1, R_2) satisfy*

$$\begin{aligned} R_1 &< \frac{1}{2} log_2 \left(\frac{|h_1|^2 P_1 (1-\tilde{\rho}^2) + N}{N(1-\tilde{\rho}^2)} \right) \\ R_2 &< \frac{1}{2} log_2 \left(\frac{|h_2|^2 P_2 (1-\tilde{\rho}^2) + N}{N(1-\tilde{\rho}^2)} \right) \\ R_1 + R_2 &< \frac{1}{2} log_2 \left(\frac{|h_1|^2 P_1 + |h_2|^2 P_2 + 2Re\{h_1 h_2{}^*\}\tilde{\rho}\sqrt{P_1 P_2} + N}{N(1-\tilde{\rho}^2)} \right) \end{aligned} \tag{3.2}$$

and where

$$\tilde{\rho} = \rho\sqrt{(1-2^{-2R_1})((1-2^{-2R_2})}. \tag{3.3}$$

Proof. See Appendix A. □

As both VQ source codewords are recovered (with high probability), the joint decoder calculates MMSE estimates $\hat{\mathbf{S}}_i$, $i \in \{1,2\}$, of the source sequences $\mathbf{S}_i$ based on the linear combinations of $\mathbf{U}_1^o$ and $\mathbf{U}_2^o$, i.e.,

$$\hat{\mathbf{S}}_i = \gamma_{i,1}\mathbf{U}_1^o + \gamma_{i,2}\mathbf{U}_2^o$$

When the transmission rates (R_1, R_2) are in the no-outage region for given channel fading gains (h_1, h_2), the minimum distortion pairs are given by [44, Theorem IV.4]

$$D_1^{(no)}(h_1,h_2) = \sigma^2 2^{-2R_1}.\frac{1-\rho^2(1-2^{-2R_2})}{1-\tilde{\rho}^2}$$
$$D_2^{(no)}(h_1,h_2) = \sigma^2 2^{-2R_2}.\frac{1-\rho^2(1-2^{-2R_1})}{1-\tilde{\rho}^2}.$$

3.2.2 Only one codeword can be decoded correctly

Consider the case where the codeword $\mathbf{U}_1^o$ can be decoded correctly while the codeword $\mathbf{U}_2^o$ cannot be correctly decoded. For this partial-outage case, the set of all rate-pairs for which only codeword $\mathbf{U}_1^o$ can be correctly decoded given by the following theorem.

Theorem 3.2. *For given $(P_1,P_2),(h_1,h_2),(\beta_1,\beta_2)$ and ρ, the codeword $\mathbf{U}_1^o$ is decodable and $\mathbf{U}_2^o$ is undecodable if and only if*

$$R_1 < \frac{1}{2}log_2\left(\frac{|h_1|^2P_1 + |h_2|^2P_2 + 2Re\{h_1h_2{}^*\}\tilde{\rho}\sqrt{P_1P_2}+N}{|h_2|^2P_2(1-\tilde{\rho}^2)+N}\right) \tag{3.4}$$
$$R_2 > \frac{1}{2}log_2\left(\frac{|h_2|^2P_2(1-\tilde{\rho}^2)+N}{N(1-\tilde{\rho}^2)}\right). \tag{3.5}$$

Proof. See Appendix A. □

The MMSE estimates, based on $\mathbf{U}_1^o$ and $\mathbf{Y}$, for the source sequences are given by

$$\hat{\mathbf{S}}_i = \gamma_{i,1}\mathbf{U}_1^o + \gamma_{i,3}\mathbf{Y}, \quad i \in \{1,2\}.$$

The linear estimator coefficients $(\gamma_{i,1}, \gamma_{i,3})$, and the corresponding MMSE $D_i^{(po1)}(h_1, h_2)$ can be deduced by letting $\alpha_i = 0, i = \{1,2\}$ in the MMSE derivation in Section 3.3.2.

The set of all rate-pairs for which the codeword $\mathbf{U}_2^o$ and $\mathbf{U}_1^o$ is undecodable is given by the following lemma.

Lemma 3.3. *For given $(P_1, P_2), (h_1, h_2), (\beta_1, \beta_2)$ and ρ, the codeword $\mathbf{U}_2^o$ is decodable and $\mathbf{U}_1^o$ is undecodable if and only if*

$$R_2 < \frac{1}{2}log_2\left(\frac{|h_1|^2P_1 + |h_2|^2P_2 + 2Re\{h_1h_2^*\}\tilde{\rho}\sqrt{P_1P_2} + N}{|h_2|^2P_2(1-\tilde{\rho}^2) + N}\right) \tag{3.6}$$

$$R_1 > \frac{1}{2}log_2\left(\frac{|h_1|^2P_1(1-\tilde{\rho}^2) + N}{N(1-\tilde{\rho}^2)}\right). \tag{3.7}$$

Proof. Follows from the previous Lemma. □

The MMSE estimates, based on $\mathbf{U}_2^o$ and $\mathbf{Y}$, for the source sequences are given by

$$\hat{\mathbf{S}}_i = \gamma_{i,2}\hat{\mathbf{U}}_2 + \gamma_{i,3}\mathbf{Y}, \quad i \in \{1,2\}.$$

The linear estimator coefficients $(\gamma_{i,2}, \gamma_{i,3})$, and the corresponding MMSE $D_i^{(po2)}(h_1, h_2)$ can be deduced from the corresponding MMSE in Section 3.3.2.

3.2.3 Neither of the codewords can be decoded correctly

The set of all rate-pairs for which neither of the codewords can be decoded is given by the following lemma.

Lemma 3.4. *For given $(P_1, P_2), (h_1, h_2), (\beta_1, \beta_2)$ and ρ, neither of the codewords can be*

decoded if

$$R_1 > \frac{1}{2} log_2 \left(\frac{|h_1|^2 P_1 + |h_2|^2 P_2 + 2\boldsymbol{Re}\{h_1 {h_2}^*\}\tilde{\rho}\sqrt{P_1 P_2} + N}{|h_2|^2 P_2 (1-\tilde{\rho}^2) + N} \right)$$
$$R_2 > \frac{1}{2} log_2 \left(\frac{|h_1|^2 P_1 + |h_2|^2 P_2 + 2\boldsymbol{Re}\{h_1 {h_2}^*\}\tilde{\rho}\sqrt{P_1 P_2} + N}{|h_1|^2 P_1 (1-\tilde{\rho}^2) + N} \right)$$
$$R_1 + R_2 > \frac{1}{2} log_2 \left(\frac{|h_1|^2 P_1 + |h_2|^2 P_2 + 2\boldsymbol{Re}\{h_1 {h_2}^*\}\tilde{\rho}\sqrt{P_1 P_2} + N}{N(1-\tilde{\rho}^2)} \right).$$

Proof. Follows from (3.2), (3.4) and (3.6) in the previous theorem and the two lemmas. □

The MMSE estimate, based on $\mathbf{Y}$, for the source sequences are given by

$$\hat{\mathbf{S}}_i = \gamma_{i,3}\mathbf{Y}, \quad i \in \{1,2\}.$$

The MMSE distortion $D_i^{(to)}(h_1, h_2)$ can be deduced by letting $\alpha_i = 0, i = \{1,2\}$ in the MMSE derivation in Section 3.3.3.

The optimization problem is to determine the optimum fixed rate-pair at the transmitter which minimizes the average MSE distortion over the fading distribution, i.e.,

$$\begin{aligned} D^{\text{JSC-VQ}} = \min_{R_1,R_2} \frac{1}{2} \sum_{i=1}^{2} \Bigg(& \int_{\mathcal{H}_{no}} D_i^{no}(h_1,h_2) f(h_1) f(h_2) dh_1 dh_2 \\ & + \int_{\mathcal{H}_{po}^{(1)}} D_i^{po1}(h_1,h_2) f(h_1) f(h_2) dh_1 dh_2 + \int_{\mathcal{H}_{po}^{(2)}} D_i^{po2}(h_1,h_2) f(h_1) f(h_2) dh_1 dh_2 \\ & + \int_{\mathcal{H}_{to}} D_i^{to}(h_1,h_2) f(h_1) f(h_2) dh_1 dh_2 \Bigg). \end{aligned}$$

Since it is difficult to determine the boundaries of the outage regions with respect to the channel fading gains, we are unable to find an explicit expression for the average MMSE. Therefore, we use a numerical optimization algorithm along with Monte-Carlo simulation to find the best achievable average MMSE.

3.2.4 Decodability of the JSC-VQ codewords with source correlation

It has been shown that the capacity of a MAC channel can be increased with correlated channel inputs [40, 44]. This may be attributed to two factors. First is that the increased

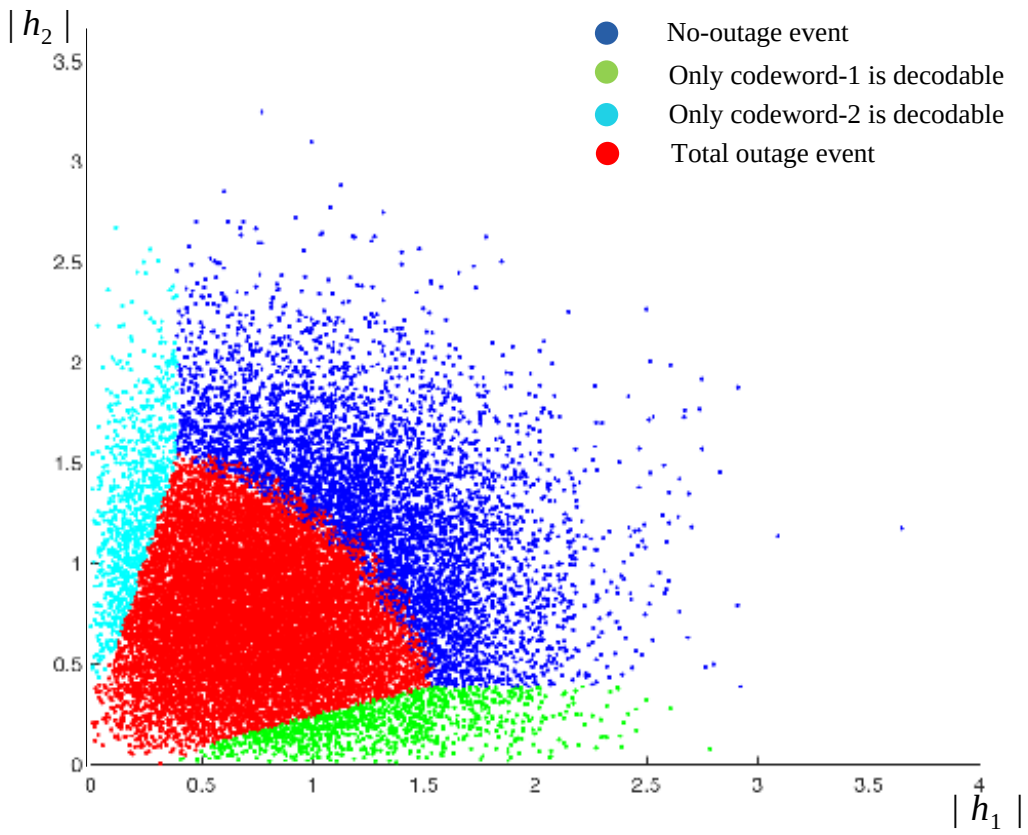

Figure 3.2: Decodability of the JSC-VQ codewrods with source correlation (low correlation), $\rho = 0.1$ and $P/N = 20dB$

effective signal power (*constructive interference*) due to the correlation between the channel inputs. Second is that given one codeword and the channel output the other codeword has a reduced uncertainty region, which allows encoders to transmit more codewords with no decoder error at the receiver (with high probability). However, when the MAC experiences fading, the codeword must be matched to the fading gains to create constructive interference in order to increase the effective capacity. If the CSI is not available to the encoders, correlated codewords can create *destructive interference* at the channel output. The strength of the received signal is determined by

$$\begin{aligned} E\{|h_1X_{1,k} + h_2X_{2,k}|^2\} &= |h_1|^2E\{|X_{1,k}|^2\} + |h_2|^2E\{|X_{2,k}|^2\} + 2\text{Re}\{h_1h_2^*\}E\{X_{1,k}X_{2,k}^*\} \\ &= |h_1|^2E\{|X_{1,k}|^2\} + |h_2|^2E\{|X_{2,k}|^2\} \\ &\quad + 2\text{Re}\{h_1h_2^*\}\rho_X\sqrt{E\{|X_{1,k}|^2\}E\{|X_{2,k}|^2\}}, \quad k = 1, \ldots, n \end{aligned} \tag{3.8}$$

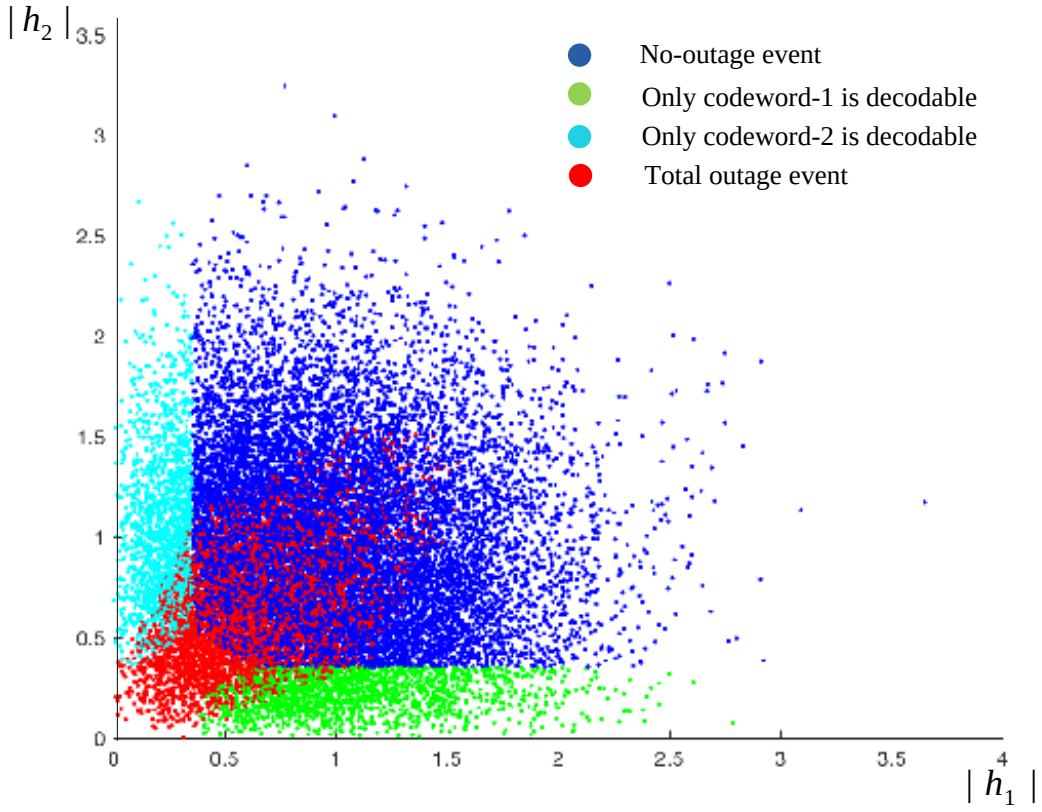

Figure 3.3: Decodability of the JSC-VQ codewrods with source correlation (high correlation), $\rho = 0.9$ and $P/N = 20dB$

where ρ_X is the correlation between the channel inputs. In equation (3.8), the term $2\text{Re}\{h_1 h_2^*\}\rho_X \sqrt{E\{|X_{1,k}|^2\}E\{|X_{2,k}|^2\}}$ determines the effect of the correlation to the received signal quality. If $\text{Re}\{h_1 h_2^*\} > 0$, the channel inputs creates constructive interference, otherwise they will interfere destructively degrading the received channel quality. However, since the CSI is available to the receiver, the asymptotic angels between the codewords can be used to improve the decodability of the codewords. Figure 3.2 illustrates the decodability of the JSC-VQ codewords with the amplitude values of the channel fading gains $(|h_1|, |h_2|)$, at a low source correlation ($\rho = 0.1$). Figure 3.3 and Figure 3.4 show the decodability of the JSC-VQ codewords at high source correlation values ($\rho = 0.9$ and $\rho = 0.98$). It can be observed that at $\rho = 0.1$ the region of total-outage event is larger than that at $\rho = 0.9$. However, at high source correlations, there is overlap of the region of total-outage event and the other decodability regions. At a very high source correlation $\rho = 0.98$, the region

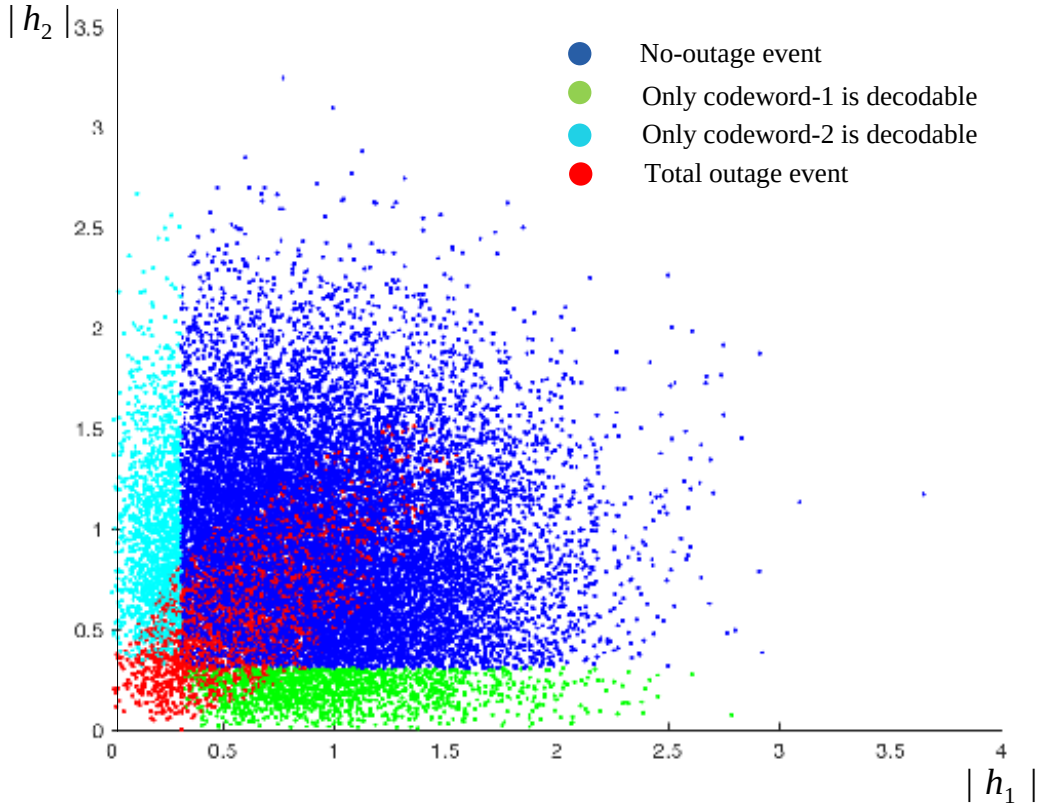

Figure 3.4: Decodability of the JSC-VQ codewrods with source correlation (very high correlation), $\rho = 0.98$ and $P/N = 20dB$

of no-outage event and the two regions of only a single codeword is decodable are further increased. However, the region of total-outage event overlaps with the other decodable regions. It can be observed that the overlap of the no-outage event is more likely when $|h_1| \approx |h_2|$. Now we can argue that the overall decodability of the JSC-VQ codewords is improved with the source correlation, while the decoder may experience outages at high CSNR instants.

3.3 A Superposition Approach: The HDA coding scheme

As the transmitters experience a range of CSNR values during the transmission, a system which send both coded and uncoded source information by superposition can be better matched to the fading distribution to achieve a lower average MMSE. The JSC scheme

analyzed in this section shares power between the coded and the uncoded transmission of the source sequence. This coding strategy is previously proposed in [44] for sending real-valued correlated Gaussian source sequences over a non fading GMAC. In the fixed channel problem in [44], the performance improvement over the JSC-VQ is mainly attributed to the optimality of uncoded transmission in the lower CSNR region. However when sending the sources over a varying channel with fixed transmitter parameters (due to CSI not being available at the transmitters), the superposition of uncoded transmission further contributed to a performance improvement as the received SNR of uncoded transmission gradually changes with the power of fading gains. To optimize the average performance of the coding scheme over the fading distribution of the BF-MAC, we compute the individual outage scenarios for each transmitter.

A description of the superimposed scheme is given below. The channel input sequence $\mathbf{X}_i$ generated by transmitter i, $i \in \{1, 2\}$, is a linear combination of the source sequence $\mathbf{S}_i$ and its rate R_i vector quantized version $\mathbf{U}_i^o$. That is

$$\mathbf{X}_i = \alpha_i \mathbf{S}_i + \beta_i \mathbf{U}_i^o,$$

where $\mathbf{u}_i^o$ is obtained as in the previous VQ scheme. The coefficient α_i and β_i are chosen so that the sequence $\mathbf{X}_i$ satisfies the average power constraint and the average MSE distortion over the fading distribution is minimized. When the optimum coefficients are computed the above two conditions are satisfied when α_i and β_i are bounded as follows

$$\alpha_i \in \left[0, \sqrt{\frac{P_i}{\sigma^2}}\right], \quad \beta_i = \sqrt{\frac{P_i - \alpha_i^2 \sigma^2 2^{-2R_i}}{\sigma^2(1 - 2^{-2R_i})}} - \alpha_i.$$

At the receiver, the joint decoder first evaluate the decodability of the codewords. The decodability of the codewords depends on encoder parameters R_i, α_i, and β_i, and the CSI h_1 and h_2. We describe different outage scenarios below.

3.3.1 Both codewords decoded correctly

When the decoder decides the codewords can be decoded with arbitrarily small probability of error, it makes a guess $(\hat{\mathbf{U}}_1, \hat{\mathbf{U}}_2)$ for the transmitted VQ sequences from the channel output sequence $\mathbf{Y} = h_1\mathbf{X}_1 + h_2\mathbf{X}_2 + \mathbf{Z}$. Then decoder computes the estimates $\hat{\mathbf{S}}_1$ and $\hat{\mathbf{S}}_2$ of the source sequences $\mathbf{S}_1$ and $\mathbf{S}_2$ as

$$\hat{\mathbf{S}}_i = \gamma_{i,1}\hat{\mathbf{U}}_1 + \gamma_{i,2}\hat{\mathbf{U}}_2 + \gamma_{i,3}\mathbf{Y}, \quad i \in \{1, 2\},$$

where the coefficients $\gamma_{i,j}$ are chosen such that $\hat{\mathbf{S}}_i = \mathrm{E}[\mathbf{S}_i|\mathbf{Y}, \hat{\mathbf{U}}_1, \hat{\mathbf{U}}_2]$. To determine explicit expressions for $\gamma_{i,j}$, the first derivative of MSE $\frac{1}{n}\mathrm{E}\left[\|\mathbf{S}_i - \hat{\mathbf{S}}_i\|^2\right]$ w.r.t. $\overline{\gamma_{ij}}$ is computed and equated the null-vector. This results in the following system of equations:

$$\begin{bmatrix} \frac{1}{n}E\|\mathbf{U}_1\|^2 & \frac{1}{n}E\langle\mathbf{U}_2, \mathbf{U}_1\rangle & \frac{1}{n}E\langle\mathbf{Y}, \mathbf{U}_1\rangle \\ \frac{1}{n}E\langle\mathbf{U}_1, \mathbf{U}_2\rangle & \frac{1}{n}E\|\mathbf{U}_2\|^2 & \frac{1}{n}E\langle\mathbf{Y}, \mathbf{U}_2\rangle \\ \frac{1}{n}E\langle\mathbf{U}_1, \mathbf{Y}\rangle & \frac{1}{n}E\langle\mathbf{U}_2, \mathbf{Y}\rangle & \frac{1}{n}E\|\mathbf{Y}\|^2 \end{bmatrix} \begin{bmatrix} \gamma_{i,1} \\ \gamma_{i,2} \\ \gamma_{i,3} \end{bmatrix} = \begin{bmatrix} \frac{1}{n}E\langle\mathbf{S}_i, \mathbf{U}_1\rangle \\ \frac{1}{n}E\langle\mathbf{S}_i, \mathbf{U}_2\rangle \\ \frac{1}{n}E\langle\mathbf{S}_i, \mathbf{Y}\rangle \end{bmatrix}.$$

For simplicity, lets define

$$\mathbf{K} \triangleq \begin{bmatrix} k_{11} & k_{12} & k_{13} \\ k_{21} & k_{22} & k_{23} \\ k_{31} & k_{32} & k_{33} \end{bmatrix} = \begin{bmatrix} \frac{1}{n}E\|\mathbf{U}_1\|^2 & \frac{1}{n}E\langle\mathbf{U}_2, \mathbf{U}_1\rangle & \frac{1}{n}E\langle\mathbf{Y}, \mathbf{U}_1\rangle \\ \frac{1}{n}E\langle\mathbf{U}_1, \mathbf{U}_2\rangle & \frac{1}{n}E\|\mathbf{U}_2\|^2 & \frac{1}{n}E\langle\mathbf{Y}, \mathbf{U}_2\rangle \\ \frac{1}{n}E\langle\mathbf{U}_1, \mathbf{Y}\rangle & \frac{1}{n}E\langle\mathbf{U}_2, \mathbf{Y}\rangle & \frac{1}{n}E\|\mathbf{Y}\|^2 \end{bmatrix}$$

and

$$\mathbf{c}_i \triangleq \begin{bmatrix} c_{i1} \\ c_{i2} \\ c_{i3} \end{bmatrix} = \begin{bmatrix} \frac{1}{n}E\langle\mathbf{S}_i, \mathbf{U}_1\rangle \\ \frac{1}{n}E\langle\mathbf{S}_i, \mathbf{U}_2\rangle \\ \frac{1}{n}E\langle\mathbf{S}_i, \mathbf{Y}\rangle \end{bmatrix},$$

where

$$k_{11} = \sigma^2(1 - 2^{-2R_1})$$

$$k_{12} = k_{21} = \sigma^2(1 - 2^{-2R_1})(1 - 2^{-2R_2})$$

$$k_{13} = k_{31}^* = (h_1\alpha_1 + h_1\beta_1 + h_2\alpha_2\rho)k_{11} + h_2\beta_2 k_{12}$$

$$k_{22} = \sigma^2(1 - 2^{-2R_2})$$

$$k_{23} = k_{32}^* = (h_2\alpha_2 + h_2\beta_2 + h_1\alpha_1\rho)k_{11} + h_1\beta_1 k_{12}$$

$$\begin{aligned} k_{33} &= \alpha_1^2|h_1|^2\sigma^2 + 2\alpha_1\beta_1|h_1|^2 k_{11} + 2\alpha_1\alpha_2 \mathbf{Re}\{h_1^* h_2\}\rho\sigma^2 + 2\alpha_1\beta_2 \mathbf{Re}\{h_1^* h_2\}\rho k_{22} \\ &\quad + \beta_1^2|h_1|^2 k_{11} + 2\beta_1\alpha_2 \mathbf{Re}\{h_1^* h_2\}\rho k_{11} + 2\beta_1\beta_2 \mathbf{Re}\{h_1^* h_2\}k_{12} + 2\alpha_2\beta_2|h_2|^2 k_{22} \\ &\quad + \alpha_2^2|h_2|^2\sigma^2 + \beta_2^2|h_2|^2 k_{22} + N. \end{aligned}$$

The coefficients $\gamma_{i,j}$ are then given by

$$\begin{bmatrix} \gamma_{i,1} \\ \gamma_{i,2} \\ \gamma_{i,3} \end{bmatrix} = \mathbf{K}^{-1} \begin{bmatrix} c_{i1} \\ c_{i2} \\ c_{i3} \end{bmatrix}, \quad i \in \{1, 2\},$$

where

$$\begin{aligned} c_{11} &= k_{11} \\ c_{12} &= \rho k_{22} \\ c_{13} &= (\alpha_1 h_1^* + \alpha_2 h_2^* \rho)\sigma^2 + h_1^*\beta_1 k_{11} + \beta_2 h_2^* k_{22} \\ c_{21} &= \rho k_{11} \\ c_{22} &= k_{22} \\ c_{23} &= (\alpha_2 h_2^* + \alpha_1 h_1^* \rho)\sigma^2 + \beta_1 h_1^* k_{11} + \beta_2 h_2^* k_{22}. \end{aligned}$$

The distortion pairs achieved for given (h_1, h_2) when both codewords decoded correctly is given by

$$D_i^{(no)}(h_1, h_2) = \sigma^2 - \gamma_{i,1}^* c_{i1} - \gamma_{i,2}^* c_{i2} - \gamma_{i,3}^* c_{i3}, \quad i \in \{1, 2\}.$$

The rate region for which both codewords can be decoded is given by the following lemma.

Lemma 3.5. *For given $(P_1, P_2), (\alpha_1, \beta_1), (\alpha_2, \beta_2), (h_1, h_2)$ and ρ, the VQ codeword pair $(\mathbf{U}_1^o, \mathbf{U}_1^o)$ can be decoded with arbitrarily small probability of error whenever (R_1, R_2)*

satisfies

$$R_1 < \frac{1}{2} log_2 \left(\frac{|\beta_1'|^2 k_{11}(1-\tilde{\rho}^2) + N'}{N'(1-\tilde{\rho}^2)} \right)$$
$$R_2 < \frac{1}{2} log_2 \left(\frac{|\beta_2'|^2 k_{22}(1-\tilde{\rho}^2) + N'}{N'(1-\tilde{\rho}^2)} \right)$$
$$R_1 + R_2 < \frac{1}{2} log_2 \left(\frac{|\beta_1'|^2 k_{11} + |\beta_2'|^2 k_{22} + 2\boldsymbol{Re}\{\beta_1'(\beta_2')^*\}\tilde{\rho}\sqrt{k_{11}k_{22}}) + N'}{N'(1-\tilde{\rho}^2)} \right)$$

for some $\alpha_1, \alpha_2, \beta_1$ and β_2 satisfying the power constraint and where

$$N' = |h_1|^2 \alpha_1^2 \nu_1 + |h_2|^2 \alpha_2^2 \nu_2 + 2\text{Re}\{h_1{}^* h_2\}\alpha_1 \alpha_2 \nu_3 + N, \tag{3.9}$$

where the expressions ν_1, ν_1, and ν_3 given in equation set following (45) in [44] is used here. with

$$\beta_1' = h_1\alpha_1(1 - a_1\tilde{\rho}) + h_1\beta_1 + h_2\alpha_2 a_2$$
$$\beta_2' = h_2\alpha_2(1 - a_2\tilde{\rho}) + h_2\beta_2 + h_1\alpha_1 a_1,$$

where a_1, a_2, η_1 and η_1 are given in (48-50) in [44].

3.3.2 Only one codeword can be decoded correctly

Consider the case when codeword-1 can be decoded correctly while codeword-2 cannot be correctly decoded. Rate pairs for this outage event is given by the following lemma.

Lemma 3.6. *For given $(P_1, P_2), (\alpha_1, \beta_1), (\alpha_2, \beta_2), (h_1, h_2)$ and ρ, the necessary and sufficient conditions that only codeword $\mathbf{U}_1^o$ but not $\mathbf{U}_2^o$ is correctly decodable are*

$$R_1 < \frac{1}{2} log_2 \left(\frac{|\beta_1'|^2 k_{11} + |\beta_2'|^2 k_{22} + 2\boldsymbol{Re}\{\beta_1'(\beta_2')^*\}\tilde{\rho}\sqrt{k_{11}k_{22}}) + N'}{|\beta_2'|^2 k_{22}(1-\tilde{\rho}^2) + N'} \right)$$
$$R_2 > \frac{1}{2} log_2 \left(\frac{|\beta_2'|^2 k_{22}(1-\tilde{\rho}^2) + N'}{N'(1-\tilde{\rho}^2)} \right).$$

The MMSE estimates for the source sequences are given by

$$\hat{\mathbf{S}}_i = \gamma_{i,1}\hat{\mathbf{U}}_1 + \gamma_{i,3}\mathbf{Y}, \quad i \in \{1, 2\},$$

where the linear estimator coefficients are given by

$$\begin{bmatrix} \gamma_{i1} \\ \\ \gamma_{i3} \end{bmatrix} = \mathbf{K}_1^{-1} \begin{bmatrix} c_{i1} \\ \\ c_{i3} \end{bmatrix}, \quad i \in \{1, 2\},$$

where

$$\mathbf{K}_1 = \begin{bmatrix} k_{11} & k_{13} \\ \\ k_{31} & k_{33} \end{bmatrix}.$$

The MMSE of this estimator is given by

$$D_i^{(po1)}(h_1, h_2) = \sigma^2 - \gamma_{i,1}^* c_{i1} - \gamma_{i,3}^* c_{i3}, \quad i \in \{1, 2\}.$$

The rate pairs for which codeword-2 can be decoded correctly codeword-1 cannot be decoded correctly is given by the following lemma.

Lemma 3.7. *For given* $(P_1, P_2), (\alpha_1, \beta_1), (\alpha_2, \beta_2), (h_1, h_2)$ *and* ρ*, the necessary and sufficient conditions that only codeword* $\mathbf{U}_2^o$ *but not* $\mathbf{U}_1^o$ *is correctly decodable are*

$$R_2 < \frac{1}{2} log_2 \left(\frac{|\beta_1'|^2 k_{11} + |\beta_2'|^2 k_{22} + 2\boldsymbol{Re}\{\beta_1'(\beta_2')^*\}\tilde{\rho}\sqrt{k_{11}k_{22}}) + N'}{|\beta_2'|^2 k_{11}(1 - \tilde{\rho}^2) + N'} \right)$$
$$R_1 > \frac{1}{2} log_2 \left(\frac{|\beta_1'|^2 k_{11}(1 - \tilde{\rho}^2) + N'}{N'(1 - \tilde{\rho}^2)} \right).$$

The MMSE estimates for the source sequences are given by

$$\hat{\mathbf{S}}_i = \gamma_{i,2} \hat{\mathbf{U}}_2 + \gamma_{i,3} \mathbf{Y}, \quad i \in \{1, 2\},$$

where the linear estimator coefficients are given by

$$\begin{bmatrix} \gamma_{i2} \\ \\ \gamma_{i3} \end{bmatrix} = \mathbf{K}_2^{-1} \begin{bmatrix} c_{i2} \\ \\ c_{i3} \end{bmatrix}, \quad i \in \{1, 2\},$$

where

$$\mathbf{K}_2 = \begin{bmatrix} k_{22} & k_{23} \\ \\ k_{32} & k_{33} \end{bmatrix}$$

and the MMSE of this estimator is given by

$$D_i^{(po2)}(h_1, h_2) = \sigma^2 - \gamma_{i,2}^* c_{i2} - \gamma_{i,3}^* c_{i3}, \quad i \in \{1, 2\}.$$

3.3.3 Neither of the codewords can be decoded correctly

In this case the rate-pair does not satisfy any of the conditions in the above scenarios, and neither of the codewords can be decoded reliably. The rate pairs for the total-outage events is given by the following lemma.

Lemma 3.8. *For given* $(P_1, P_2), (\alpha_1, \beta_1), (\alpha_2, \beta_2), (h_1, h_2)$ *and* ρ*, neither* $\mathbf{U}_1^o$ *nor* $\mathbf{U}_2^o$ *is correctly decodable if*

$$\begin{aligned}
R_1 &> \frac{1}{2} log_2 \left(\frac{|\beta_1'|^2 k_{11} + |\beta_2'|^2 k_{22} + 2Re\{\beta_1'(\beta_2')^*\}\tilde{\rho}\sqrt{k_{11}k_{22}}) + N'}{|\beta_2'|^2 k_{22}(1-\tilde{\rho}^2) + N'} \right) \\
R_2 &> \frac{1}{2} log_2 \left(\frac{|\beta_1'|^2 k_{11} + |\beta_2'|^2 k_{22} + 2Re\{\beta_1'(\beta_2')^*\}\tilde{\rho}\sqrt{k_{11}k_{22}}) + N'}{|\beta_1'|^2 k_{11}(1-\tilde{\rho}^2) + N'} \right) \\
R_1 + R_2 &> \frac{1}{2} log_2 \left(\frac{|\beta_1'|^2 k_{11} + |\beta_2'|^2 k_{22} + 2Re\{\beta_1'(\beta_2')^*\}\tilde{\rho}\sqrt{k_{11}k_{22}}) + N'}{N'(1-\tilde{\rho}^2)} \right).
\end{aligned}$$

The MMSE estimate for the source sequences are given by

$$\hat{\mathbf{S}}_i = \gamma_{i,3}\mathbf{Y}, \quad i \in \{1, 2\}. \tag{3.10}$$

The MMSE is given by

$$D_i^{(to)}(h_1, h_2) = \sigma^2 - \gamma_{i,3}^* c_{i3}, \quad i \in \{1, 2\}.$$

where the linear estimator coefficient is given by

$$\gamma_{i3} = \frac{c_{i3}}{k_{i3}}, \quad i \in \{1, 2\}.$$

Lemmas 3.5, 3.6, 3.7 and 3.8 can be proven by combining the arguments used in the proof of [44, Lemma F.1] and the proofs of Theorem 3.2 and Lemma 3.1 given in Appendix A. As in the proof of [44, Lemma F.1], we choose β_1', β_2' and N' such that the MAC input

output relationship $\mathbf{Y} = \beta_1' \mathbf{U}_1^o + \beta_1' \mathbf{U}_1^o + \mathbf{W}'$ satisfies the properties needed to analyze the JSC-VQ scheme. Here $\mathbf{W}'$ is the independent interference to the VQ codewords $\mathbf{U}_1^o$ and $\mathbf{U}_2^o$, and β_1', β_2' and N' are functions of the fading gains h_1 and h_2.

The optimization problem is to determine the optimum fixed rate-pair (R_1, R_2) and the coefficient α_i and β_i, $i \in \{1, 2\}$ which minimizes the average MMSE distortion over the fading distribution, i.e.,

$$
\begin{aligned}
D^{\text{JSC-VQ-HDA}} = \min_{R_1, R_2, \alpha_1, \alpha_2} \frac{1}{2} \sum_{i=1}^{2} \Bigg(& \int_{\mathcal{H}_{no}} D_i^{no}(h_1, h_2) f(h_1) f(h_2) dh_1 dh_2 \\
& + \int_{\mathcal{H}_{po}^{(1)}} D_i^{po1}(h_1, h_2) f(h_1) f(h_2) dh_1 dh_2 + \int_{\mathcal{H}_{po}^{(2)}} D_i^{po2}(h_1, h_2) f(h_1) f(h_2) dh_1 dh_2 \\
& + \int_{\mathcal{H}_{to}} D_i^{to}(h_1, h_2) f(h_1) f(h_2) dh_1 dh_2 \Bigg).
\end{aligned}
$$

Since evaluating the boundaries of the outage regions with respect to the channel fading gains is not mathematically feasible, we use Monte Carlo simulation methods to compute the average MMSE for given R_1, R_2, α_i and, β_i. The convexity of the optimization problem is not known. Therefore, a global optimization tool is used to find the achievable average MMSE.

3.4 Numerical Results and Discussion

In this section we present a set of numerical results to analyze the performance of the JSC-VQ scheme and the HDA scheme which combines coded and uncoded transmission of the source (JSC-VQ-HDA). In [44], the numerical results are presented which demonstrate the superior performance of the JSC-VQ-HDA scheme in communicating correlated Gaussian sources over fixed (non-fading) GMAC. In our experiment setup we consider communication of correlated Gaussian sources over Rayleigh BF-GMAC. The fading coefficients (h_1, h_2) are assumed to be independent normally distributed random variables with zero-mean and unit variance. The average MSE is computed over 10,000 channel realizations. We assume that the transmitter powers are equal to 1 ($P_1 = P_2 = 1$).

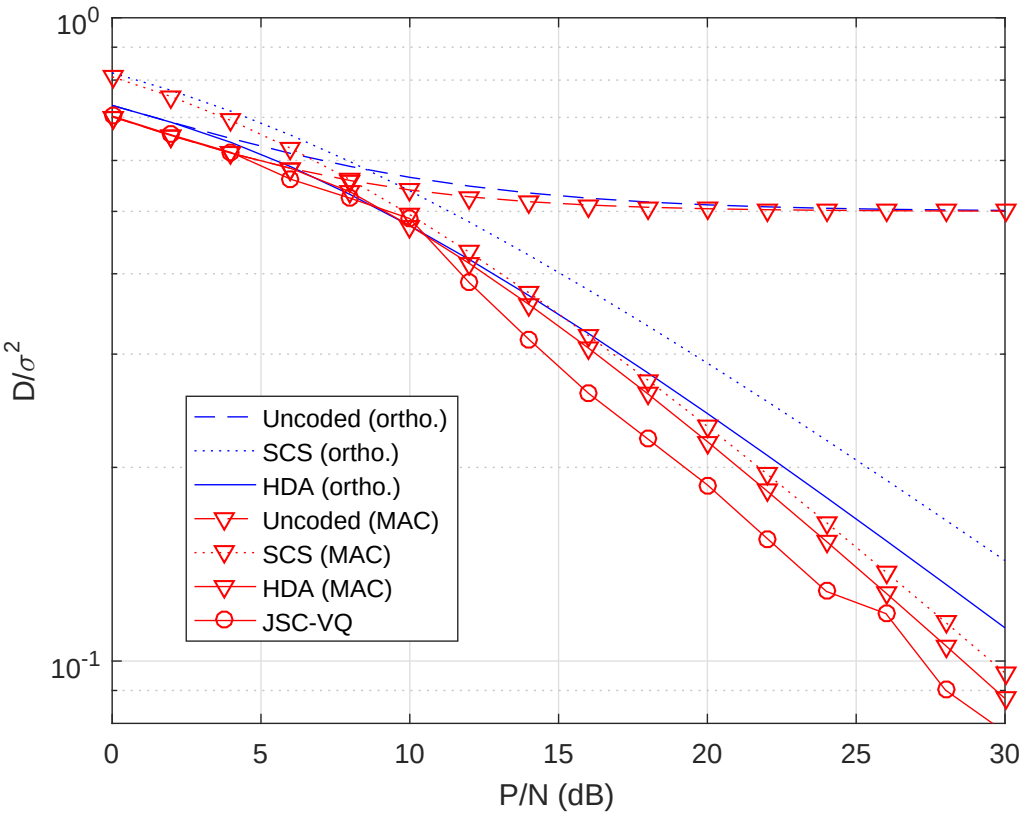

Figure 3.5: Performance comparison of different coding scheme assuming uncorrelated sources.

3.4.1 Sending uncorrelated Gaussian sources over BF-MAC

In order to compare the performance of the JSC-VQ scheme against the bounds derived in Chapter 2, we first consider sending uncorrelated source over the BF-MAC. Fig. 3.5 compares the MMSE achieved over a range of P/N values. It can be observed that JSC-VQ scheme is superior to the HDA schemes which use source-channel separation in the digital part. This performance difference is due to the fact that the JSC-VQ scheme the digital codewords are constructed using the source VQ sequences, and therefore the receiver can estimate a source sequences even when the corresponding digital transmitter is in outage.

3.4.2 Sending Correlated Gaussian Sources Over Fading MAC

In the performance analyzes of the communication of correlated Gaussian sources, we consider the same fading GMAC and the transmitters with equal powers. In order to evaluate

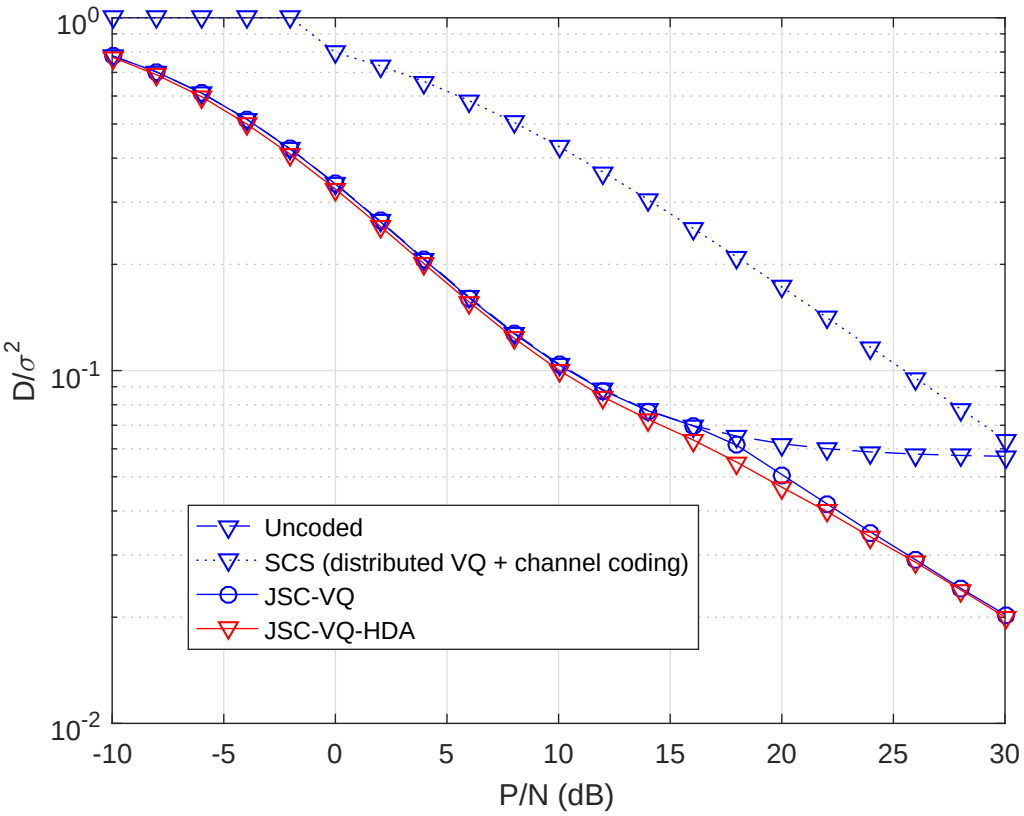

Figure 3.6: Performance of different coding schemes sending correlated sources ($\rho = 0.9$).

the performance of the proposed JSC-VQ and JSC-VQ-HDA schemes we use Monte Carlo simulation techniques due to the high complexity in determining the boundaries of the individual outage regions. In particular, we use Monte Carlo simulation techniques to compute the MSE distortion average over the fading distribution. Fig. 3.6 shows the performance of JSC-VQ-HDA, JSC-VQ, the SCS based (with distributed VQ), and uncoded transmission over the BF-MAC P/N.

The performance of the uncoded transmission is significantly better compared to the SCS coding scheme for a range of low P/N values. However, as the P/N increases the performance of the uncoded scheme deteriorates, i.e., the performance of the uncoded scheme levels off as $P/N \to \infty$. In the uncoded transmission, a part of the correlated inputs by one transmitter act as independent noise to the other transmitter. Note that one channel input can be written as a function of other channel input $X_2 = aX_1 + W$, where W

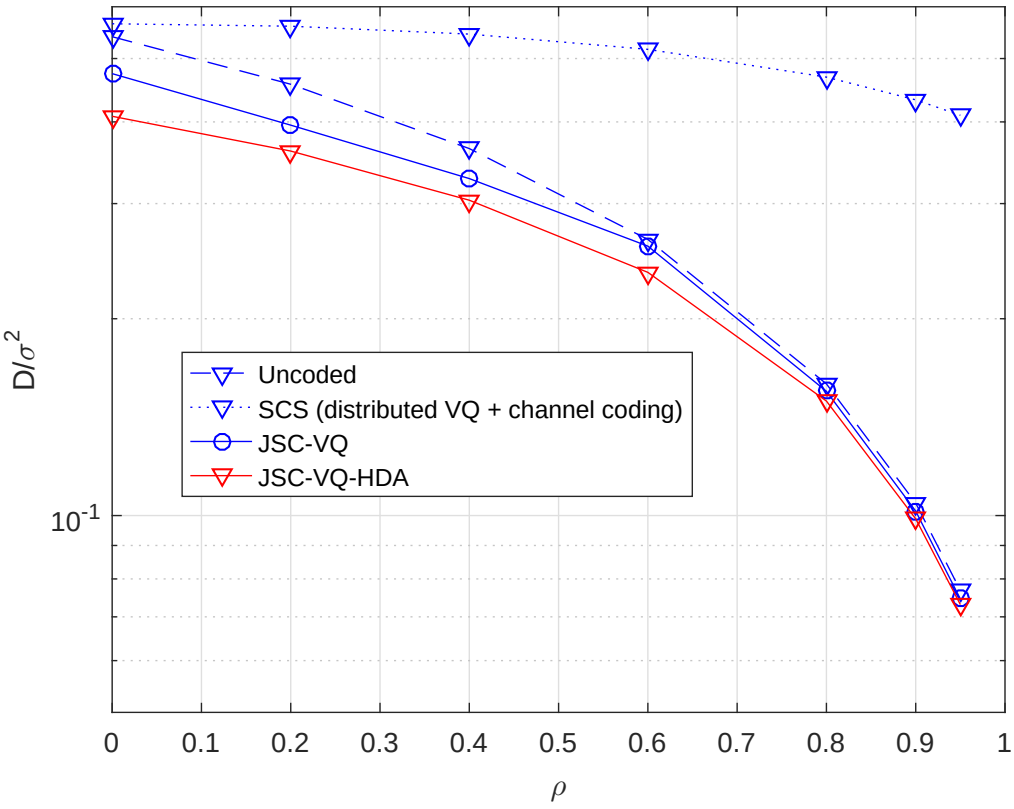

Figure 3.7: D/σ^2 vs ρ ($P/N = 10$ dB).

is independent noise. In the symmetric case the average distortion of the uncoded scheme approaches $\sigma^2(1-\rho)/2$. The HDA scheme outperforms both the uncoded scheme and the separation-based approach after some P/N value. Below a certain P/N value the HDA scheme simply operates as an uncoded scheme by letting $R_i \to \infty$. The direct VQ transmission performs as close to the HDA scheme for low P/N values. This is mainly due to the fact that both system operates nearly as the uncoded system. However, as P/N increases, the probability of correctly decoding the codewords increases which amounts to performance improvement. However, the HDA system outperforms the direct VQ transmission as P/N further increases. This can be attributed to the fact that receiver signal quality of analog coding gradually increases with the channel gains.

The performance curves of the coding systems against the correlation coefficient (ρ) are shown in Fig. 3.7 and Fig. 3.8 for P/N values 10 dB and 30 dB, respectively. In Fig.

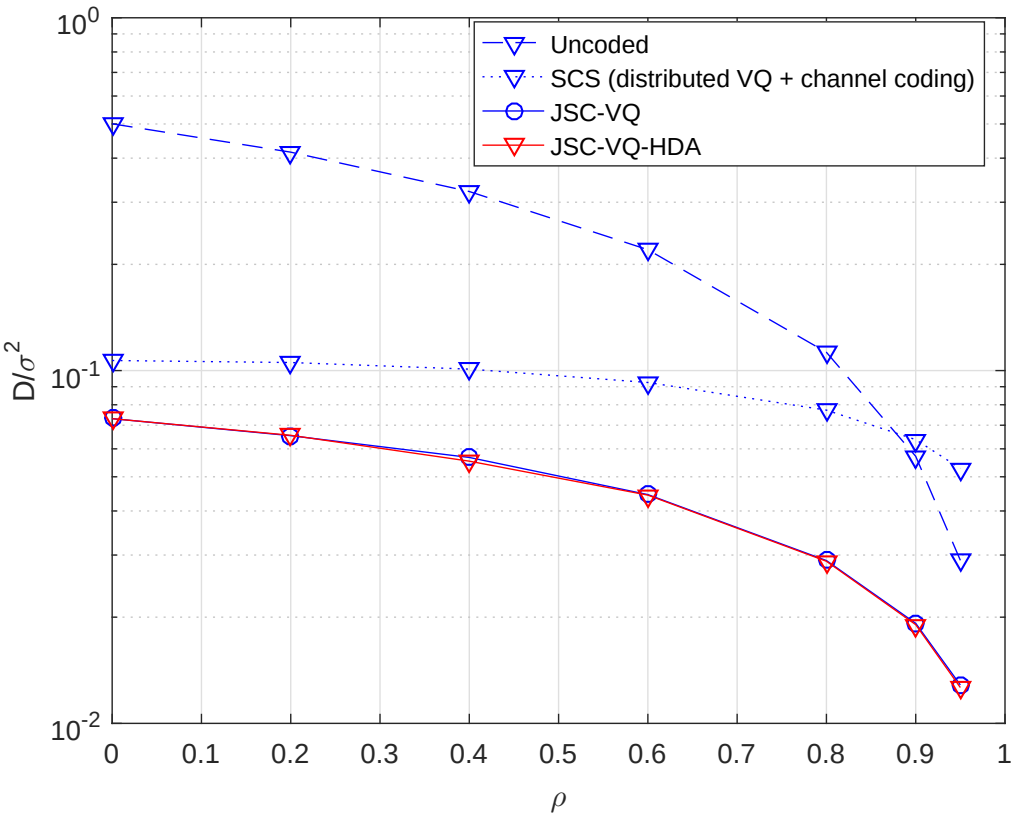

Figure 3.8: D/σ^2 vs ρ ($P/N = 30$ dB).

3.7, for $P/N = 10$ dB, the HDA scheme clearly outperforms both direct VQ, the uncoded scheme and the separation based coding scheme for the range $0 < \rho < 0.6$. However as ρ increases the performance curves of the HDA scheme, the direct VQ transmission and the uncoded transmission converge to equal performance. In Fig. 3.7, for $P/N = 30$ dB, the HDA scheme and the direct VQ transmission show equal performance over all ρ values. This is due to that at very high CSNR values, both scheme can achieve almost zero outage probability in decoding source-channel codewords with a sufficiently high encoding rate. However, the coding scheme based on source-channel separation is significantly inferior to the direct VQ codeword transmission. This is due to that the direct VQ codeword transmission is able to improve the effective channel capacity by letting channel inputs to be correlated.

Chapter 4

Practical Joint Source-Channel Coding Based on Trellis Coded Quantization for Correlated Sources and BF-GMAC

4.1 Introduction

In chapter 2, we discussed implementations of two JSC coding schemes for BF-GMAC and Gaussian sources where the generation of the channel codes are dependent on the joint pdf of the sources. In contrast to channel coding based on source-channel separation, the JSC-VQ scheme which sends an optimally vector quantized source sequence directly over the MAC generates channel input symbols with the maximum mutual dependency. The decoding of the codewords is based on measuring the Euclidean distance from superimposed *typical channel codewords* to the received waveform, subject to the *typical angle* between the channel codewords pairs. In Sec.3.2, we argued that, when averaged over the channel fading distribution, the rate regions for individual decodability of the JSC-VQ scheme, compared to that of separation based coding, are enlarged, as a result of the mutual correlation between the sources. This can be attributed two factors. First, the constructive interference created by the correlated channel symbols, when the fading gains (h_1, h_2) sat-

isfy the condition $\text{Re}\{h_1, h_2^*\} > 0$, and second the knowledge of typical angle between the transmitted codewords reduces the area containing one codeword respect to the other codeword on the surface of the hypersphere, which in return reduces the uncertainty in decoding.

Motivated by the superior performance of the JSC-VQ coding scheme, in this chapter we propose a practical code design to send Gaussian sources over BF-GMAC when CSI is not available at the transmitters. The proposed coding scheme is designed to mimic the principle behind the JSC-VQ scheme (see Fig. 4.1). The key challenges arise in designing such a practical coding scheme are:

1. Developing a finite block encoder that mimics a rate-distortion optimal VQ (which requires an infinite block encoder)

2. The joint detection of the VQ codewords from the MAC output, with a tractable computational complexity.

In designing the coding strategy, the encoder structure must lead to a codeword construction that enables the joint detection of the codewords considering their joint probability distribution. The practical VQ approaches, such as tree searched VQ [52, 53] or structured VQ based on lattices [54] do not lend themselves to computationally feasible joint detection. On the other hand, trellis coded quantization (TCQ) proposed in [55] generates a structured codebook which leads to a computationally feasible joint decoding structure. TCQ is one of the best known practical realizations of VQ and is capable of achieving average distortion within 1 to 2 dB of the distortion-rate function of a Gaussian source [55]. Therefore, we argue that the use of TCQ to generate source-channel codewords may achieve performance very close to the theoretical bound derived in Chapter 3. The main contribution of this chapter is a joint-detection algorithm that can decode TCQ source-channel codewords according to various decoder outage scenarios as discussed in Section 3.2.

Practical JSC code designs proposed in the literature, in general, consider a fixed MAC, i.e., CSI is assumed known at the transmitters. For example, Murugan *et al.* [56] propose a

low complexity cooperative source-channel coding scheme based on the use of low-density generator matrix codes. In [57], a practical design approach is presented for sending correlated binary sources over GMAC using systematic irregular low-density parity check (LDPC) codes, where the LDPC code is optimized for the joint source probabilities. Multiterminal (MT) source coding problem is closely related our problem in the high CSNR regime (lossless channel). In [58], a practical MT code design is proposed based on separating encoding into analog and digital parts, where TCQ is employed for compression of the analog part and LDPC codes are employed for distributed compression (Slepian-Wolf coding [29]) of the digital part.

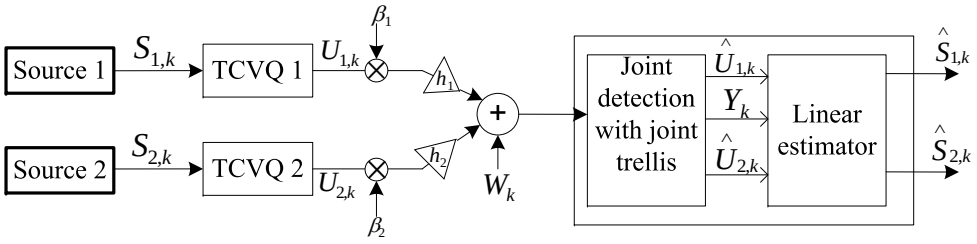

Figure 4.1: Source-channel TCVQ code over BF-GMAC.

4.2 A Practical Approach to Low Complexity JSC Coding: Trellis Encoding and Joint Sequential Detection

A novel approach to implementing a JSC coding scheme for GMAC, which is capable achieving performance close to the theoretical bound in Chapter 3 is described in the following sections. The functional block diagram of this scheme is depicted in Fig. 4.1. The encoder's function is to approximate a sequence of Gaussian source symbols by a source-channel codeword with the minimum possible MSE. What makes TCQ ideal for this is the fact that computational complexity of encoding a sequence grows linearly rather than exponentially with the sequence length. At the common receiver the transmitted codewords are detected first, and then the source components are linearly estimated based on the decoded

codewords, as done in the JSC-VQ scheme considered to obtain the theoretical bound. An important feature of TCQ is the use of a structured codebook with an expanded set of quantization levels. The structured codebook enables the optimal joint detection at the common receiver, of quantized sequences from two TCQs, with a computational complexity only linear in the sequence length. Furthermore, an expanded codebook can be efficiently used for quantization with a reduced nominal encoding rate by using the Ungerboek's set partitioning technique [59]. TCQ employs a deterministic codebook, and therefore inherits computationally simple encoding structure. In [60], the TCQ technique in [55] is generalized to use VQ at trellis transitions. The generalized VQ based source compression is called trellis-coded vector quantization (TCVQ). TCVQ enables the use of fractional rates at the transmitter which the standard fixed rate TCQ does not allow. The fractional rates allow the encoders to operate at rates closer to the optimum rate that achieves the minimum distortion. We will refer to JSC coding schemes proposed in this chapter as joint source-channel TCQ (JSC-TCQ) or joint source-channel TCVQ (JSC-TCVQ).

4.3 Trellis Coded Quantization

This section summarizes the basics of TCQ. More details can be found in [60]. The main idea behind TCQ is to encode a sequence of samples using a trellis of a finite state machine, where the branches of the trellis are assigned scalar codebooks, and a source sample is quantized at each transition. This enables quantization of a long vector of source samples using a sequence of scalar quantization decisions, yet achieve performance close to optimal VQ. In order to determine the next state, current source sample is quantized by each of the M quantizer codebooks assigned to M branches leaving the state, and the corresponding MSE value is computed. The expanded codebook is found using the Lloyd-Max algorithm [61], and the expanded codebook is divided into sub codebooks and distributed over the trellis branches to achieve the desired reduced encoding rate. The encoder uses the Viterbi algorithm [62] to find the sequence of branches through the trellis which corresponds to

the minimum MSE of quantizing a sequence of given L samples. In TCQ, the use of scalar quantization restricts encoding rate to integer values. This limitation is overcome by using TCVQ where vector codebooks, rather than scalar codebooks, are used in trellis branches. In quantizing a sequence of L samples, TCVQ employs l dimensional VQ at each trellis transition, and the Viterbi algorithm to search over L/l transitions.

Other than achieving better rate-distortion performance and realizing fractional coding rates, the use of TCVQ in the proposed JSC coding scheme can have another objective. In the JSC-TCQ scheme, a TCQ is used at each input of the GMAC to quantize a sequence of Gaussian samples into a sequence of continuous-valued channel symbols which are transmitted (after scaling to meet the power constraint) over the channel. This is suitable for real-valued baseband channels (e.g. phase shift-keying (PSK)). On the other hand, when more general complex baseband transmission is required, (e.g. quadrature amplitude modulation (QAM)), JSC-TCVQ based on 2-dimensional TCVQ ($l = 2$) can be used to map complex Gaussian source symbols to complex channel symbols.

In the next section we describe in detail the proposed JSC-TCVQ scheme. This includes JSC-TCQ as a special case.

4.4 JSC-TCVQ System Implementation

In the communication system depicted in Fig. 4.1, $\mathbf{S}_i, i \in \{1, 2\}$, is a sequence of L-dimensional Gaussian source symbols and $\mathbf{U}_i$ is the corresponding sequence of TCVQ output symbols. We use the following TCVQ structure for encoding of the source sequence.

Consider a TCVQ used to encode a Gaussian sequence. Let R be the encoding rate (bits/symbol) of the TCQ, L the length of a source sequence being encoded, l a positive integer such that L/l is an integer, and M a positive integer. Also the product RL (number of bits per source sequence) is assumed to be an integer. Now consider an N-state trellis with 2^M branches entering and leaving each trellis state. It is assumed that a l dimensional vector of reproduction symbols are produced at each trellis transition, and therefore each

branch may be uniquely labeled by a subset of l dimensional reproduction source symbols. Consequently, M/l bits/symbol are required to uniquely specify a sequence of branches through the trellis. There are L/l consecutive branches in the trellis that correspond to a sequence of L source samples. We use the Viterbi algorithm to find the optimum sequence of reproduction symbols $\mathbf{U}_i, i = 1, \ldots, L/l$ that minimizes the MSE, for a given trellis, branch labeling and a set of reproduction symbols.

Now consider TCVQs at each input of the two-input GMAC. Let the rate of the TCVQ used on source i be R_i bits/sample, $i = 1, 2$. For $R_i > 0, \tilde{R}_i \geq 0, M \geq 1, L \geq l$ and $R_i L$ and $\tilde{R}_i L$ integers satisfying $R_i L \geq M$, form a codebook, say $\mathcal{C}_i$, of $2^{(R_i+\tilde{R}_i)L}$ vector codewords. Note that codebook $\mathcal{C}_i$ of TCVQ i has $2^{\tilde{R}_i L}$ times as many codewords than the number of codewords in the equivalent L-dimensional VQ seen by the length L input sequence. Let $K_i = \tilde{R}_i l + M$ and partition the codebook, into 2^K subsets, denoted as $\tilde{\mathcal{C}}_{i,1}, \tilde{\mathcal{C}}_{i,2} \ldots, \tilde{\mathcal{C}}_{i,2^K}$. Each subset has $2^{R_i l - M}$ reconstruction vectors. For notational convenience we will drop source index i in the rest of the description of the encoding process.

An N-state trellis with 2^M branches entering and leaving each state, where each branch is labeled with one of the subsets, $\tilde{\mathcal{C}}_k$. In order to optimize the encoding process, all codewords in the codebook $\mathcal{C}$ are expected to be assigned to at least one branch. Therefore, there must be $N \geq 2^{\tilde{R}l}$ trellis states. The choice of the trellis and the branch labeling plays an important role in achieving good encoder performance. The details of such TCVQ design aspects are outlined in [60]. Next we describe the encoding of source sequence $\mathbf{S}\,(= \mathbf{S}_i, i = 1, 2)$, using the above TCVQ. Let the source sequence $\mathbf{S} \equiv \left(\mathbf{S}_1, \mathbf{S}_2, \ldots, \mathbf{S}_{L/l}\right)$ and the TCVQ output be $\mathbf{U} \equiv \left(\mathbf{U}_1, \mathbf{U}_2, \ldots, \mathbf{U}_{L/l}\right)$, i.e., both source and TCVQ output sequences are written as an augmentation of "sub-vectors" of dimension l. Given an initial state of the trellis, M bits specify a sub set $\tilde{\mathcal{C}}_k$ that is chosen for encoding during a trellis transition which produces a sub codeword $\mathbf{U}_i$ of dimension l. Therefore, M bits/sub-vector specify a unique sequence of branches, and thus a unique sequence of subset codebooks. The remaining $Rl - M$ bits/sub-vector specify a unique codeword chosen from each subset, so that the transmission rate of the encoder is RL bits/source-sequence. The encoding is

done in two steps as follows:

1. Let the branch metric for a branch labeled with subset $\tilde{\mathcal{C}}_i$ be the distortion found in step (1).

2. Use the Viterbi algorithm to find the path with the minimum distortion through the trellis.

3. At the i-th trellis transition, for each input sub-vector, $\mathbf{S}_i, i \in \{1, 2, \ldots, L/l\}$, find the closest codeword in each subset $\tilde{\mathcal{C}}_i$ assigned to any branch leaving the current state and corresponding distortion (squared error).

Fig 4.2 depicts the Ungerboeck's four-state amplitude modulation trellis with a scalar quantizer codebook of nominal rate $R = 2$ and codebook expansion rate $\tilde{R} = 1$.

Recall from Chapter 3 that the input and output of an optimal VQ for a Gaussian source are asymptotically jointly Gaussian. This is a requirement for achieving the JSC-VQ bound. In order to verify if this requirement is (at least approximately) met by a TCQ, we have determined the histogram estimate of the pdf of the TCQ output by encoding Gaussian sequences of length $L = 500$, which is shown Fig. 4.3. It appears that, provided L is sufficiently large, TCQ output is approximately Gaussian as well.

The TCVQ codeword $\mathbf{U}_i$, generated after L/l trellis state transitions, is transmitted over the fading GMAC, as shown in Fig. 4.1. The resulting sequence of L channel output symbols is given by

$$\mathbf{Y} = h_1\beta_1\mathbf{U}_1 + h_2\beta_2\mathbf{U}_2 + \mathbf{W}.$$

The reconstruction method of recovering the source symbols is described next.

Motivated by JSC-VQ used in Section 3.2 to derive the theoretical performance bound, JSC-TCVQ also uses two stage decoding scheme. In the first stage the TCVQ codewords are jointly detected to minimize the probability of error. TCVQ codewords and the channel output sequence are used to estimate the source sequences $\mathbf{S}_1$ and $\mathbf{S}_2$. In the following section, we describe the joint detection algorithm. Given the joint distribution of $(\mathbf{S}_1, \mathbf{S}_2)$

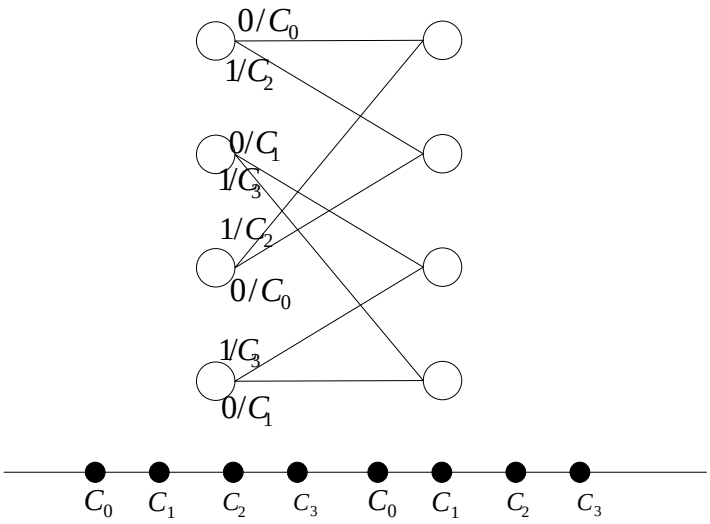

Figure 4.2: Ungerboeck's four-state amplitude modulation trellis with codebook partitioned for 2 bits/sample TCQ

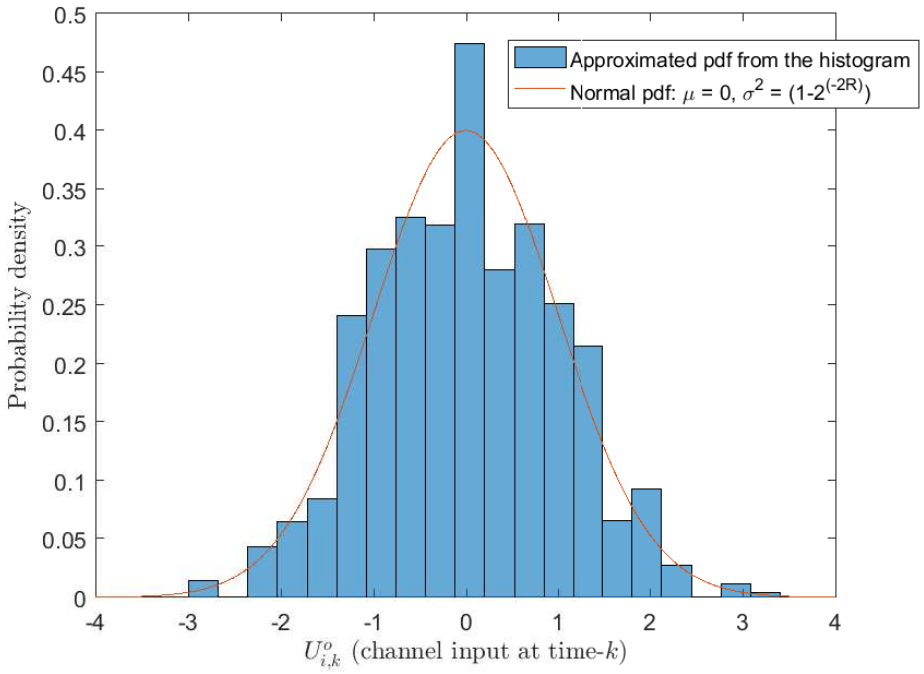

Figure 4.3: The approximated pdf of the TCQ output codeword symbols. ($R = 4$ with a codebook expansion factor of 2)

and the channel output the optimal detector is the maximum a posteriori (MAP) detector. We will also consider an alternative maximum likelihood (ML) detector which has a much lower complexity than the joint MAP detector. While the MAP detection uses the joint

distribution of the source-channel codewords, the ML detection only uses the marginal distributions which results in a performance loss.

4.4.1 MAP Detector

We assume that the sets of all possible rate pairs (R_1, R_2) for which various decoder outage events occur (decodability regions for rates) in JSC-TCVQ are the same as those of the JSC-VQ scheme in Section 3.2. With the knowledge of the channel gains (h_1, h_2) at the receiver, the joint detector determines the decodability of the source-channel codewords. The decodability of the codewords can be classified into three scenarios, i.e., 1) Reliable decoding of both codewords, 2) Only one of the codewords can be decoded reliably, and 3) Neither of the codewords can be decoded reliably. The decoded codewords and the received MAC output sequence are used as the input to the linear estimator whose coefficients are also the same those in the JSC-VQ scheme. The decoder operation according to each decodability scenario is outlined below.

Both codewords can be decoded

In the case both codewords can be decoded, the MAP detection of $\mathbf{U}_1$ an $\mathbf{U}_2$ is given by

$$\begin{aligned}(\mathbf{u}_1^o, \mathbf{u}_2^o) &= \arg\max_{\mathbf{u}_1,\mathbf{u}_2} f\left(\mathbf{u}_1, \mathbf{u}_2|\mathbf{y}\right) \\ &= \arg\max_{\mathbf{u}_1,\mathbf{u}_2} \frac{f\left(\mathbf{y}|\mathbf{u}_1, \mathbf{u}_2\right) P\left(\mathbf{u}_1, \mathbf{u}_2\right)}{f\left(\mathbf{y}\right)}. \end{aligned} \tag{4.1}$$

Using the fact that $f\left(\mathbf{y}\right)$ is a constant for given $\mathbf{y}$, and the expressions for pdf $f\left(\mathbf{y}|\mathbf{u}_1, \mathbf{u}_2\right)$, (4.1) can be simplified as

$$(\mathbf{u}_1^o, \mathbf{u}_2^o) = \arg\min_{\mathbf{u}_1,\mathbf{u}_2} \frac{\|\mathbf{y} - (h_1\mathbf{u}_1 + h_2\mathbf{u}_2)\|^2}{2N} - \log\left(P\left(\mathbf{u}_1, \mathbf{u}_2\right)\right).$$

The joint probability distribution $P\left(\mathbf{u}_1, \mathbf{u}_2\right)$ may be computed by Monte-Carlo simulations.

The joint detection of $\mathbf{u}_1$ and $\mathbf{u}_2$ is done by considering the "joint trellis" consisting of all the possible combinations of legitimate branch sequences followed by the TCQ trel-

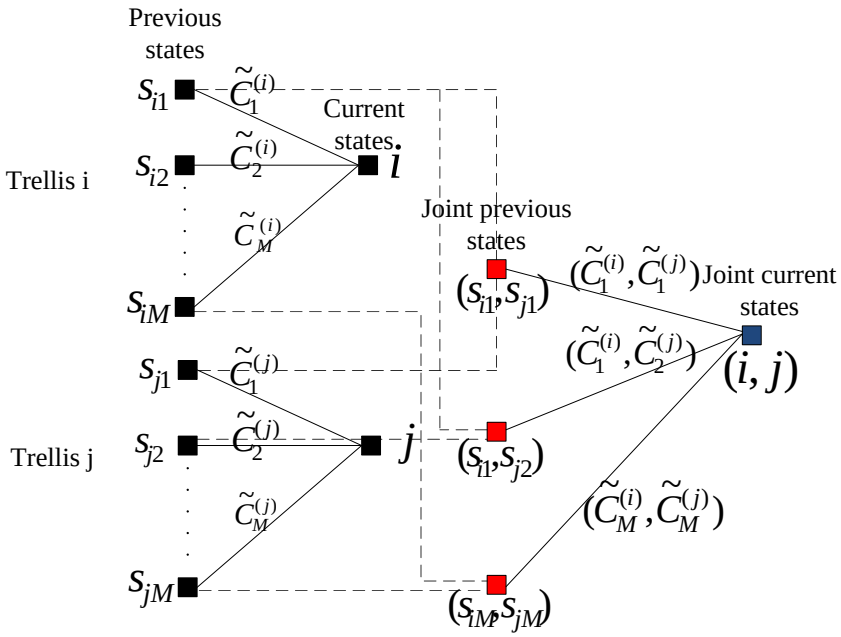

Figure 4.4: Construction of the joint trellis.

lises used for encoding the two source components. The joint trellis has N^2 states and M^2 branches entering and leaving each state (see Fig. 4.4). Let i and j be the indices for branches in trellis 1 and trellis 2, respectively, and tuple (i, j) is the index for the corresponding branch in the joint trellis. Each branch of the joint trellis is assigned a subset $\tilde{\mathcal{C}}_{i,j}$, where $\tilde{\mathcal{C}}_{i,j}$ is the cartesian product $\tilde{\mathcal{C}}_i \times \tilde{\mathcal{C}}_j$. Given the initial conidtions of the two encoder trellises, the branch metric used at the n-th trellis transition is given by

$$\lambda_i = \frac{1}{N}\mathrm{Re}\left\{\sum_{m=1+(i-1)l}^{il} y_m^*(h_1 u_{1m} + h_2 u_{2m})\right\} - \frac{1}{2N}\sum_{m=1+(i-1)l}^{il} |h_1 u_{1m} + h_2 u_{2m}|^2 - \sum_{m=1+(i-1)l}^{il} \log\left(P\left(u_{1,m}, u_{2,m}\right)\right) \tag{4.2}$$

However, numerically estimating $P\left(u_{1,m}, u_{2,m}\right)$ for all possible transmission rates can be computationally intensive. Therefore we make the reasonable assumption that the joint distribution of the TCVQ output symbols is equal to the joint distribution of the VQ output symbols. Consequently, we assume that $\mathbf{U}_1, \mathbf{U}_2$ and $\mathbf{Y}$ are circularly symmetric Gaussian random vectors. Then, the covariance matrix between vectors $\mathbf{U}_1$ and $\mathbf{U}_2$ can be approxi-

mated by the covariance matrix $\text{cov}(U_{1,k}, U_{2,k}) = E\left([U_{1,k}U_{2,k}][U_{1,k}U_{2,k}]^H\right)$ resulting from the optimal VQ of the source vectors $\mathbf{S}_1$ and $\mathbf{S}_2$, i.e.,

$$\text{cov}(U_{1,k}, U_{2,k}) = \begin{bmatrix} \tilde{\sigma}_1^2 & \tilde{\rho}\tilde{\sigma}_1\tilde{\sigma}_2 \\ \tilde{\rho}\tilde{\sigma}_1\tilde{\sigma}_2 & \tilde{\sigma}_2^2 \end{bmatrix},$$

where $\tilde{\sigma}_1 = \sigma\sqrt{1-2^{-2R_1}}$, $\tilde{\sigma}_2 = \sigma\sqrt{1-2^{-2R_2}}$, and $\tilde{\rho} = \rho\sqrt{(1-2^{-2R_1})(1-2^{-2R_2})}$. Now by substituting for $P(\mathbf{u}_{1,m}, \mathbf{u}_{2,m})$ in (4.2) we get

$$\lambda_i = \text{Re}\left\{\frac{1}{N}\sum_{m=1+(i-1)l}^{il} y_m^*(h_1u_{1m} + h_2u_{2m})\right\} - \frac{1}{2N}\sum_{m=1+(i-1)l}^{il} |h_1u_{1m} + h_2u_{2m}|^2 + \frac{1}{2}\sum_{m=1+(i-1)l}^{il} [u_{1,m}\, u_{2,m}]^* \left[\text{cov}(u_{1,m}, u_{2,m})\right]^{-1} [u_{1,m}\, u_{2,m}]^T.$$

The implementation of the joint detection of $\mathbf{u}_1$ and $\mathbf{u}_2$ using the joint trellis defined above is summarized in Algorithm 1.

The estimated source sequence is then given by the linear estimator

$$\hat{\mathbf{s}}_i = \gamma_{i,1}\mathbf{u}_1^o + \gamma_{i,2}\mathbf{u}_2^o,$$

where $[\gamma_{i,1}, \gamma_{i,2}]^T$ is the coefficients of the MMSE linear estimator derived in Section 3.2.

Only one codeword can be decoded

If the joint decoder determines only one codeword is decodable for given fading gains (h_1, h_2), the detection of the decodable codeword $\mathbf{U}_i$ is given by

$$\mathbf{u}_i^o = \underset{\mathbf{u}_i}{\text{argmax}} f\left(\mathbf{u}_i|\mathbf{y}\right), \quad i = 1, 2.$$

For clarity of explanation, let $i = 1$. Then the decoding of $\mathbf{u}_1$ can be written

$$\begin{aligned} \mathbf{u}_1^o &= \underset{\mathbf{u}_1}{\text{argmax}} f\left(\mathbf{u}_1|\mathbf{y}\right) \\ &= \underset{\mathbf{u}_1}{\text{argmax}} f\left(\mathbf{y}|\mathbf{u}_1\right) P(\mathbf{u}_1). \end{aligned} \tag{4.3}$$

Algorithm 1: The joint detection algorithm when both codewords are decodable.

Input: BF-MAC output sequence of length L: $\mathbf{y} = \{\mathbf{y}_1, \mathbf{y}_2, \ldots, \mathbf{y}_{L/l}\}$,
Subsets of the expanded codebook $\tilde{\mathcal{C}}_i$ at trellis $\nu \in \{1, 2\}$: $\left\{\tilde{\mathcal{C}}_{\nu,1}, \tilde{\mathcal{C}}_{\nu,2}, \ldots, \tilde{\mathcal{C}}_{\nu,J}\right\}$
Incoming branches/states at state $i \in \{1, 2, \ldots, N\}$: $S_{in}(i) = \{s_{i1}, s_{i2}, \ldots, s_{iM}\}$
Subset assigned to branch s_{im} at state $i \in \{1, 2, \ldots, N\}$: $\tilde{C}_m^{(i)}, m = 1, 2, \ldots, M$
(index $j \in \{1, 2, \ldots, N\}$ is used to indicate a state from other trellis respectively)

$t = 0$
Total path metric $\mathbf{\Lambda}_a^t(i, j) = \infty, \forall (i, j)$ and $(i, j) \neq (0, 0)$ and $\mathbf{\Lambda}_a^t(0, 0) = 0$
vec_$U_\nu^t(i, j) \leftarrow$ {an empty array} - to store detected channel symbols
for $t = 1$ *to* L/l **do**
    $\mathbf{y}_t \leftarrow \left[y_{(t-1)l+1}, \ldots, y_{tl}\right]$
    for $(i, j) \in \{1, \ldots N\} \times \{1, \ldots N\}$ **do**
        for $(\tilde{C}_{m_1}^{(i)}, \tilde{C}_{m_2}^{(j)}) \in \left\{\tilde{C}_1^{(i)}, \ldots, \tilde{C}_M^{(i)}\right\} \times \left\{\tilde{C}_1^{(j)}), \ldots, \tilde{C}_M^{(j)}\right\}$ **do**
            $s_1 = S_{in}(m_1)$
            $s_2 = S_{in}(m_2)$
            [λ^o, temp_$u_1(s_1, s_2)$, temp_$u_2(s_1, s_2)$] $\leftarrow$ Compute λ (4.2) $\forall (\mathbf{u}_1, \mathbf{u}_2) \in \tilde{C}_{m_1}^{(i)} \times \tilde{C}_{m_2}^{(j)}$, return minimum λ, and corresponding $\mathbf{u}_1$ and $\mathbf{u}_2$
            $\Lambda_a^{temp}(s_1, s_2) \leftarrow \Lambda_a^{t-1}(s_1, s_2) + \lambda^o$
        end
        $(s_1^o, s_2^o) \leftarrow (s_1, s_2)$ corresponding to the minimum value in $\Lambda_a^{temp}(s_1, s_2)$
        $u_1^o =$ temp_$u_1(s_1^o, s_2^o)$
        $u_2^o =$ temp_$u_2(s_1^o, s_2^o)$
        vec_$U_1^t(i, j) \leftarrow \left\{\text{vec_}U_1^{t-1}(s_1^o, s_2^o), u_1^o\right\}$ - updating detected sequence
        vec_$U_2^t(i, j) \leftarrow \left\{\text{vec_}U_2^{t-1}(s_1^o, s_2^o), u_2^o\right\}$
        $\Lambda_a^t(s_1, s_2) \leftarrow \Lambda_a^{temp}(s_1^o, s_2^o)$
    end
end

Since only $\mathbf{u}_1$ is decodable, $\mathbf{u}_1^o$ that minimizes the error probability is searched over trellis-1 using the Viterbi algorithm. The path metric for the MAP detection is found by evaluating (4.3). By using the fact that $\mathbf{u}_1$, $\mathbf{u}_2$ and $\mathbf{y}$ are iid sequences, (4.3) can be written as

$$\mathbf{u}_1^o = \underset{\mathbf{u}_1}{\text{argmax}} \sum_{\mathbf{u}_2} \prod_{m=1}^{L} f\left(y_m|u_{1m}, u_{2m}\right) P(u_{1m}|u_{2m}) P(u_{2m}), \tag{4.4}$$

where the conditional pdf $f\left(y_m|u_{1m}, u_{2m}\right)$ is Gaussian with mean zero and variance N; and the pmfs $P(u_{1m}|u_{2m})$ and $P(u_{2m})$ may be numerically estimated by Monte-Carlo simulations. In order to reduce the computational burden at the decoder, we make the assumption that the joint pdf of the optimal VQ output symbols equal to the joint distribution of the TCVQ output symbols. Then (4.4) can be written as

$$\begin{aligned}\mathbf{u}_1^o &= \underset{\mathbf{u}_1}{\text{argmax}} \int \prod_{m=1}^{L} f\left(y_m|u_{1m}, u_{2m}\right) f(u_{1m}|u_{2m}) f(u_{2m}) du_{2m} \\ &= \underset{\mathbf{u}_1}{\text{argmax}} \prod_{m=1}^{L} f(u_{1m}) \int f\left(y_m|u_{1m}, u_{2m}\right) f(u_{2m}|u_{1m}) du_{2m}. \end{aligned} \tag{4.5}$$

Here $f(u_{1m}) = \mathcal{CN}\left(0, \tilde{\sigma}_1^2\right)$ and $f(u_{2m}|u_{1m}) = \mathcal{CN}\left(\tilde{\rho}\frac{\tilde{\sigma}_2}{\tilde{\sigma}_1} u_{1m}, \tilde{\sigma}_{2|1}^2\right)$ where $\tilde{\sigma}_{2|1}^2 = \tilde{\sigma}_2^2(1 - \tilde{\rho}^2)$. By substituting for pdfs, it can be shown that (4.5) is equivalent to

$$\mathbf{u}_1^o = \underset{\mathbf{u}_1}{\text{argmin}} \sum_{m=1}^{L} \frac{|y_m - \beta_1 h_1 u_{1m}|^2}{N} + \left(\frac{1}{\tilde{\sigma}_1^2} + \frac{\tilde{\rho}^2}{\tilde{\sigma}_1^2(1 - \tilde{\rho}^2)}\right) |u_{1m}|^2 - \nu_{1m}, \tag{4.6}$$

where

$$\nu_{1m} = \frac{|(y_m - \beta_1 h_1 u_{1m}) h_2^* \beta_2 \tilde{\sigma}_{2|1}^2 + \tilde{\rho}\frac{\tilde{\sigma}_2}{\tilde{\sigma}_1} u_{1m} N|^2}{\beta_2^2 |h_2|^2 \tilde{\sigma}_{2|1}^2 + N}.$$

From (4.6), the branch metric $\lambda_i^{(1)}$ corresponding to i-th transition can be written as

$$\lambda_i^{(1)} = \sum_{m=1+(i-1)l}^{il} \frac{|y_m - \beta_1 h_1 u_{1m}|^2}{N} + \left(\frac{1}{\tilde{\sigma}_1^2} + \frac{\tilde{\rho}^2}{\tilde{\sigma}_1^2(1 - \tilde{\rho}^2)}\right) |u_{1m}|^2 - \nu_{1m}, \tag{4.7}$$

The detection of $\mathbf{u}_1$ is summarized in Algorithm 2. The estimated source sequence $\mathbf{S}_i$

Algorithm 2: The detection algorithm when only $\mathbf{u}_1$ is decodable.

Input: BF-MAC output sequence of length L: $\mathbf{y} = \{\mathbf{y}_1, \mathbf{y}_2, \ldots, \mathbf{y}_{L/l}\}$,
Subsets of the expanded codebook $\tilde{\mathcal{C}}_1$ at trellis 1: $\left\{\tilde{\mathcal{C}}_{1,1}, \tilde{\mathcal{C}}_{1,2}, \ldots, \tilde{\mathcal{C}}_{1,J}\right\}$
Incoming branches/states at state $i \in \{1, 2, \ldots, N\}$: $S_{in}(i) = \{s_{i1}, s_{i2}, \ldots, s_{iM}\}$
Subset assigned to branch s_{im} at state $i \in \{1, 2, \ldots, N\}$: $\tilde{C}_m^{(i)}, m = 1, 2, \ldots, M$

$t = 0$
Total path metric $\mathbf{\Lambda}_a^t(i) = \infty, \forall i$ and $i \neq 0$ and $\mathbf{\Lambda}_a^t(0) = 0$
vec_$U_1^t(i) \leftarrow$ {an empty array} - to store detected channel symbols
for $t = 1$ *to* L/l **do**
    $\mathbf{y}_t \leftarrow \left[y_{(t-1)l+1}, \ldots, y_{tl}\right]$
    for $i \in \{1, \ldots N\}$ **do**
        for $\tilde{C}_{m_1}^{(i)} \in \left\{\tilde{C}_1^{(i)}, \ldots, \tilde{C}_M^{(i)}\right\}$ **do**
            $s_1 = S_{in}(m_1)$
            [λ^o, temp_$u_1(s_1)$, temp_$u_2(s_1)$] $\leftarrow$ Compute λ (4.14) $\forall \mathbf{u}_1 \in \tilde{C}_{m_1}^{(i)}$, return minimum λ, and corresponding $\mathbf{u}_1$
            $\Lambda_a^{temp}(s_1) \leftarrow \Lambda_a^{t-1}(s_1) + \lambda^o$
        end
        $s_1^o \leftarrow s_1$ corresponding to the minimum value in $\Lambda_a^{temp}(s_1)$
        $u_1^o =$ temp_$u_1(s_1^o, s_2^o)$
        vec_$U_1^t(i, j) \leftarrow \left\{\text{vec_}U_1^{t-1}(s_1^o, s_2^o), u_1^o\right\}$ - updating detected sequence
        $\Lambda_a^t(s_1) \leftarrow \Lambda_a^{temp}(s_1^o)$
    end
end

is then given by the linear estimator

$$\hat{\mathbf{s}}_i = \gamma_{i,1}\mathbf{u}_1^o + \gamma_{i,3}\mathbf{y} \quad i \in \{1,2\}.$$

Similarly we can derive the branch metric for the case when only codeword $\mathbf{u}_2$ is decodable. Then, using the Viterbi algorithm, the codeword that maximizes $P(\mathbf{u_2}|\mathbf{y})$ is found searching the trellis 2.

When neither of the codewords are decodable, the source sequences are linearly estimated using the channel output sequence y, i.e.,

$$\hat{\mathbf{s}}_i = \gamma_{i,3}\mathbf{y} \quad i \in \{1,2\}.$$

4.4.2 ML Detector

As a bench mark, we evaluate the performance of the JSC-TCVQ with ML detection criterion at the joint detector. ML detection maximizes the probability of the received sequence $\mathbf{y}$ given the channel codewords $\mathbf{u}_1, \mathbf{u}_2$. The path metric$\lambda_i$ for ML detection is computed below.

Both codewords can be decoded

The detected sequence can be written as

$$(\mathbf{u}_1^o, \mathbf{u}_2^o) = \arg\max_{\mathbf{u}_1,\mathbf{u}_2} f\left(\mathbf{y}|\mathbf{u}_1, \mathbf{u}_2\right), \tag{4.8}$$

where $f\left(\mathbf{y}|\mathbf{u}_1, \mathbf{u}_2\right)$ is pdf of $\mathbf{y}$ given codewords $\mathbf{u}_1$ and $\mathbf{u}_2$. Since the conditional pdf is Gaussian, hence (4.8) can be written as

$$\begin{aligned}
(\mathbf{u}_1^o, \mathbf{u}_2^o) &= \arg\min_{\mathbf{u}_1,\mathbf{u}_2} \|\mathbf{y} - (h_1\mathbf{u}_1 + h_2\mathbf{u}_2)\|^2 \\
&= \arg\min_{\mathbf{u}_1,\mathbf{u}_2} \|\mathbf{y}\|^2 - 2\text{Re}\left\{\langle \mathbf{y}, h_1\mathbf{u}_1 + h_2\mathbf{u}_2\rangle\right\} + \|h_1\mathbf{u}_1 + h_2\mathbf{u}_2\|^2 \\
&= \arg\max_{\mathbf{u}_1,\mathbf{u}_2} 2\text{Re}\left\{\langle \mathbf{y}, h_1\mathbf{u}_1 + h_2\mathbf{u}_2\rangle\right\} - \|h_1\mathbf{u}_1 + h_2\mathbf{u}_2\|^2.
\end{aligned}$$

For ML detection, the joint trellis's branch metric is given by

$$\lambda_i = \text{Re}\left\{ \sum_{m=1+(i-1)l}^{il} y_m^*(h_1 u_{1m} + h_2 u_{2m}) \right\} - \frac{1}{2} \sum_{m=1+(i-1)l}^{il} |h_1 u_{1m} + h_2 u_{2m}|^2. \quad (4.9)$$

Only one codeword can be decoded

the detection of the decodable codeword $\mathbf{U}_i$ is given by

$$\mathbf{u}_i^o = \underset{\mathbf{u}_i}{\text{argmax}} f\left(\mathbf{y}|\mathbf{u}_i\right), \quad i = 1, 2.$$

For clarity of explanation, let $i = 1$. Then the decoding of $\mathbf{u}_1$ can be written

$$\mathbf{u}_1^o = \underset{\mathbf{u}_1}{\text{argmax}} f\left(\mathbf{y}|\mathbf{u}_1\right). \quad (4.10)$$

The path metric for the ML detection, in this decoder state, is found by evaluating (4.10). By using the fact that $\mathbf{u}_1$, $\mathbf{u}_2$ and $\mathbf{y}$ are iid sequences, (4.3) can be written as

$$\mathbf{u}_1^o = \underset{\mathbf{u}_1}{\text{argmax}} \sum_{\mathbf{u}_2} \prod_{m=1}^{L} f\left(y_m|u_{1m}, u_{2m}\right) P(u_{2m}|u_{1m}). \quad (4.11)$$

Assuming that the joint distribution of the TCVQ output symbols is equal to the joint pdf of the optimal VQ output symbols, (4.11) can be written as

$$\mathbf{u}_1^o = \underset{\mathbf{u}_1}{\text{argmax}} \prod_{m=1}^{L} \int f\left(y_m|u_{1m}, u_{2m}\right) f(u_{2m}|u_{1m}) du_{2m}. \quad (4.12)$$

By substituting for pdfs, it can be shown that (4.12) is equivalent to

$$\mathbf{u}_1^o = \underset{\mathbf{u}_1}{\text{argmin}} \sum_{m=1}^{L} \frac{|y_m - \beta_1 h_1 u_{1m}|^2}{N} + \frac{\tilde{\rho}^2}{\tilde{\sigma}_1^2(1-\tilde{\rho}^2)} |u_{1m}|^2 - \nu_{1m}, \quad (4.13)$$

where

$$\nu_{1m} = \frac{|(y_m - \beta_1 h_1 u_{1m}) h_2^* \beta_2 \tilde{\sigma}_{2|1}^2 + \tilde{\rho} \frac{\tilde{\sigma}_2}{\tilde{\sigma}_1} u_{1m} N|^2}{\beta_2^2 |h_2|^2 \tilde{\sigma}_{2|1}^2 + N}.$$

From (4.13), the branch metric $\lambda_i^{(1)}$ corresponding to i-th transition can be written as

$$\lambda_i^{(1)} = \sum_{m=1+(i-1)l}^{il} \frac{|y_m - \beta_1 h_1 u_{1m}|^2}{N} + \left(\frac{1}{\tilde{\sigma}_1^2} + \frac{\tilde{\rho}^2}{\tilde{\sigma}_1^2(1-\tilde{\rho}^2)} \right) |u_{1m}|^2 - \nu_{1m}, \qquad (4.14)$$

Similarly we can derive the branch metric for the case when only codeword $\mathbf{u}_2$ is decodable.

The detection of the TCVQ channel codewords and estimation of the source sequences are done similar to the reconstruction process in the MAP detection.

4.5 Numerical Results

In this section we present a set of numerical results to analyze the performance of the proposed practical JSC-TCQ/TCVQ coding scheme. Even though the superior performance of source compression using TCQ and TCVQ has been established in literature, the performance of a joint source-channel code, based on trellis-coded quantization over a MAC is not known. The performance of the proposed code relies on the strength of the channel code implemented and the source estimation. The four scenarios for the decodability of the received channel codes are determined as described in Section 4.4.1. The JSC-TCQ/TCVQ encoders have been designed so that their rates are approximately equal to the optimal VQs in the ideal JSC-VQ for the same source correlation and the channel distribution.

In this experimental setup, we consider sending a pair of Gaussian sources, each with a unit variance ($\sigma^2 = 1$). The source components are assumed to be correlated with correlation coefficient $0 < \rho < 1$ ($\rho = 0.9$ is assumed, unless mentioned otherwise). The initial expanded codebook for TCQ is generated using the generalized Lloyd algorithm [61]. The length of the input source sequence is $L = 500$ symbols. The fading coefficients are assumed to be independent and normally distributed random variables with zero-mean and unit variance (Rayleigh fading). We assume that the transmitter powers are equal to 1 ($P_i = 1, i \in \{1, 2\}$). The average distortion is obtained over 1000 channel realizations. The joint decoder, after determining the outage scenario for given fading gains, is implemented for the MAP detection of the codewords (ML detection is employed for comparison). The

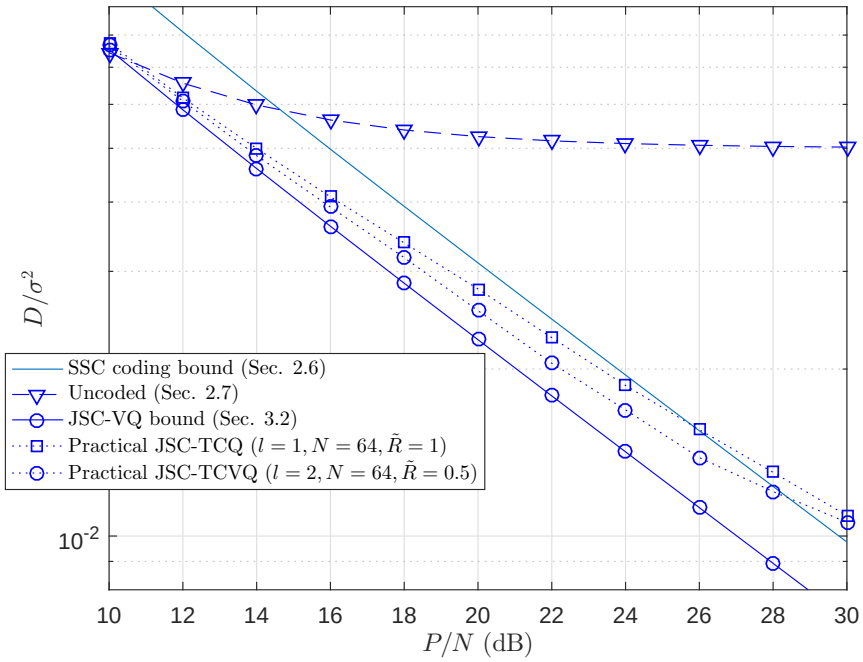

Figure 4.5: Performance of JSC-TCQ and JSC-TCQ (N=64), for correlated sources with $\rho = 0.9$ and non-fading GMAC.

JSC coding scheme is optimized over the transmission rate, subject to $Rl \in \mathbb{Z}^+$. Here l is the dimension of the branch VQ used in TCVQ. For example, if 2-dimensional VQ is used the rates can only be integer multiples of 0.5 bits/sample. In [44], JSC-VQ is used to obtain a theoretical upper bound for the performance achievable in communicating correlated Gaussian sources over a GMAC with no-fading has been presented. We can compare the performance achievable with practical JSC-TCVQ for this case, by setting $h_1 = h_2 = 1$. Fig. 4.5 compares the performance of TCVQ with the JSC-VQ bound in [44]. It interesting to note that both JSC-TCQ and JSC-TCVQ are able to achieve lower MMSE than even the theoretical lower bound of SSC coding, unless the P/N ratio is very high (> 26 dB). This suggests that no practical SSC coding scheme, which use finite block coding, is unlikely to outperform JC-TCQ/TCVQ in reality. The performance gap between JSC-TCQ and JSC-TCVQ seen here can be obviously attributed to the superior performance of VQ over scalar quantization, and to the fact that TCVQ allows to chose fractional rates in the design optimization procedure, where as with JSC-TCQ an integer approximation has to

be made, see Tables 4.1 and 4.2. These tables also show the average MSE of at the stages of the two stage decoder. Clearly the linear estimation based on prior knowledge of source correlation (second stage) improves on the joint sequence detection (first stage).

Table 4.1: Quantization rates and average MSEs of two stage decoding in JSC-TCQ used in Fig. 4.5.

$P/N(dB)$	Rate (bits/sample)		Average MSE	
	JSC-VQ (theoretical)	JSC-TCQ	Detection	Estimation
10	10	10	0.0843	0.0774
12	1.85	2	0.0672	0.0617
14	1.92	2	0.0545	0.0500
16	2.12	2	0.0446	0.0409
18	2.24	2	0.0368	0.0338
20	2.48	2	0.0304	0.0279
22	2.61	3	0.0248	0.0228
24	2.91	3	0.0204	0.0187
26	3.17	3	0.0169	0.0156
28	3.23	3	0.0142	0.0130
30	3.41	4	0.0119	0.0109

Table 4.2: Quantization rates and average MSEs of two stage decoding in JSC-TCVQ used in Fig. 4.5.

$P/N(dB)$	Rate (bits/sample)		Average MSE	
	JSC-VQ (theoretical)	JSC-TCVQ	Detection	Estimation
10	10	10	0.0827	0.0766
12	1.85	2	0.0657	0.0609
14	1.92	2	0.0524	0.0485
16	2.12	2	0.0423	0.0392
18	2.24	2.5	0.0343	0.0318
20	2.48	2.5	0.0275	0.0255
22	2.61	2.5	0.0221	0.0205
24	2.91	3	0.0182	0.0169
26	3.17	3	0.0150	0.0139
28	3.23	3.5	0.0130	0.0120
30	3.41	3.5	0.0114	0.0106

In the following experiments we consider the communication over block-fading MAC, and the average MSE given by (2.2). Recall that our main assumption is that, the transmitters are unaware of the fading gain values, but they use the knowledge of pdf of the fading

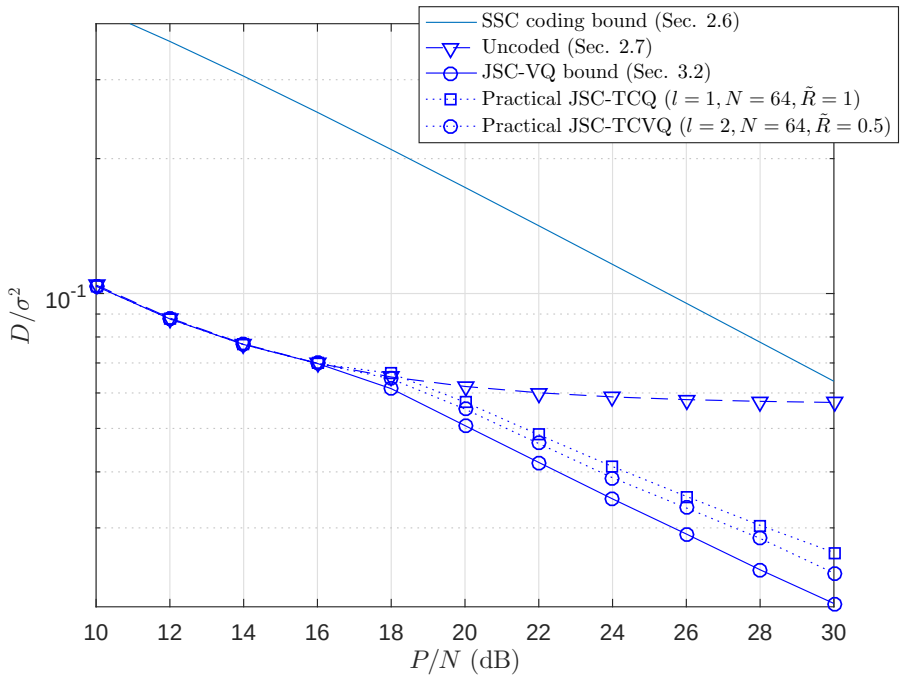

Figure 4.6: Performance of JSC-TCQ and JSC-TCVQ (N=64), for correlated Gaussian sources ($\rho = 0.9$) and BF-GMAC.

gains to optimize the transmitter parameter. The fading gains h_1 and h_2 are assumed to be independent Gaussian random variables with zero mean and unit variance. The common receiver has the perfect knowledge of the fading gains. Fig. 4.6, shows the average performance of JSC-TCQ and JSC-TCVQ against several theoretically achievable performance bounds. The performance curve of the JSC-TCVQ lies closer to the theoretical performance bound of JSC-VQ over the range 10-30 dB P/N range. It can be noticed that for low P/N the JSC-VQ performance bound coincide with the performance of the uncoded scheme. For these P/N values both JSC-VQ and JSC-TCVQ operate as the uncoded scheme by using very high transmission rates (total outage scenario). Table 4.3 and Table 4.4, list the optimum encoding rates and the average distortions at the two decoding stages.

Fig. 4.7 shows the effectiveness of the codebook expansion in JSC-TCVQ while the nominal transmission rate is kept unchanged. As can be seen, the JSC-TCVQ with codebook expansion rate $\tilde{R} = 1$ outperforms the JSC-TCVQ coding with codebook expansion rate $\tilde{R} = 0.5$. This result indicates that the joint detection is not affected by increasing the

Table 4.3: Quantization rates and average MSEs of two stage decoding in JSC-TCQ used in Fig. 4.6.

$P/N(dB)$	Rate (bits/sample)		Average MSE	
	JSC-VQ (theoretical)	JSC-TCQ	Detection	Estimation
10	10	10	0.1127	0.1039
12	10	10	0.0952	0.0878
14	10	10	0.0835	0.0770
16	10	10	0.0758	0.0698
18	2.10	2	0.0720	0.0663
20	2.23	2	0.0621	0.0572
22	2.43	2	0.0525	0.0484
24	2.71	3	0.0446	0.0411
26	2.95	3	0.0383	0.0353
28	3.15	3	0.0330	0.0304
30	3.39	4	0.0287	0.0264

Table 4.4: Quantization rates and average MSEs of two stage decoding in JSC-TCVQ used in Fig. 4.6.

$P/N(dB)$	Rate (bits/sample)		Average MSE	
	JSC-VQ (theoretical)	JSC-TCVQ	Detection	Estimation
10	10	10	0.1143	0.1039
12	10	10	0.0966	0.0878
14	10	10	0.0847	0.0770
16	10	10	0.0768	0.0698
18	2.10	2	0.0710	0.0645
20	2.23	2.5	0.0608	0.0552
22	2.43	2.5	0.0509	0.0463
24	2.71	3	0.0427	0.0388
26	2.95	3	0.0366	0.0332
28	3.15	3.5	0.0313	0.0284
30	3.39	3.5	0.0262	0.0238

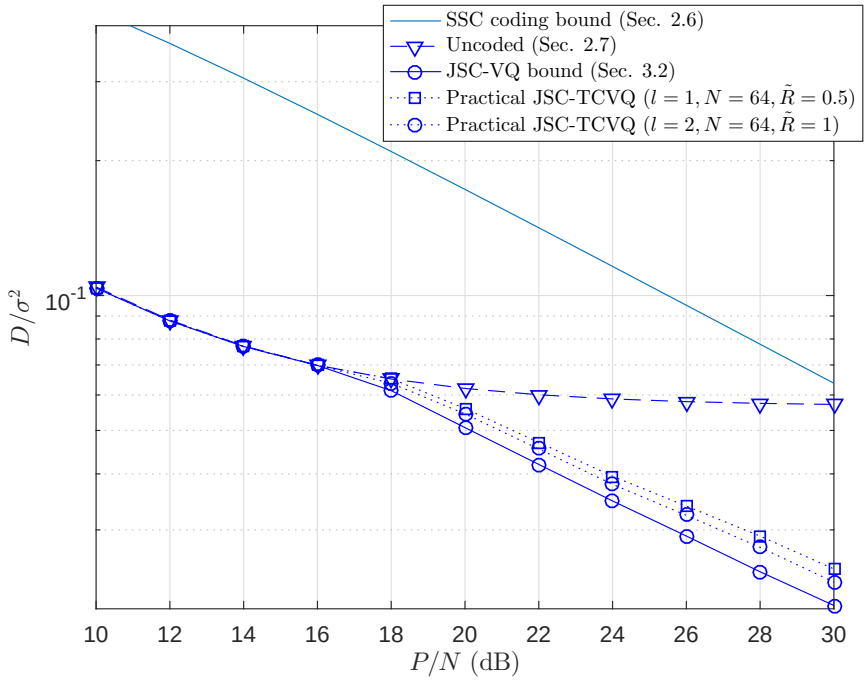

Figure 4.7: Performance comparison of JSC-TCVQ (N=32) with different deferent codebook expansion rates, for correlated sources ($\rho = 0.9$) and BF-GMAC.

effective encoder rate corresponding to the expanded codebook.

Fig. 4.8 shows performance of JSC-TCVQ with different number of states N. As expected the average MSE decrease with the number of states. However the MSE value seems to levels off as N increases. This can be attributed to the leveling off of the performance of TCVQ source compression [60]. As N increases, effectively there are more VQ codewords to encode a source sequence; however since these codewords are generated as a combinatorial sequence of a finite alphabet, the effectiveness of increasing the trellis size seems to vanish after some N value.

Fig. 4.9 shows a performance comparison between MAP detection and ML detection at the joint decoder for different source correlation values. The numerical results show that the performance gap between MAP and ML detection widens as ρ increases. This is obviously because the ML detection ignores the correlation between the source-channel codewords, whereas MAP detection uses the joint conditional distribution of the source-channel codewords given the MAC output.

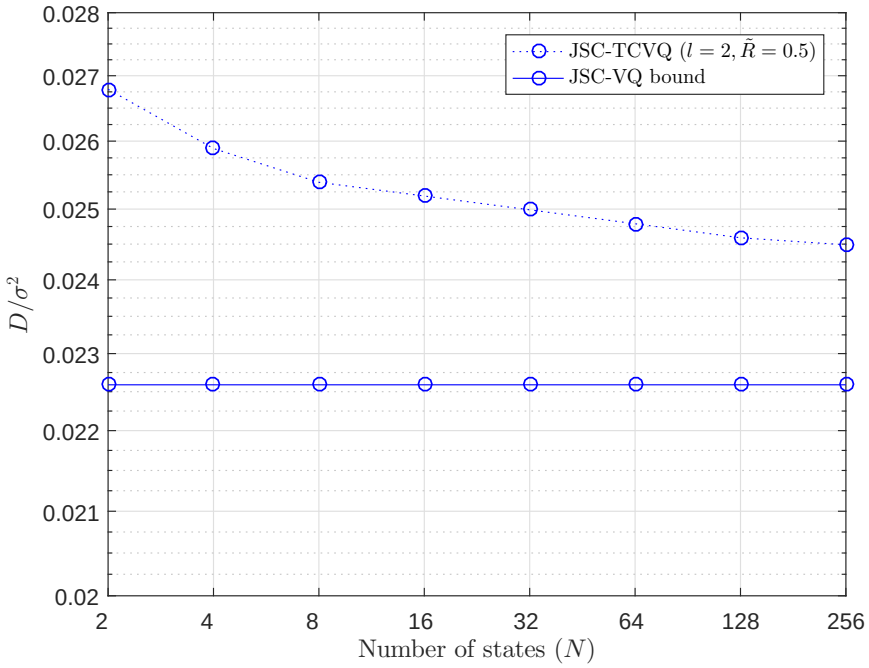

Figure 4.8: Performance of JSC-TCVQ with number of trellis states (N), for correlated sources ($\rho = 0.9$) and BF-GMAC with P/N = 30 dB.

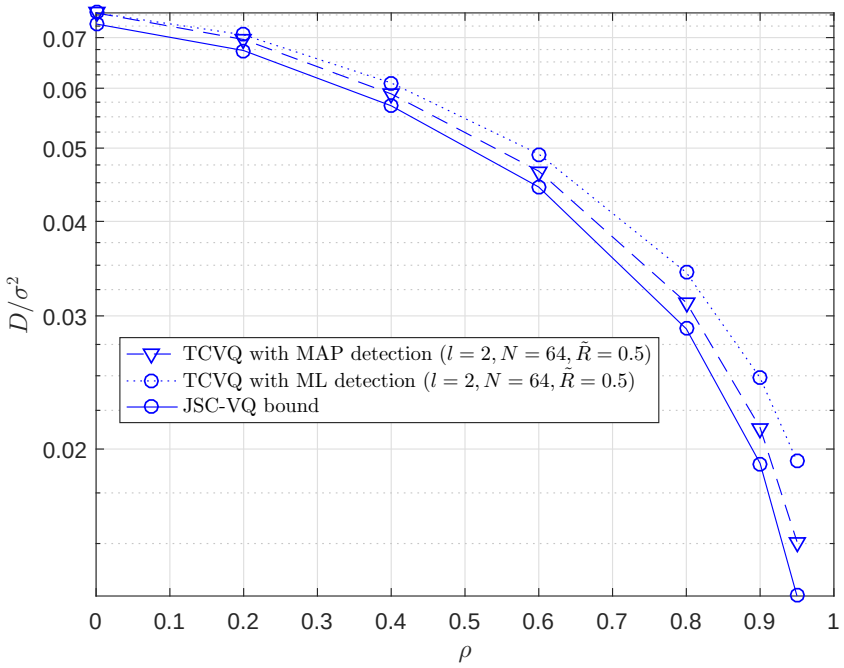

Figure 4.9: Performance comparison between MAP detection and ML detection (P/N =30 dB).

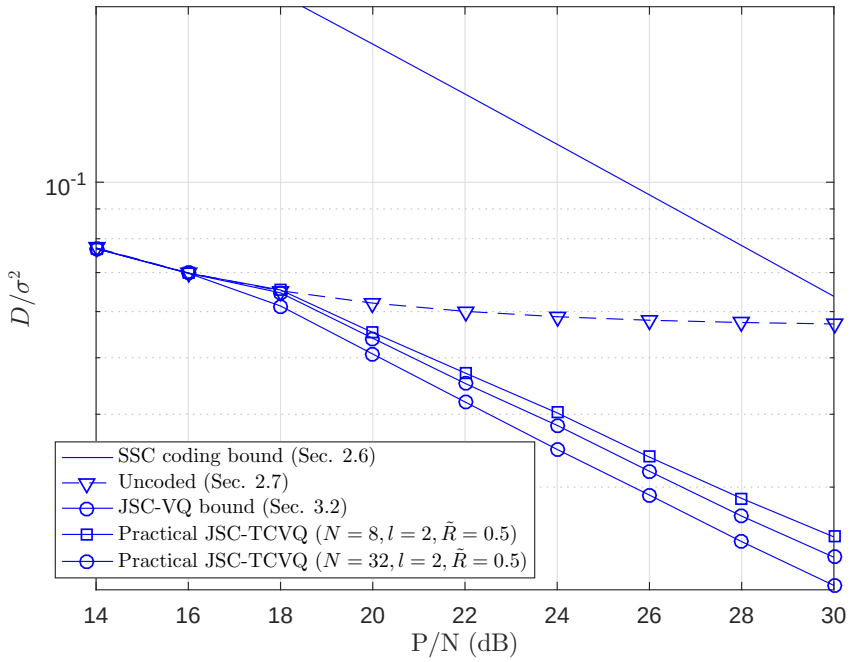

Figure 4.10: Performance comparison of JSC-TCVQ with complex baseband communication.

To demonstrate the application of JSC-TCVQ for communication over complex baseband GMAC, L 2-dimensional source symbols are transmitted using L complex channel symbols. As can be seen in Fig. 4.10 the MSE comparison between different schemes are similar to that observed for the communication over real Gaussian MAC. Also it can be noticed that the MSE curves corresponding to JSC-TCVQ transmission over the complex channel and the real-valued channels are very close. This is due to the fact that in the complex transmission, both the real-valued channel and the imaginary channel share the transmitter power, and each of the channels has an AWGN component with noise power (variance) $N/2$, and therefore each channel has the same P/N average CSNR value. However, in the real-valued transmission system, the channel has noise power N. Since the complex transmission has 3 dB less noise per symbol transmitted, the MSE for the real transmission at a certain CSNR is comparable to the MSE for the complex transmission at CSNR $-$ 3dB.

4.6 Conclusion

The practical JSC coding scheme proposed in this Chapter has drawn inspiration from the superior performance of TCQ/TCVQ in a source compression and the implications of the theoretical performance bound of the JSC-VQ coding scheme presented in Chapter 3. The structured source codeword construction in TCQ/TCVQ allows us to implement a joint channel-codeword detection algorithm with low computational complexity. The numerical results have shown that the JSC-TCVQ code can perform closer to the JSC-VQ bound than other alternatives such as SSC coding, uncoded transmission, and HDA coding. In fact, JSC-TQ can outperform the best achievable performance bounds for these schemes most of the time. From the numerical results, we can argue that JSC-TCVQ scheme employs a "good" joint channel code for the given source correlation and the channel fading distribution, and two stage decoding can be effectively used to match the encoder parameters to the inevitable outage scenarios to mtitigate the effect of the channel uncertainity at the transmitters.

Chapter 5

Conclusions and Future Work

In this thesis we have investigated the problem of communicating correlated Gaussian sources over a BF-GMAC when there is no CSI at the transmitters. For this problem, neither the theoretical bounds of achievable performance nor practical coding methods that can at least perform close to theoretical limits in a provable manner are known. The research presented in this thesis is an attempt to answer these questions. The thesis has made important contributions in terms of both establishing upper bounds to achievable performance and proposing a practically realizable coding scheme that can achieve performance close to the best known bound. The main conclusions of this thesis area s follows.

5.1 Conclusions

- In Chapter 2, an upper bound to achievable MMSE has been derived by considering a HDA coding scheme. For comparison, the achievable MMSEs of conventional source-channel separation-based coding and simple uncoded transmission have also been derived and used as benchmarks. Furthermore, we have considered the communication over an orthogonal MAC where the channel symbols are transmitted by splitting the channel bandwidth so that there is no interference between the channel inputs. The achievable MMSEs are computed by considering all decoder outage

scenarios of the digital code and optimizing the encoder parameters to minimize the MSE averaged over the fading distribution. Through numerical results we have shown that the HDA coding scheme can outperform the source-channel separation approach and the uncoded scheme as P/N (CSNR) increases. Interestingly, HDA coding over the orthogonal MAC shows slightly lower MMSE for P/N values from 5 - 10. This shows the effect of interference due to outages in the digital code at lower CSNR values. However, HDA (MAC) coding scheme shows lower MSE for CSNR > 12 dB.

- In Chapter 3, upper bounds to the achievable MMSE have been derived by considering JSC coding schemes that use source dependent channel codewords. Unlike the channel codes that ignore the correlation between the source to be transmitted over a MAC, a source dependent channel code can create constructive or destructive interference between digital channel inputs in an optimal manner and improve the performance. The main contribution here is the study of a joint source-channel vector quantizer (JSC-VQ) scheme which is designed to maximize the mutual dependency between the channel inputs. One key problem we solved is that deriving the necessary and sufficient conditions for various scenarios for correct decodablity of transmitted codewords. These scenarios arise due to the fact that, in the absence of CSI, the transmitters are forced to use fixed-rate coding. Motivated by previous work in the literature, an HDA extension of the JSC-VQ scheme has also been considered. While the established bounds have no close-form expressions, they can be numerically evaluated. Our numerical results show that unlike in the case of non-fading GMAC as considered in [44], uncoded transmission is no longer optimal at low CSNRs, when there is channel fading and CSI is not available to the transmitters. In particular, the HDA version of the JSC-VQ scheme can outperform uncoded transmission at low CSNRs.

- In Chapter 4, a practical JSC coding scheme that mimics the coding principle used in

the JSC-VQ scheme used to establish the bounds in Chapter 3 has been developed. The problem with the JSC-VQ scheme is that it relies on infinite-dimensional VQ for JSC coding. In order to practically implement a coding scheme that can come close to the JSC-VQ bound, we used trellis coded quantization (TCQ) with an expanded codebook in place of infinite dimensional VQs. It is well known that TCQ can outperform high-dimensional VQs (such as lattice VQ) at a much lower computational complexity. More importantly, TCQ provides a path to tractable decoding of the very long codewords required to approach JSC-VQ bound. The problem of joint detection of the TCQ codewords was solved by developing a four state joint decoder based on the Viterbi algorithm. Simulation results show that the proposed JSC coding scheme perform closer to the JSC-VQ bound than the other alternatives such as SSC coding, uncoded transmission, and conventional HDA coding. We conclude that the proposed JSC-TCVQ scheme is the best known practical transmission scheme to date for communicating correlated sources over a BF-MAC when CSI is not available to the transmitters.

5.2 Future Work

- In the conventional SSC coding of correlated sources in Chapter 2, distributed VQ is employed with channel coding to minimize MSE. Since the source correlation is fully exploited in the distributed VQ stage, both channel codewords must be decoded to estimate the sources. However, when transmitting over a BF-MAC with no transmitter CSI the probability of only a single codeword is decoded increases with the transmission rates. In this partial outage case, the recovered VQ index cannot be used to recover any source information. In order to optimize the SSC coding to decoder outages, a possible solution is to develop a source compression scheme such that the source correlation is at least partially exploited.

- Situations where a partial CSI is available to transmitters arise in practical commu-

nication systems. Examples of partial CSI are *uncertain CSI*, where uncertainty may be induced by channel estimation or prediction errors, and *limited CSI* which may appear with quantized feedback. Designing a JSC code that takes errors in CSI estimation in to account can draw inspirations from the work presented in Chapter 2 and 3. Unlike in our problem, where fading (CSI) distribution remains fixed, in partial CSI case, the distribution of the estimated CSI will vary over time. Therefore variation of the channel distribution over successive code blocks, and the uncertainty of the CSI during one code block must be considered to optimize the coding scheme.

Appendix A

Proof of Lemma 3.1 and Theorem 3.2

We start by summarizing the proof of [44, Theorem IV.4]. The code construction, encoding, and decoding in the JSC-VQ scheme as follows. Let $\epsilon > 0$ be a fixed constant and rates R_1 and R_2 be fixed. The VQ codebook $\mathcal{C}_i \subset \mathbb{C}^n, i = 1, 2$, is generated by independently drawing 2^{nR_i} vectors of length n from the the surface of the origin-centered sphere of radius $r_i = \sqrt{n\sigma^2(1 - 2^{-2R_i})}$ in $\mathbb{C}^n$. The encoder for source i uses $\mathcal{C}_i$ and vector quantizes the source sequences $\mathbf{s}_i$ to generate a codeword $\mathbf{u}_i^o \in \mathcal{C}_i$. The code vector then scaled to meet the power constraint and transmitted over the GMAC without any further encoding. Crucial to the proof given in [44] is the geometric view of the VQ encoder. To this end, consider the cosine angle between any pair of non-zero vectors $\mathbf{w}$ and $\mathbf{v}$ is defined by

$$\cos(\mathbf{w}, \mathbf{v}) = \frac{\text{Re}\{\langle \mathbf{w}, \mathbf{v} \rangle\}}{\|\mathbf{w}\|\|\mathbf{v}\|}.$$

Let the $\mathcal{F}(\mathbf{s}_i, \mathcal{C}_i)$ be all $\mathbf{u}_i \in \mathcal{C}_i$ for which $\cos(\mathbf{s}_i, \mathbf{u}_i)$ is between $\sqrt{1 - 2^{-2R_i}}(1 \pm \epsilon)$. The VQ encoder for source $\mathbf{s}_i$ into the codeword $\mathbf{u}_i^o$ as follows. If $\mathcal{F}(\mathbf{s}_i, \mathcal{C}_i) = \emptyset$ then set $\mathbf{u}_i^o = 0$. Otherwise, $\mathbf{u}_i^o$ is the code vector $\mathbf{u}_i \in \mathcal{F}(\mathbf{s}_i, \mathcal{C}_i)$ with the smallest $|\cos(\mathbf{s}_i, \mathbf{u}_i) - \sqrt{1 - 2^{-2R_i}}|$. The channel input is then formed as $\mathbf{x}_i = \beta_i \mathbf{u}_i^o$, where β_i is given by (3.1). Upon reception of the GMAC output $\mathbf{y}$ due to both transmitters, the receiver derives the source estimate $(\hat{\mathbf{s}}_1, \hat{\mathbf{s}}_2)$ in two steps. First, the receiver obtains a guess $(\hat{\mathbf{u}}_1, \hat{\mathbf{u}}_2)$ for the channel input codeword pair $(\mathbf{u}_1^o, \mathbf{u}_2^o)$ by finding the jointly typical pair $(\mathbf{u}_1, \mathbf{u}_2) \in \mathcal{C}_1 \times \mathcal{C}_2$ such that

$\beta_1\mathbf{u}_1 + \beta_2\mathbf{u}_2$ has the smallest Euclidean distance to the channel output $\mathbf{y}$. A jointly typical-pair is defined as $(\mathbf{u}_1, \mathbf{u}_2)$ for which $\tilde{\rho} - \cos(\mathbf{u}_1, \mathbf{u}_2) \leq 7\epsilon$, where $\epsilon > 0$ and $\tilde{\rho}$ is given by (3.3), which is the correlation between the transmitted VQ codewords $(\mathbf{u}_1^o, \mathbf{u}_2^o)$. Note that, guessing the channel inputs based on the output $\mathbf{y}$ in this case is akin to channel decoding in SSC coding, but the use of the correlation $\tilde{\rho}$ to define a jointly typical set amounts to JSC decoding. In the second step, the source estimates are obtained by computing the MMSE linear estimates of the source sequences, given $\mathbf{y}$ and the already decoded VQ codewords $(\hat{\mathbf{u}}_1, \hat{\mathbf{u}}_2)$.

Given the channel output $\mathbf{y}$, let $\mathcal{E}_{\hat{U}}$ be the error event that there exists a jointly-typical codeword pair $(\hat{\mathbf{u}}_1, \hat{\mathbf{u}}_2) \neq (\mathbf{u}_1, \mathbf{u}_2)$ for which

$$\|\mathbf{y} - (\beta_1\hat{\mathbf{u}}_1 + \beta_1\hat{\mathbf{u}}_1)\| \leq \|\mathbf{y} - (\beta_1\mathbf{u}_1^o + \beta_1\mathbf{u}_1^o)\|.$$

It can be shown that, for sufficiently large n, the probability of joint decoding error $\Pr(\mathcal{E}_{\hat{U}}) \to 0$ as $n \to \infty$ if the rates (R_1, R_2) satisfy the constraints [44, Lemma D.1]

$$R_1 < \frac{1}{2}\log_2\left(\frac{P_1(1-\tilde{\rho}^2)+N}{N(1-\tilde{\rho}^2)}\right) \tag{A.1}$$

$$R_2 < \frac{1}{2}\log_2\left(\frac{P_2(1-\tilde{\rho}^2)+N}{N(1-\tilde{\rho}^2)}\right) \tag{A.2}$$

$$R_1 + R_2 < \frac{1}{2}\log_2\left(\frac{P_1+P_2+2\tilde{\rho}\sqrt{P_1P_2}+N}{N(1-\tilde{\rho}^2)}\right). \tag{A.3}$$

A.1 Proof of Lemma 3.1

Consider the decoder JSC-VQ in a system where the GMAC exhibits block fading h_i for transmitted codeword $\beta_i\mathbf{u}_i^o$. The channel output is given by $\mathbf{y} = \beta_1\mathbf{u}_1^o + \beta_1\mathbf{u}_1^o + \mathbf{w}$, where $\mathbf{u}_i^o \in \mathbb{C}^n, h_i \in \mathbb{C}, i = 1, 2$, and $\mathbf{w} \in \mathbb{C}^n$. The set of (R_1, R_2) pairs for which both VQ codewords are decodable can be obtained straightforwardly by replacing $\mathbf{u}_1^o$ and $\mathbf{u}_2^o$ by their scaled versions in the proof of [44, Lemma D.1].

A.2 Proof of Theorem 3.2

We give proof to that when rate pair $(R_1, R_2) \in \mathcal{R}_i^{po}$, defined by (3.5), the codeword u_i^o can be recovered with arbitrarily small probability of decoding error, while the codeword u_j^o cannot be recovered reliably at the receiver. In the proof, for clarity, we will consider the case of codeword u_1^o can be recovered (i.e., $i = 1$). To this end, we first introduce an error event related to a decoding error at the receiver. This error event occurs if the decoder attempts to decode $\mathbf{u}_1$ without knowing the decodability of $\mathbf{u}_2$. This event is denoted by $\mathcal{E}_{\hat{\mathbf{U}}_1}^o$ consists of all tuples $(\mathbf{s}_1, \mathbf{s}_2, \mathcal{C}_1, \mathcal{C}_2, \mathbf{z})$ for which there exists pair $(\tilde{\mathbf{u}}_1, \tilde{\mathbf{u}}_2)$ so that $\tilde{\mathbf{u}}_1 \neq \mathbf{u}_1^o$ in $\mathcal{C}_1$ and $\mathbf{u}_2 \in \mathcal{C}_2$, and this error event precisely defined by

$$\mathcal{E}_{\hat{\mathbf{U}}_1}^* = \Bigg\{ (\mathbf{s}_1, \mathbf{s}_2, \mathcal{C}_1, \mathcal{C}_2, \mathbf{z}) : \exists \tilde{\mathbf{u}}_1 \in \mathcal{C}_1 \backslash \{\mathbf{u}_1^o\} \text{ and } \exists \tilde{\mathbf{u}}_2 \in \mathcal{C}_2 \text{ s.t.}$$

$$|\tilde{\rho} - \cos \measuredangle(\tilde{\mathbf{u}}_1, \tilde{\mathbf{u}}_2)| \leq 7\epsilon \text{ and } ||y - (h_1\beta_1\tilde{\mathbf{u}}_1 + h_2\beta_2\tilde{\mathbf{u}}_2)||^2 \leq ||y - (h_1\beta_1\mathbf{u}_1^o + h_2\beta_2\mathbf{u}_2^o)||^2 \Bigg\} \tag{A.4}$$

Note that a decoding error occurs only if $(\mathbf{s}_1, \mathbf{s}_2, \mathcal{C}_1, \mathcal{C}_2, \mathbf{z}) \in \mathcal{E}_{\hat{\mathbf{U}}_1}^o$. The main results of this section is given by the following Lemma.

Lemma A.1. *For every $\delta > 0$ and $0.3 > \epsilon > 0$, there exists an $n_4'(\delta, \epsilon) \in \mathbb{N}$ such that for all $n > n_4'(\delta, \epsilon)$*

$$Pr[\mathcal{E}_{\hat{\mathbf{U}}_1}^o] < 9\delta, \quad \textit{whenever } R_1 \in \mathcal{R}_1(\epsilon),$$

where

$$\mathcal{R}_1(\epsilon) = \left\{ R_1 < \frac{1}{2} log_2 \left(\frac{|h_1|^2 P_1 + |h_2|^2 P_2 + 2Re\{h_1 h_2{}^*\}\tilde{\rho}\sqrt{P_1 P_2} + N}{|h_2|^2 P_2 (1 - \tilde{\rho}^2) + N} - \xi_{15}\epsilon \right) \right\}$$

To prove Lemma A.1, as in [44], we define three auxiliary events related to source sequences, encoder output sequences, and channel error sequences. The first auxiliary error event $\mathcal{E}_{\mathbf{S}}$ corresponds to an atypical source output sequence. In [44], $\mathcal{E}_{\mathbf{S}}$ is given in (83), and we will use the same definition except that the source sequence are on n-dimensional

complex plain, i.e., $(\mathbf{s}_1, \mathbf{s}_2) \in \mathbb{C}^n \times \mathbb{C}^n$. The second auxiliary event $\mathcal{E}_{\mathbf{S}}$ corresponds to an atypical additive noise sequences, and is given by (84) in [44] where $\mathbf{z} \in \mathbb{C}^n$. The third auxiliary event $\mathcal{E}_{\mathbf{X}}$ and is given by the union of three events given by (85)-(87) in [44]. To prove Lemma A.1 we now start with the decomposition

$$\begin{aligned}\Pr[\mathcal{E}^o_{\hat{\mathbf{U}}_1}] &= \Pr[\mathcal{E}^o_{\hat{\mathbf{U}}_1} \cap \mathcal{E}^c_{\mathbf{S}} \cap \mathcal{E}^c_{\mathbf{X}} \cap \mathcal{E}^c_{\mathbf{Z}}] + \Pr[\mathcal{E}^o_{\hat{\mathbf{U}}_1} | \mathcal{E}_{\mathbf{S}} \cup \mathcal{E}_{\mathbf{X}} \cup \mathcal{E}_{\mathbf{Z}}] \Pr[\mathcal{E}_{\mathbf{S}} \cup \mathcal{E}_{\mathbf{X}} \cup \mathcal{E}_{\mathbf{Z}}] \\ &\leq \Pr[\mathcal{E}^o_{\hat{\mathbf{U}}_1} \cap \mathcal{E}^c_{\mathbf{S}} \cap \mathcal{E}^c_{\mathbf{X}} \cap \mathcal{E}^c_{\mathbf{Z}}] + \Pr[\mathcal{E}_{\mathbf{S}}] + \Pr[\mathcal{E}_{\mathbf{X}}] + \Pr[\mathcal{E}_{\mathbf{Z}}], \end{aligned} \tag{A.5}$$

where we have used the shorthand notation $\Pr[\mathcal{E}_\nu]$ for $\Pr[(\mathbf{S}_1, \mathbf{S}_2, \mathcal{C}_1, \mathcal{C}_2, \mathbf{Z}) \in \mathcal{E}_\nu]$, where $\mathcal{E}^c_\nu$ denotes the complement of $\mathcal{E}_\nu$. Lemma A.1 now follows from upper bounding the probability terms on the RHS of (A.5).

Lemma A.2. *For every $\delta > 0$ and $\epsilon > 0$ there exists an $n'_1(\delta, \epsilon) \in \mathbb{N})$ such that for all $n > n'_1(\delta, \epsilon) \in \mathbb{N})$*

$$Pr[\mathcal{E}_{\mathbf{S}}] < \delta.$$

Proof. See [44, Lemma D.2]. □

Lemma A.3. *For every $\delta > 0$ and $\epsilon > 0$ there exists an $n'_3(\delta, \epsilon) \in \mathbb{N})$ such that for all $n > n'_3(\delta, \epsilon) \in \mathbb{N})$*

$$Pr[\mathcal{E}_{\mathbf{Z}}] < \delta.$$

Proof. See [44, Lemma D.3]. □

Lemma A.4. *For every $\delta > 0$ and $0.3 > \epsilon > 0$ there exists an $n'_3(\delta, \epsilon) \in \mathbb{N})$ such that for all $n > n'_3(\delta, \epsilon) \in \mathbb{N})$*

$$Pr[\mathcal{E}_{\mathbf{X}}] < 6\delta.$$

Proof. See [44, Lemma D.4]. □

Lemma A.5. *For every $\delta > 0$ and every $\epsilon > 0$ there exists some $n''_4(\delta, \epsilon) \in \mathbb{N}$ the following*

condition holds true

$$Pr[\mathcal{E}^*_{\hat{\mathbf{U}}_1} \cap \mathcal{E}^c_{\mathbf{S}} \cap \mathcal{E}^c_{\mathbf{X}} \cap \mathcal{E}^c_{\mathbf{Z}}] \leq \delta, \quad \textit{if}$$
$$R_1 < \frac{1}{2} log_2 \left(\frac{|h_1|^2 P_1 + |h_2|^2 P_2 + 2Re\{h_1 {h_2}^*\}\tilde{\rho}\sqrt{P_1 P_2} + N}{|h_2|^2 P_2 (1-\tilde{\rho}^2) + N} - \xi_{15}\epsilon \right) \tag{A.6}$$

where ξ_{15} is a positive constant determined by P_1, P_2, h_1, h_2 and N.

We now start with a lemma that will be used to prove (A.6).

Lemma A.6. *Let $\varphi_j \in [0, \pi]$ be the angle between $\mathbf{y}$ and $\mathbf{u}_1(j)$, and let the set $\mathcal{E}_{\hat{\mathbf{U}}_1^{*'}}$ be defined as*

$$\mathcal{E}^{*'}_{\hat{\mathbf{U}}_1} \equiv \Bigg\{ (\mathbf{s}_1, \mathbf{s}_1, \mathcal{C}_1, \mathcal{C}_2, \mathbf{z}) : \exists \mathbf{u}_1(j) \in \mathcal{C}_1 \backslash \{\mathbf{u}_1^o\} \textit{ and } \mathbf{u}_2(l) \in \mathcal{C}_2 \textit{ s.t.}$$
$$\cos\varphi_j \geq \sqrt{\frac{|h_1|^2 P_1 + Re\{h_1 h_2^*\}\tilde{\rho}\sqrt{P_1 P_2} - \xi'' \epsilon}{\sqrt{|h_1|^2 P_1 (|h_1|^2 P_1 + |h_2|^2 P_2 + 2Re\{h_1 h_2^*\}\tilde{\rho}\sqrt{P_1 P_2} + N) + \xi_2 \epsilon}}}$$
$$\textit{and } \cos(u_1(j), u_2(l)) \geq \tilde{\rho} - 7\epsilon \Bigg\} \tag{A.7}$$

and where ξ'' and ξ_5 depend only on P_1, P_2, and N. Then, for every sufficiently small $\epsilon > 0$

$$\left(\mathcal{E}^*_{\hat{\mathbf{U}}_1} \cap \mathcal{E}^c_{\mathbf{Z}} \cap \mathcal{E}^c_{\mathbf{S}} \cap \mathcal{E}^c_{\mathbf{X}} \right) \subseteq \left(\mathcal{E}^{*'}_{\hat{\mathbf{U}}_1} \cap \mathcal{E}^c_{\mathbf{Z}} \cap \mathcal{E}^c_{\mathbf{S}} \cap \mathcal{E}^c_{\mathbf{X}} \right)$$

and, in particular

$$Pr\left[\mathcal{E}^*_{\hat{\mathbf{U}}_1} \cap \mathcal{E}^c_{\mathbf{Z}} \cap \mathcal{E}^c_{\mathbf{S}} \cap \mathcal{E}^c_{\mathbf{X}} \right] \leq Pr\left[\mathcal{E}^{*'}_{\hat{\mathbf{U}}_1} \cap \mathcal{E}^c_{\mathbf{Z}} \cap \mathcal{E}^c_{\mathbf{S}} \cap \mathcal{E}^c_{\mathbf{X}} \right]$$

Proof. We note that the error event $\mathcal{E}^*_{\hat{\mathbf{U}}_1}$ to occur, there must exist codewords $\mathbf{u}_1(j) \in \mathcal{C}_1 \backslash \{\mathbf{u}_1^o\}$, and codeword $\mathbf{u}_2(l) \in \mathcal{C}_2$ (decodability is unknown) such that

$$|\tilde{\rho} - \cos \measuredangle(\tilde{\mathbf{u}}_1, \tilde{\mathbf{u}}_2)| \leq 7\epsilon \tag{A.8}$$

and

$$||y - (h_1\beta_1\tilde{\mathbf{u}}_1 + h_2\beta_2\tilde{\mathbf{u}}_2)||^2 \leq ||y - (h_1\beta_1\mathbf{u}_1^o + h_2\beta_2\mathbf{u}_2^o)||^2. \tag{A.9}$$

We state a sequence of statement related to Condition (A.8) and Condition (A.8). **A)** For every $(\mathbf{s}_1, \mathbf{s}_2, \mathcal{C}_1, \mathcal{C}_2, \mathbf{z}) \in \mathcal{E}_{\mathbf{X}} \cap \mathcal{E}_{\mathbf{Z}}$, the following implication holds.

$$\Big(||y - (h_1\beta_1\tilde{\mathbf{u}}_1 + h_2\beta_2\tilde{\mathbf{u}}_2)||^2 \leq ||y - (h_1\beta_1\mathbf{u}_1^o + h_2\beta_2\mathbf{u}_2^o)||^2)\Big) \tag{A.10}$$
$$\Rightarrow \Big((\text{Re}\langle \mathbf{y}, \beta_1 h_1 u_1(j)\rangle \geq n(|h_1|^2 P_1 + \text{Re}\{h_1 {h_2}^*\}\tilde{\rho}\sqrt{P_1 P_2} - \xi_{13}\epsilon)\Big),$$

where ξ_{13} only depends on P_1, P_2, h_1, h_2 and z.

We start by rewriting the LHS of (A.7) as

$$\begin{aligned}
&\text{Re}(\langle \mathbf{y}, \beta_1 h_1 \mathbf{u}_1(j) + \beta_2 h_2 \mathbf{u}_2(l)\rangle) \\
&\geq ||h_1\beta_1\mathbf{u}_1^o + h_2\beta_2\mathbf{u}_2^o||^2 + \text{Re}(\langle \mathbf{z}, h_1\beta_1\mathbf{u}_1^o + h_2\beta_2\mathbf{u}_2^o\rangle) \\
&\quad + \frac{1}{2}\left\{||h_1\beta_1\mathbf{u}_1(j) + h_2\beta_2\mathbf{u}_2(l)||^2 - ||h_1\beta_1\mathbf{u}_1^o + h_2\beta_2\mathbf{u}_2^o||^2\right\} \\
&\geq ||h_1\beta_1\mathbf{u}_1^o + h_2\beta_2\mathbf{u}_2^o||^2 - n(h_1\sqrt{P_1 N}\epsilon + h_2\sqrt{P_2 N}\epsilon) \\
&\quad + \text{Re}(\langle h_1\beta_1\mathbf{u}_1(j), h_2\beta_2\mathbf{u}_2(l)\rangle) - \text{Re}(\langle h_1\beta_1\mathbf{u}_1^o, h_2\beta_2\mathbf{u}_2^o\rangle) \\
&\geq ||h_1\beta_1\mathbf{u}_1^o + h_2\beta_2\mathbf{u}_2^o||^2 - n\xi_1\epsilon + n\text{Re}\{h_1 h_2^*\}\left\{\tilde{\rho}\sqrt{P_1 P_2}(1 - 7\epsilon) - \tilde{\rho}\sqrt{P_1 P_2}(1 + 7\epsilon)\right\} \\
&\geq ||h_1\beta_1\mathbf{u}_1^o + h_2\beta_2\mathbf{u}_2^o||^2 - n\xi_2\epsilon
\end{aligned} \tag{A.11}$$

By rewriting RHS of the above inequality (A.11)

$$\begin{aligned}
&\text{Re}\{\langle h_1\beta_1\mathbf{u}_1^o + h_2\beta_2\mathbf{u}_2^o, \beta_1 h_1\mathbf{u}_1(j) + \beta_2 h_2\mathbf{u}_2(l)\rangle\} \\
&\geq ||h_1\beta_1\mathbf{u}_1^o + h_2\beta_2\mathbf{u}_2^o||^2 - \text{Re}\{\langle \mathbf{z}, \beta_1 h_1\mathbf{u}_1(j) + \beta_2 h_2\mathbf{u}_2(l)\rangle\} - n\xi_2\epsilon \\
&\geq ||h_1\beta_1\mathbf{u}_1^o + h_2\beta_2\mathbf{u}_2^o||^2 - (h_1\sqrt{P_1 N}\epsilon + h_2\sqrt{P_2 N}\epsilon) - n\xi_2\epsilon \\
&\geq ||h_1\beta_1\mathbf{u}_1^o + h_2\beta_2\mathbf{u}_2^o||^2 - n\xi_3\epsilon
\end{aligned} \tag{A.12}$$

Fig. A.12 illustrates an example of vectors $h_1\beta_1\mathbf{u}_1(j), h_2\beta_2\mathbf{u}_2(j)$ and in the complex vector space $\mathbb{C}^n$. Let angles ϕ, θ and γ are defined as $\phi = \sphericalangle(h_1\beta_1\mathbf{u}_1(j), h_1\beta_1\mathbf{u}_1^o + h_2\beta_2\mathbf{u}_2^o)$, $\theta = \sphericalangle(h_1\beta_1\mathbf{u}_1(j) + h_2\beta_2\mathbf{u}_2(j), h_1\beta_1\mathbf{u}_1^o + h_2\beta_2\mathbf{u}_2^o)$ and $\gamma = \sphericalangle(h_1\beta_1\mathbf{u}_1(j), h_1\beta_1\mathbf{u}_1(j) +$

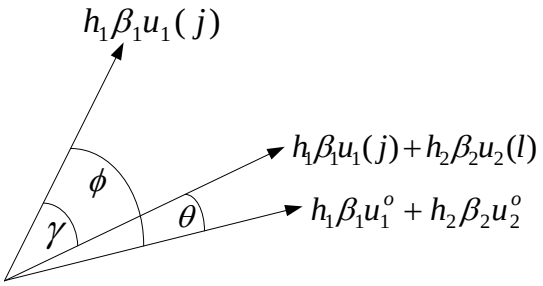

Figure A.1: The definition of asymptotic angles.

$h_2\beta_2\mathbf{u}_2(j)$). The respective cosine values of ϕ, θ and γ are given by

$$\cos\phi = \frac{\mathrm{Re}\{\langle h_1\beta_1\mathbf{u}_1^o + h_2\beta_2\mathbf{u}_2^o, \beta_1 h_1\mathbf{u}_1(j)\rangle\}}{||h_1\beta_1\mathbf{u}_1^o + h_2\beta_2\mathbf{u}_2^o||.||\beta_1 h_1\mathbf{u}_1(j||}$$
$$\cos\theta = \frac{\mathrm{Re}\{\langle h_1\beta_1\mathbf{u}_1^o + h_2\beta_2\mathbf{u}_2^o, \beta_1 h_1\mathbf{u}_1(j) + \beta_2 h_2\mathbf{u}_2(l)\rangle\}}{||h_1\beta_1\mathbf{u}_1^o + h_2\beta_2\mathbf{u}_2^o||.||\beta_1 h_1\mathbf{u}_1(j) + \beta_2 h_2\mathbf{u}_2(l)||}$$
$$\cos\gamma = \frac{\mathrm{Re}\{\langle \beta_1 h_1\mathbf{u}_1(j), \beta_1 h_1\mathbf{u}_1(j) + \beta_2 h_2\mathbf{u}_2(l)\rangle\}}{||\beta_1 h_1\mathbf{u}_1(j)||.||\beta_1 h_1\mathbf{u}_1(j) + \beta_2 h_2\mathbf{u}_2(l)||}$$

Recalling that $||\beta_i\mathbf{u}_i||= \sqrt{nP_i},\ i \in \{1,2\}$, $||\beta_i\mathbf{u}_i^o||= \sqrt{nP_i}$, $|\tilde{\rho} - \cos\sphericalangle(\mathbf{u}_1(j), \mathbf{u}_2(l))|< 7\epsilon|$ and $|\tilde{\rho} - \cos\sphericalangle(\mathbf{u}_1^o, \mathbf{u}_2^o)|< 7\epsilon|$, it can be shown that

$$|\|h_1\beta_1\mathbf{u}_1^o + h_2\beta_2\mathbf{u}_2^o\|^2 - \|h_1\beta_1\mathbf{u}_1(j) + h_2\beta_2\mathbf{u}_2(l)\|^2| \leq n\xi_4\epsilon \tag{A.13}$$

$$\tag{A.14}$$

By substituting the following can be written

$$\begin{aligned}\cos\theta &\geq \frac{\|h_1\beta_1\mathbf{u}_1^o + h_2\beta_2\mathbf{u}_2^o\|^2 - n\xi_3\epsilon}{\|h_1\beta_1\mathbf{u}_1^o + h_2\beta_2\mathbf{u}_2^o\|\sqrt{\|h_1\beta_1\mathbf{u}_1^o + h_2\beta_2\mathbf{u}_2^o\| + n\xi_4\epsilon}} \\ &\geq \frac{1-\xi_5\epsilon}{\sqrt{1+\xi_6\epsilon}}.\end{aligned} \tag{A.15}$$

For $\epsilon \to 0$ choose ξ_7, s.t., $\frac{1}{\sqrt{1+\xi_6\epsilon}} > 1 - \xi_7\epsilon$. Then, it follows that

$$\begin{aligned}\cos\theta &\geq (1-\xi_5\epsilon)(1-\xi_7\epsilon) \\ &\geq 1 - \xi_8\epsilon\end{aligned} \tag{A.16}$$

With $\phi \leq \gamma + \theta$ (equality holds true when vectors $h_1\beta_1\mathbf{u}_1(j)$, $h_1\beta_1\mathbf{u}_1(j) + h_2\beta_2\mathbf{u}_2(l)$ and $h_1\beta_1\mathbf{u}_1^o + h_2\beta_2\mathbf{u}_2^o$ are on the same plane). Note that $0 \leq \gamma \leq \pi$ and $0 \leq \theta < \frac{\pi}{2}$, and then it

follows

$$\begin{aligned}\cos\phi &\geq \cos(\gamma+\theta)\\ &= \cos\gamma\cos\theta - \sin\gamma\sin\theta\\ &= \cos\gamma\cos\theta - \sin\gamma\sqrt{1-\cos^2\theta}\\ &\geq \cos\gamma(1-\xi_8\epsilon) - \sin\gamma\sqrt{\xi_8\epsilon}. \end{aligned} \tag{A.17}$$

As $\epsilon \to 0$ let $(\cos\gamma\xi_8\epsilon - \sin\gamma\sqrt{\xi_8\epsilon}) \to \xi_9\epsilon$, where ξ_9 is only a function of P_1, P_2, h_1, h_2 and N. Now (A.17) can be written as

$$\cos\phi \geq \cos\gamma - \xi_9\epsilon. \tag{A.18}$$

By revisiting the definition of ϕ and γ, (A.18) can be rewritten as

$$\frac{\text{Re}\{\langle h_1\beta_1\mathbf{u}_1(j), h_1\beta_1\mathbf{u}_1^o + h_2\beta_2\mathbf{u}_2^o\rangle\}}{\|h_1\beta_1\mathbf{u}_1(j)\|\|h_1\beta_1\mathbf{u}_1^o + h_2\beta_2\mathbf{u}_2^o\|} \geq \frac{\text{Re}\{\langle h_1\beta_1\mathbf{u}_1(j), h_1\beta_1\mathbf{u}_1(j) + h_2\beta_2\mathbf{u}_2(l)\rangle\}}{\|h_1\beta_1\mathbf{u}_1(j)\|\|h_1\beta_1\mathbf{u}_1(j) + h_2\beta_2\mathbf{u}_2(l)\|} - \xi_9\epsilon \tag{A.19}$$

Recalling that $|\|h_1\beta_1\mathbf{u}_1^o + h_2\beta_2\mathbf{u}_2^o\|^2 - \|h_1\beta_1\mathbf{u}_1(j) + h_2\beta_2\mathbf{u}_2(l)\|^2| \leq n\xi_4\epsilon$, (A.20) can be written as

$$\begin{aligned}\text{Re}\{\langle\overline{h_1\beta_1\mathbf{u}_1(j)}, h_1\beta_1\mathbf{u}_1^o + h_2\beta_2\mathbf{u}_2^o\}\rangle &\geq \text{Re}\{\langle h_1\beta_1\mathbf{u}_1(j), h_1\beta_1\mathbf{u}_1(j) + h_2\beta_2\mathbf{u}_2(l)\}\rangle - n\xi_{10}\epsilon\\ &\geq n\left(P_1 + \text{Re}\{h_1h_2^*\}\tilde{\rho}\sqrt{P_1P_2}(1-7\epsilon)\right) - n\xi_{10}\epsilon\\ &= n\left(P_1 + \text{Re}\{h_1h_2^*\}\tilde{\rho}\sqrt{P_1P_2}\right) - n\xi_{11}\epsilon. \end{aligned} \tag{A.20}$$

Since $\mathbf{z} \in \mathcal{E}_\mathbf{z}$, $\text{Re}\{\langle\mathbf{z}, h_1\beta_1\mathbf{u}_1(j)\rangle\} \geq -n|h_1|\sqrt{P_1N}\epsilon$, we can write the real component of the inner product between received signal vector $\mathbf{y}$ and $h_1\beta_1\mathbf{u}_1(j)$ as follows

$$\begin{aligned}\text{Re}\{\langle h_1\beta_1\mathbf{u}_1(j), \mathbf{y}\rangle\} &= \text{Re}\{\langle h_1\beta_1\mathbf{u}_1(j), h_1\beta_1\mathbf{u}_1^o + h_2\beta_2\mathbf{u}_2^o\rangle\} + \text{Re}\{\langle h_1\beta_1\mathbf{u}_1(j), \mathbf{z}\rangle\}\\ &\geq n\left(P_1 + \text{Re}\{h_1h_2^*\}\tilde{\rho}\sqrt{P_1P_2}\right) - n\xi_{11}\epsilon - n|h_1|\sqrt{P_1N}\epsilon\\ &= n\left(P_1 + \text{Re}\{h_1h_2^*\}\tilde{\rho}\sqrt{P_1P_2}\right) - n\xi_{12}\epsilon. \end{aligned} \tag{A.21}$$

B) For every $(\mathbf{s}_1, \mathbf{s}_2, \mathcal{C}_1, \mathcal{C}_2, \mathbf{z}) \in \mathcal{E}_{\mathbf{X}}^c \cap \mathcal{E}_{\mathbf{Z}}^c$, the following statement is true

$$\|\mathbf{y}\|^2 \leq n(|h_1|^2 P_1 + |h_2|^2 P_2 + 2\text{Re}\{h_1 h_2^*\}\tilde{\rho}\sqrt{P_1 P_2} + N + \xi_{13}\epsilon) \tag{A.22}$$

where ξ_{13} is only a function of P_1, P_2, h_1 and h_2. The proof is straight forward. **C)** For every $(\mathbf{s}_1, \mathbf{s}_2, \mathcal{C}_1, \mathcal{C}_2, \mathbf{z}) \in \mathcal{E}_{\mathbf{X}}^c$, the following hold true

$$\|h_1\beta_1\mathbf{u}_1(j)\| \leq |h_1|\sqrt{nP_1}. \tag{A.23}$$

This is due to the average power constraint. **D)** For every $(\mathbf{s}_1, \mathbf{s}_2, \mathcal{C}_1, \mathcal{C}_2, \mathbf{z}) \in \mathcal{E}_{\mathbf{X}}^c \cap \mathcal{E}_{\mathbf{Z}}^c$, the following implication holds

$$\begin{aligned}
&|\tilde{\rho} - \cos\sphericalangle(h_1\mathbf{u}_1(j), h_1\mathbf{u}_2(l))| < 7\epsilon \text{ and} \\
&\|\mathbf{y} - (\beta_1 h_1\mathbf{u}_1(j) + \beta_2 h_2\mathbf{u}_2(l))\|^2 \leq \|\mathbf{y} - (\beta_1 h_1\mathbf{u}_1^o + \beta_2 h_2\mathbf{u}_2^o)\|^2 \Rightarrow \\
&\qquad \cos\sphericalangle(\mathbf{y}, h_1\beta_1\mathbf{u}_1(j)) \geq \Delta(\epsilon)
\end{aligned} \tag{A.24}$$

where

$$\Delta(\epsilon) \equiv \sqrt{\frac{|h_1|^2 P_1 + \text{Re}\{h_1 h_2^*\}\tilde{\rho}\sqrt{P_1 P_2} - \xi''\epsilon}{\sqrt{|h_1|^2 P_1(|h_1|^2 P_1 + |h_2|^2 P_2 + 2\text{Re}\{h_1 h_2^*\}\tilde{\rho}\sqrt{P_1 P_2} + N) + \xi_2''\epsilon}}} \tag{A.25}$$

The Statement D follows by rewriting the $\cos\sphericalangle(\mathbf{y}, h_1\beta_1\mathbf{u}_1(j))$ as

$$\cos\sphericalangle(\mathbf{y}, h_1\beta_1\mathbf{u}_1(j)) = \frac{\text{Re}\{\langle\mathbf{y}, h_1\beta_1\mathbf{u}_1(j)\rangle\}}{\|\mathbf{y}\|\|h_1\beta_1\mathbf{u}_1(j)\|} \tag{A.26}$$

and then lower bounding $\langle\text{Re}\{\mathbf{y}, h_1\beta_1\mathbf{u}_1(j)\rangle\}$ using A) and upper bounding $\|\mathbf{y}\|$ and $\|h_1\beta_1\mathbf{u}_1(j)\|$ using B) and C), respectively. The Lemma now follows by D)

$$\left(\mathcal{E}_{\hat{\mathbf{U}}_1}^* \cap \mathcal{E}_{\mathbf{Z}}^c \cap \mathcal{E}_{\mathbf{S}} \cap \mathcal{E}_{\mathbf{X}}\right) \subseteq \left(\mathcal{E}_{\hat{\mathbf{U}}_1}^{*'} \cap \mathcal{E}_{\mathbf{Z}}^c \cap \mathcal{E}_{\mathbf{S}} \cap \mathcal{E}_{\mathbf{X}}\right)$$

and, therefore

$$\text{Pr}\left[\mathcal{E}_{\hat{\mathbf{U}}_1}^* | \mathcal{E}_{\mathbf{Z}}^c \cap \mathcal{E}_{\mathbf{S}} \cap \mathcal{E}_{\mathbf{X}}\right] \leq \text{Pr}\left[\mathcal{E}_{\hat{\mathbf{U}}_1}^{*'} | \mathcal{E}_{\mathbf{Z}}^c \cap \mathcal{E}_{\mathbf{S}} \cap \mathcal{E}_{\mathbf{X}}\right] \tag{A.27}$$

□

The following lemma will also be used for the proof of (A.6).

Lemma A.7. *For every $\Delta \in (0,1]$, let the set $\mathcal{G}$ be given by*

$$\mathcal{G} = \{(\mathbf{s}_1, \mathbf{s}_2, \mathcal{C}_1, \mathcal{C}_2, \mathbf{z}) : \exists \mathbf{u}_1(j) \backslash \{\mathbf{u}_1^o\}. \textit{ s.t. } \cos \sphericalangle(\mathbf{y}, h_1\beta_1\mathbf{u}_1(j)) \geq \Delta\}$$

Then

$$\left(R_1 < -\frac{1}{2}(1-\Delta^2)\right) \Rightarrow \left(lim_{n\to\infty} Pr[\mathcal{G}|\mathcal{E}^c_{\mathbf{X}_1}] = 0, \quad \epsilon > 0\right)$$

Proof. The proof will simply follows from [44, Lemma D.7] by letting

$$\mathbf{w}(\mathbf{s}_1, \mathbf{s}_2, \mathcal{C}_1, \mathcal{C}_2, \mathbf{z}) \stackrel{\Delta}{=} \frac{\mathbf{y}}{h_1\beta_1}, \tag{A.28}$$

in [44, Identity (92)]. Note that [44, Lemma D.7] is true for any fixed vector $\mathbf{w}(\mathbf{s}_1, \mathbf{s}_2, \mathcal{C}_1, \mathcal{C}_2, \mathbf{z})$. The proof of [44, Lemma D.7] is based on the argument that the conditional probability of $\mathbf{u}_1(j)$ lies inside the polar cap surface of half-angle = arccosΔ for all $\mathbf{u}_1(j) \neq \mathbf{u}_1^o$ conditional on $\mathbf{u}_1^o$ approaches 0 as $n \to \infty$, if

$$R_1 < -\frac{1}{2}(1-\Delta^2).$$

Therefore, [44, Lemma D.7] holds true irrespective of $\mathbf{w}(\mathbf{s}_1, \mathbf{s}_2, \mathcal{C}_1, \mathcal{C}_2, \mathbf{z})$ vector. □

Proof of Lemma A.5. We start the proof of (A.6) by writing

$$\Pr\left[\mathcal{E}^*_{\hat{\mathbf{U}}_1} \cap \mathcal{E}^c_{\mathbf{Z}} \cap \mathcal{E}^c_{\mathbf{S}} \cap \mathcal{E}^c_{\mathbf{X}}\right] \stackrel{a)}{\leq} \Pr\left[\mathcal{E}^{*'}_{\hat{\mathbf{U}}_1} \cap \mathcal{E}^c_{\mathbf{Z}} \cap \mathcal{E}^c_{\mathbf{S}} \cap \mathcal{E}^c_{\mathbf{X}}\right] \qquad \stackrel{b)}{\leq} \Pr\left[\mathcal{E}^{*'}_{\hat{\mathbf{U}}_1} \mid \mathcal{E}^c_{\mathbf{X}_1}\right]$$

where $a)$ follows by Lemma A.6 and $b)$ follows because $\mathcal{E}^c_{\mathbf{X}} \in \mathcal{E}^c_{\mathbf{X}_1}$. We can complete the proof of (A.6) by combining (A.29) with Lemma A.7. This gives that for every $\delta > 0$ and every $\epsilon > 0$ there exists some $n_4'(\delta, \epsilon)$ we have $\Pr\left[\mathcal{E}^*_{\hat{\mathbf{U}}_1} \cap \mathcal{E}^c_{\mathbf{Z}} \cap \mathcal{E}^c_{\mathbf{S}} \cap \mathcal{E}^c_{\mathbf{X}}\right] < \delta$ whenever

$$\begin{aligned} R_1 &< -\frac{1}{2}\log_2\left(\frac{|h_2|^2P_2(1-\tilde{\rho}^2)+N}{|h_1|^2P_1+|h_2|^2P_2+2\text{Re}\{h_1h_2^*\}\tilde{\rho}\sqrt{P_1P_2}+N} + \xi_{14}\epsilon\right) \\ &\leq \frac{1}{2}\log_2\left(\frac{|h_1|^2P_1+|h_2|^2P_2+2\text{Re}\{h_1h_2^*\}\tilde{\rho}\sqrt{P_1P_2}+N}{|h_2|^2P_2(1-\tilde{\rho}^2)+N} - \xi_{15}\epsilon\right) \end{aligned} \tag{A.29}$$

where ξ_{15} is a positive constant determined by P_1, P_2, h_1, h_2 and N. □

Now we can prove Lemma A.1 by recalling A.5.

Proof Lemma A.1.

$$\Pr[\mathcal{E}^o_{\hat{\mathbf{U}}_1}] \leq \Pr[\mathcal{E}^o_{\hat{\mathbf{U}}_1} \cap \mathcal{E}^c_{\mathbf{S}} \cap \mathcal{E}^c_{\mathbf{X}} \cap \mathcal{E}^c_{\mathbf{Z}}] + \Pr[\mathcal{E}_{\mathbf{S}}] + \Pr[\mathcal{E}_{\mathbf{X}}] + \Pr[\mathcal{E}_{\mathbf{Z}}] \tag{A.30}$$

$$\leq \Pr[\mathcal{E}^o_{\hat{\mathbf{U}}_1} \mid \mathcal{E}^c_{\mathbf{S}} \cap \mathcal{E}^c_{\mathbf{X}} \cap \mathcal{E}^c_{\mathbf{Z}}] + \Pr[\mathcal{E}_{\mathbf{S}}] + \Pr[\mathcal{E}_{\mathbf{X}}] + \Pr[\mathcal{E}_{\mathbf{Z}}] \tag{A.31}$$

$$\leq \Pr[\mathcal{E}^o_{\hat{\mathbf{U}}_1} \mid \mathcal{E}^c_{\mathbf{X}_1}] + \Pr[\mathcal{E}_{\mathbf{S}}] + \Pr[\mathcal{E}_{\mathbf{X}}] + \Pr[\mathcal{E}_{\mathbf{Z}}] \tag{A.32}$$

Now by combining Lemma A.2, Lemma A.3, Lemma A.4 and Lemma A.7, we have that for every $\delta > 0$ and $0.3 > \epsilon > 0$, there exists an $n'_4(\delta, \epsilon) \in \mathbb{N}$ such that for all $n > n'_4(\delta, \epsilon)$ we have $\Pr[\mathcal{E}_{\mathbf{Z}}] < 9\delta$ whenever

$$R_1 < \frac{1}{2}\log_2\left(\frac{|h_1|^2P_1 + |h_2|^2P_2 + 2\mathrm{Re}\{h_1{h_2}^*\}\tilde{\rho}\sqrt{P_1P_2} + N}{|h_2|^2P_2(1-\tilde{\rho}^2) + N} - \xi_{15}\epsilon\right). \tag{A.33}$$

□

We have completed the main part of the Theorem 3.2, that is if $R_1 \in \mathcal{R}_1(\epsilon)$ codeword 1 can be recovered regardless of the decodability of codeword 2. Now we consider decoding codeword 2 given that codeword 1 is decoded. To this end, we introduce the error event related to decoding of codeword 2 when codeword 1 is correctly recovered. This error event is denoted by $\mathcal{E}_{\hat{\mathbf{U}}_2}$ and consists of all tuples $(\mathbf{s}_1, \mathbf{s}_2, \mathcal{C}_1, \mathcal{C}_2, \mathbf{z})$ for which there exists $\tilde{\mathbf{u}}_2 \neq \mathbf{u}_2^o$ in $\mathcal{C}_2$ and $\tilde{\mathbf{u}}_1 = \mathbf{u}_1^o$ in $\mathcal{C}_1$, which is precisely defined by

$$\mathcal{E}_{\hat{\mathbf{U}}_2} = \Bigg\{ (\mathbf{s}_1, \mathbf{s}_1, \mathcal{C}_1, \mathcal{C}_2, \mathbf{z}) : \exists \tilde{\mathbf{u}}_2 \in \mathcal{C}_2 \backslash \{\mathbf{u}_2^o\} \text{ s.t.}$$

$$|\tilde{\rho} - \cos\measuredangle(\mathbf{u}_1^o, \tilde{\mathbf{u}}_2)| \leq 7\epsilon \text{ and } ||y - (h_1\beta_1\mathbf{u}_1^o + h_2\beta_2\tilde{\mathbf{u}}_2)||^2 \leq ||y - (h_1\beta_1\mathbf{u}_1^o + h_2\beta_2\mathbf{u}_2^o)||^2 \Bigg\} \tag{A.34}$$

Now we state the following lemma to complete the proof of Theorem 3.2

Lemma A.8.

$$R_2 > \frac{1}{2}log_2\left(\frac{|h_2|^2P_2(1-\tilde{\rho}^2) + N}{N(1-\tilde{\rho}^2)}\right), \tag{A.35}$$

then Pr$[\mathcal{E}_{\hat{\mathbf{U}}_2}]$ *cannot be made arbitrarily small.*

Proof. By decomposing the error event $\mathcal{E}_{\hat{\mathbf{U}}_2}$ we can write

$$\begin{aligned}\Pr[\mathcal{E}_{\hat{\mathbf{U}}_2}] &= \Pr[\mathcal{E}_{\hat{\mathbf{U}}_2} \cap \mathcal{E}_{\mathbf{S}}^c \cap \mathcal{E}_{\mathbf{X}}^c \cap \mathcal{E}_{\mathbf{Z}}^c] + \Pr[\mathcal{E}_{\hat{\mathbf{U}}_1}^o | \mathcal{E}_{\mathbf{S}} \cup \mathcal{E}_{\mathbf{X}} \cup \mathcal{E}_{\mathbf{Z}}] \Pr[\mathcal{E}_{\mathbf{S}} \cup \mathcal{E}_{\mathbf{X}} \cup \mathcal{E}_{\mathbf{Z}}] \\ &\leq \Pr[\mathcal{E}_{\hat{\mathbf{U}}_2} \cap \mathcal{E}_{\mathbf{S}}^c \cap \mathcal{E}_{\mathbf{X}}^c \cap \mathcal{E}_{\mathbf{Z}}^c] + \Pr[\mathcal{E}_{\mathbf{S}}] + \Pr[\mathcal{E}_{\mathbf{X}}] + \Pr[\mathcal{E}_{\mathbf{Z}}] \end{aligned} \tag{A.36}$$

From [44, Condition (90) in Lemma D.5] it follows that if

$$R_2 > \frac{1}{2}\log_2\left(\frac{|h_2|^2 P_2(1-\tilde{\rho}^2) + N}{N(1-\tilde{\rho}^2)}\right). \tag{A.37}$$

then the term $\Pr[\mathcal{E}_{\hat{\mathbf{U}}_2} \cap \mathcal{E}_{\mathbf{S}}^c \cap \mathcal{E}_{\mathbf{X}}^c \cap \mathcal{E}_{\mathbf{Z}}^c]$ cannot be made arbitrarily small. □

The proof of Theorem 3.2 follows by combining Lemma A.1 and Lemma A.8.

Bibliography

[1] C. E. Shannon, "A mathematical theory of communication," *Bell Syst. Tech. J.*, vol. 27, pp. 379–423, 623–656, July and Oct. 1948.

[2] T. Cover and J. Thomas, *Elements of Information Theory*, 2nd ed. John Wiley, 2006.

[3] C. Shannon, "Coding theorems for a discrete source with a fidelity criterion," *IRE Nat. Conv. Rec.*, pp. 142–163, Mar. 1959.

[4] T. Berger, *Rate Distortion Theory*. Prentice Hall, Englewood Cliffs, New Jersey, 1971.

[5] N. Farvardin and V. Vaishampayan, "On the performance and complexity of channel-optimized vector quantizers," *IEEE Trans. Inform. Theory*, vol. 37, pp. 155–159, Jan. 1991.

[6] H. Kumazawa, M. Kasahara, and T. Namekawa, "A construction of vector quantizers for noisy channels," *Electronics and Engineering in Japan*, vol. 67-B, pp. 39–47, Jan. 1984.

[7] A. Kurtenbach and P. Wintz, "Quantizing for noisy channels," *IEEE Trans. Commun. Technol.*, vol. COM-17, pp. 291–302, Apr. 1969.

[8] K. Zeger and A. Gersho, "Vector quantizer design for memoryless noisy channels," in *Proc. IEEE Int. Conf. Commun. (ICC), Philadephia, PA*, 1988, pp. 1593–1597.

[9] N. Farvardin, "A study of vector quantization for noisy channels," *IEEE Trans. Inform. Theory*, vol. 36, pp. 799–809, July 1990.

[10] K. Zeger and A. Gersho, "Pseudo-Gray coding," *IEEE Trans. Communications*, vol. 38, pp. 2147–2158, Dec. 1990.

[11] N. Phamdo and N. Farvardin, "Optimal detection of discrete Markov sources over memoryless channels," *IEEE Trans. Inform. Theory*, vol. 40, pp. 186–193, Jan. 1994.

[12] F. Alajaji, N. Phamdo, and T. Fuja, "Channel codes that exploits the residual redundancy in CELP-encoded speech," *IEEE Trans. on Speech and Audio Processing*, vol. 4, pp. 325–336, Sept. 1996.

[13] J. Kroll and N. Phamdo, "Analysis and design of trellis codes optimized for a binary symmetric Markov source with MAP detection," *IEEE Trans. Inform. Theory*, vol. 44, pp. 2977–2987, Nov. 1998.

[14] B. Srinivas, R. Ladner, M. Azizoğlu, and E. Riskin, "Progressive transmission of images using MAP detection over channels with memory," *IEEE Trans. on Image Processing*, vol. 8, pp. 462–475, Apr. 1999.

[15] T. Goblick Jr., "Theoretical limitations on the transmission of data from analog sources," *IEEE Trans. Inform. Theory*, vol. 11, pp. 558–567, Oct. 1965.

[16] C. Shannon, "Communication in the presence of noise," *Proceedings of the IRE*, vol. 37, no. 1, pp. 10 – 21, Jan. 1949.

[17] A. Wyner and J. Ziv, "On communication of analog data from a bounded space," *The Bell System Technical Journal*, vol. 48, pp. 3139–3172, Dec. 1969.

[18] J. Ziv, "The behavior of analog communication systems," *IEEE Trans. Inform. Theory*, vol. 16, pp. 587–594, Sept. 1970.

[19] E. Biglieri, J. Proakis, and S. Shamai, "Fading channels: information-theoretic and communications aspects," *IEEE Trans. Inform. Theory*, vol. 44, no. 6, pp. 2619–2692, Oct. 1998.

[20] L. Li, N. Jindal, and A. Goldsmith, "Outage capacities and optimal power allocation for fading multiple-access channels," *IEEE Trans. Inform. Theory*, vol. 51, no. 4, pp. 1326–1347, Apr. 2005.

[21] M. Gastpar, B. Rimoldi, and M. Vetterli, "To code, or not to code: Lossy source-channel communication revisited," *IEEE Trans. Inform. Theory*, vol. 49, no. 5, p. 1147–1158, May 2003.

[22] U. Mittal and N. Phamdo, "Hybrid digital-analog (HDA) joint source-channel codes for broadcasting and robust communications," *IEEE Trans. Inform. Theory*, vol. 48, no. 5, p. 1082–1102, May 2002.

[23] M. Skoglund, N. Phamdo, and F. Alajaji, "Hybrid digital–analog source–channel coding for bandwidth compression/expansion," *IEEE Transactions on Information Theory*, vol. 52, no. 8, pp. 3757–3763, 2006.

[24] L. Yu, H. Li, and W. Li, "Wireless scalable video coding using a hybrid digital-analog scheme," *IEEE Transactions on Circuits and Systems for Video Technology*, vol. 24, no. 2, pp. 331–345, 2014.

[25] Y. Wang, F. Alajaji, and T. Linder, "Hybrid digital-analog coding with bandwidth compression for gaussian source-channel pairs," *IEEE Transactions on Communications*, vol. 57, no. 4, pp. 997–1012, 2009.

[26] T. M. Cover, "Broadcast channels," *IEEE Trans. Inform. Theory*, vol. IT-18, no. 1, pp. 2–14, Jan. 1972.

[27] S. Shamai (Shitz), "A broadcast strategy for the Gaussian slowly fading channel," in *in Proc. IEEE Int. Symp. Information Theory, Ulm, Germany*, Jun. 1997, p. 150.

[28] C. Ng, D. Gunduz, A. Goldsmith, and E. Erkip, "Distortion minimization in Gaussian layered broadcast coding with successive refinement," *IEEE Trans. Inform. Theory*, vol. 55, no. 11, pp. 5074–5086, Nov. 2009.

[29] D. Slepian and J. Wolf, "Noiseless coding of correlated information sources," *IEEE Trans. Inform . Theory*, vol. IT-19, pp. 47l–480, July 1973.

[30] A. Wyner and J. Ziv, "The rate-distortion function for source coding with side information at the decoder," *IEEE Trans. Inform . Theory*, vol. 22, no. 1, pp. 1–10, Jan. 1976.

[31] T. Berger, "Multiterminal source coding," *The Inform. Theory Approach to Communications, G. Longo, Ed., New York: Springer-Verlag*, vol. 229, pp. 171–231, 1977.

[32] S. Tung, *Multiterminal Rate-distortion Theory*. Ph. D. Dissertation, School of Electrical Engineering, Cornell University, Ithaca, NY, 1978.

[33] Y. Oohama, "Gaussian multiterminal source coding," *IEEE Trans. Inform.*, vol. 43, p. 1912–1923, Nov. 1997.

[34] A. Wagner, S. Tavildar, and P. Viswanath, "The rate region of the quadratic gaussian two-terminal source coding problem," *IEEE Trans. Inform. Theory*, vol. 54, May 2008.

[35] L. Song, R. Yeung, and N. Cai, "A separation theorem for single-source network coding," *IEEE Trans. Inform. Theory*, vol. 52, no. 5, p. 1861–1871, May 2006.

[36] A. Ramamoorthy, K. Jain, P. Chou, and M. Effros, "Separating distributed source coding from network coding," *IEEE Trans. Inform. Theory*, vol. 52, no. 6, p. 2785–2795, June 2006.

[37] M. Agarwal and S. Mitter, "Communication to within a fidelity criterion over unknown networks by reduction to reliable communication problems over unknown networks," 2010. [Online]. Available: http://arxiv.org/abs/1002.1300

[38] S. Jalali and M. Effros, "On the separation of lossy source-network coding and channel coding in wireline networks," in *Proc. IEEE International Symposium on Information Theory Proceedings*, June 2010, pp. 500–504.

[39] C. Tian, J. Chen, S. Diggavi, and S. Shamai, "Optimality and approximate optimality of source-channel separation in networks," in *Proc. IEEE International Symposium on Information Theory Proceedings*, June 2010, pp. 495–499.

[40] T. Cover, A. El-Gamal, and M. Salehi, "Multiple access channels with arbitrarily correlated sources," *IEEE Trans. Inform. Theory*, vol. IT-26, no. 6, p. 648–657, Nov. 1980.

[41] G. Dueck, "A note on the multiple access channel with correlated sources," *IEEE Trans. Inform. Theory*, vol. IT-27, no. 3, p. 232–235, Mar. 1981.

[42] W. Kang and S. Ulukus, "A single-letter upper bound for the sum rate of multiple access channels with correlated sources," Nov. 2005. [Online]. Available: http://arxiv.org/pdf/cs.IT/0511096

[43] M. Salehi, "Multiple-access channels with correlated sources," in *in Proc. IEEE Int. Symp. Information Theory (ISIT)*, Sep. 1995, p. 17–22.

[44] A. Lapidoth and S. Tinguely, "Sending a bivariate Gaussian over a Gaussian MAC," *IEEE Trans. Inform. Theory*, vol. 56, no. 6, p. 2714–2752, Jun. 2010.

[45] N. Prasad, G. Yue, M. A. Khojastepour, X. Wang, and M. Madihian, "Optimal successive group decoder for the slow-fading multiple access channel," in *2006 40th Annual Conference on Information Sciences and Systems*, Mar. 2006, pp. 1025–1030.

[46] R. Narasimhan, "Individual outage rate regions for fading multiple access channels," in *Proc. IEEE International Symposium on Information Theory Proceedings*, Jun. 2007.

[47] V. Kafedziski, "Rate allocation for transmission of two Gaussian sources over multiple access fading channels," *IEEE Communications Letters*, vol. 16, no. 11, pp. 1784–1787, Nov. 2012.

[48] T. Ramstad, "Shannon mappings for robust communication," *Telektronikk*, pp. 98(1):114–128, 2002.

[49] S. Y. Chung, *On the Construction of Some Capacity-Approaching Coding Schemes*. Ph.D. thesis, Massachusetts Institute of Technology, 2000.

[50] M. Hassanin, O. Fresnedo, J. Garcia-Frias, and L. Castedo, "Analog joint source channel coding for Gaussian multiple access channels," *Springer Lecture Notes in Computer Science*, vol. 8310, pp. 21–32, Dec. 2013.

[51] P. J. Schreier, "A unifying discussion of correlation analysis for complex random vectors," *IEEE Transactions on Signal Processing*, vol. 56, no. 4, Apr. 2008.

[52] P. A. Chou, T. Lookabaugh, and R. M. Gray, "Optimal pruning with applications to tree-structured source coding and modeling," *IEEE Transactions on Information Theory*, vol. 35, no. 2, pp. 299–315, March 1989.

[53] A. Buzo, A. Gray, R. Gray, and J. Markel, "Speech coding based upon vector quantization," vol. 5, pp. 15–18, 1980.

[54] T. Eriksson and E. Agrell, *Lattice-based quantization Part II*, 1996.

[55] M. W. Marcellin and T. R. Fischer, "Trellis coded quantization of memoryless and gauss-markov sources," *IEEE Transactions on Communications*, vol. 38, no. 1, pp. 82–93, 1990.

[56] A. D. Murugan, P. K. Gopala, and H. E. Gamal, "Correlated sources over wireless channels: cooperative source-channel coding," *IEEE Journal on Selected Areas in Communications*, vol. 22, no. 6, pp. 988–998, 2004.

[57] I. Shahid and P. Yahampath, "Distributed joint source-channel code design for GMAC using irregular LDPC codes," *J Wireless Com Network 2014*, vol. 3, 2014. [Online]. Available: https://doi.org/10.1186/1687-1499-2014-3

[58] Y. Yang, V. Stankovic, Z. Xiong, and W. Zhao, "On multiterminal source code design," *IEEE Transactions on Information Theory*, vol. 54, no. 5, pp. 2278–2302, May. 2008.

[59] G. Ungerboeck, "Channel coding with multilevel/phase signals," *IEEE Transactions on Information Theory*, vol. 28, no. 1, pp. 55–67, 1982.

[60] T. R. Fischer, M. W. Marcellin, and M. Wang, "Trellis-coded vector quantization," *IEEE Transactions on Information Theory*, vol. 37, no. 6, pp. 1551–1566, 1991.

[61] A. Gresho and R. M. Gray, *Vector Quantization and Signal Compression*. Kluwer Academic Publishers, 1992.

[62] G. D. Forney, "The Viterbi algorithm," *Proceedings of the IEEE*, vol. 61, no. 3, pp. 268–278, 1973.

Publications

- C. Illangakoon and P. Yahampath,“On Achievable Distortion in Sending Gaussian Sources over a Bandwidth-Matched Gaussian MAC with No Transmitter CSI”, Entropy 2019, 21, 992.
- C. Illangakoon and P. Yahampath, “Hybrid Digital-Analog Communication of a Bivariate Gaussian Source over a Fading MAC”, 2016 IEEE 84th Vehicular Technology Conference (VTC-Fall), Montreal, 2016.
- C. Illangakoon and P. Yahampath, “Optimal CDMA Signatures for Correlated Sources With a Multi-Antenna Receiver”, Canadian Workshop on Information Theory, 2015.
- C. Illangakoon and P. Yahampath, “On Joint Source-Channel Decoding and Interference Cancellation in CDMA-Based Large-Scale Wireless Sensor Networks”, IEEE International Conference on Acoustics, Speech and Signal processing, 2013.